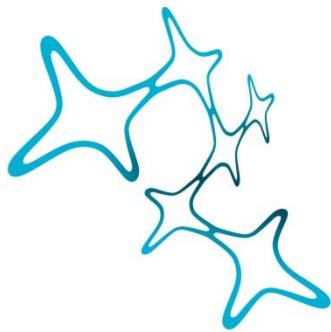

CONTROL OF WALKING BEHAVIOR BY HORIZONTAL OPTIC FLOW DETECTORS IN *DROSOPHILA*

Christian Busch



Graduate School of
Systemic Neurosciences
LMU Munich



Dissertation der
Graduate School of Systemic Neurosciences der
Ludwig-Maximilians-Universität München

10th of February 2020

Supervisor

Prof. Dr. Alexander Borst

Max-Planck-Institute of Neurobiology, Martinsried, Germany

First Reviewer: Prof. Dr. Alexander Borst

Second Reviewer: Dr. Ruben Portugues

Date of Submission: 10.02.2020

Date of Defense: 28.07.2020

SUMMARY

Complex behaviors are based on sensory feedback signals that enable animals to control for dynamic changes and unintended deviations within their surroundings. While signals from different sensory modalities can be used for this purpose, visual signals particularly contain valuable information. Thus, sighted animals often rely on visual feedback when navigating through the world. Optic flow provides important feedback about self-motion, which is likely to be incorporated in course control and locomotion behavior. However, the mechanism by which optic flow modulates the behavioral response is not yet fully understood.

Due to its relative small number of neurons and the large number of genetic tools available, *Drosophila melanogaster* is a model organism well suited to investigate neural circuits of visually driven behavior. Significant progress has been made during the last decades to depict how *Drosophila* reliably extracts and processes information to control its motion. It is known that *Drosophila* has dedicated optic flow sensing neurons, which respond to specific optic flow fields. Nevertheless, further research is required to unravel the specific contribution of these neurons to visually-driven locomotion.

This cumulative thesis consists of two published studies. In the first study, my colleagues and I investigated the application of novel anion channelrhodopsins as optogenetic silencers in the visual system of *Drosophila melanogaster*. To this end, we characterized the anion channelrhodopsins GtACR1 and GtACR2 and we performed patch-clamp recordings from tangential cells expressing GtACR1, which showed strong and light-sensitive photocurrents with minor light induced artifacts. Furthermore, we demonstrated that GtACR1 can be used to introduce fast and reversible hyperpolarization within the optic lobe of *Drosophila* without compromising visual processing.

In the second study, my colleagues and I investigated the potential contribution of optic flow information to course control in *Drosophila melanogaster*. *Drosophila*'s horizontal system (HS) cells respond to horizontal optic flow by depolarizing for front-to-back motion and hyperpolarizing for back-to-front motion. Using optogenetic tools such as GtACR1, I introduced unilateral de- and hyperpolarization in HS cells, which evoked turning behavior in opposite directions. Thus, both de- and hyperpolarizing signals are transmitted to downstream pathways and are used as steering signals. Furthermore, I also introduced bilateral de- and hyperpolarization in HS cells, which evoked a reduction in walking velocity. These results indicate a functional architecture where HS cell signals are split into two decelerating pathways. Asymmetric deceleration signals from HS cells can therefore mediate bi-directional turning by specifically reducing the motor activity of one side.

Taken together, the findings presented in this thesis underline the applicability, advantages and challenges of using optogenetic tools in the visual system of *Drosophila* and further broaden our understanding of the contributions of HS cells to the steering behavior of walking flies.

CONTENTS

1	INTRODUCTION	1
1.1	The Relevance of Visual Feedback for Course Control	1
1.1.1	Control of Self-Motion by Sensory Feedback	1
1.1.2	The Necessity of Computing Visual Feedback	2
1.1.3	Optic Flow	3
1.1.4	Self-Motion Information from Rotational and Translational Optic Flow	3
1.1.5	Visual Feedback from Voluntary and Involuntary Movements	5
1.2	Requirements for Optic Flow Detection	5
1.2.1	General Requirements for Local Motion Detection	5
1.2.2	Local Motion Detectors	6
1.2.3	Wide-Field Integration of Local Motion Signals	8
1.3	Visual Processing in <i>Drosophila</i>	9
1.3.1	The Compound Eye	9
1.3.2	Retina	10
1.3.3	Lamina, Medulla and Lobula	12
1.3.4	Optic Flow Detectors in the Lobula Plate	13
1.4	Probing the Mechanisms Underlying Visually Guided Course Control	17
1.4.1	Optomotor Response	17
1.4.2	Tethered Walking Setup	18
1.5	Evidence for Behavioral Roles of Optic Flow Neurons	18
1.6	Aim of Thesis and Overview of Published Work	20
2	METHODS AND TOOLS IN CIRCUITS NEUROSCIENCE	22
2.1	Access to Neural Populations	22
2.1.1	The Binary Expression System GAL4-UAS	22
2.1.2	Split-GAL4 and GAL80	23
2.1.3	Other Binary Systems and Techniques	24
2.1.4	Libraries of Driver Lines	25
2.2	Effectors and Reporters	25
2.2.1	Fluorescence Proteins	25
2.2.2	Functional Reporters	25
2.2.3	Ablation	27
2.2.4	Silencing	27
2.2.5	Activation	27
2.3	Optogenetics	28
2.3.1	Intrinsic Parameters of Optogenetic Tools	28
2.3.2	Opsins	29
2.3.3	Neuronal Activators	29
2.3.4	Neuronal Inhibitors	31
2.3.5	Synthetic Retinal Analogues	32
2.3.6	Step-Function Opsins	32
2.4	Physiological Techniques	32

2.4.1	Whole-Cell Patch Clamp Recording	32
2.4.2	Two-Photon Imaging	33
2.5	Methods for Structural Analysis	33
2.5.1	Effector Based Anatomical Analysis	34
2.5.2	Electron Microscopy	34
3	PUBLICATIONS	37
3.1	Optogenetic Neuronal Silencing in <i>Drosophila</i> during Visual Processing	37
3.2	Bi-directional Control of Walking Behavior by Horizontal Optic Flow Sensors	51
4	DISCUSSION	73
4.1	Neural Activity Manipulations	73
4.1.1	Possibilities of Neural Silencing	74
4.1.2	Considerations for Using Optogenetic Tools	75
4.1.3	Optogenetic Manipulations in Visual Circuits	76
4.1.4	Optimizing GtACR1	79
4.2	The Role of HS Cells for Behavior	80
4.2.1	Response Properties Supporting Role in Course Control	80
4.2.2	The Effect of Acute Manipulations on Tethered Walking	81
4.2.3	Redundancy in the Lobula Plate Network	81
4.2.4	Downstream Pathways	82
4.2.5	Visual Control of Walking Velocity	83
4.2.6	Behavioral Importance of HS Cell Signals	83
4.3	Future Directions	84
4.3.1	Unrestrained Behavioral Experiments	84
4.3.2	Unilateral Optogenetic Manipulations during Unrestrained Behavior	85
4.3.3	Recording Neural Activity with Bioluminescence Indicators	87
4.4	Conclusion	87
	Bibliography	89

LIST OF FIGURES

Figure 1	Illustration of <i>Drosophila melanogaster</i> and its feedback signals during self-motion	2
Figure 2	Illustration of optic flow as vector field	4
Figure 3	Schematic overview of rotations and translations	4
Figure 4	The <i>Hassenstein and Reichardt</i> (HR) detector	7
Figure 5	Three-arm hybrid detector	8
Figure 6	Illustration of the architecture of an optic flow selective neuron	9
Figure 7	Schematic overview of the visual information flow	10

Figure 8	Horizontal system (HS) cells	14
Figure 9	Layered structure of the lobula plate	15
Figure 10	Tethered walking setup	19
Figure 11	Illustration of the working principle of the GAL4-UAS system	23
Figure 12	Split-GAL4 and GAL80	24
Figure 13	Illustration of selected optogenetic channels	30
Figure 14	Exemplary illustration of the suitable parameter range of an optogenetic tool	78
Figure 15	Proposed optimization of GtACR1 by spectral shift	79
Figure 16	Symmetric and unilateral expression patterns of HS cell specific driver lines (split-GAL4 HS lines)	86

Complex behaviors require sensory feedback, as animals must constantly control for dynamic changes and unintended deviations within their surroundings. For this purpose, feedback signals from different sensory modalities are used.

Visual systems provide important information about the environment. Thus, sighted animals often rely on visual feedback when navigating through the world. Particularly interesting feedback signals during locomotion behavior are retinal image shifts and rotations, also known as optic flow. Unintended deviations from a planned course can be detected and avoided based on the perceived optic flow patterns. *Drosophila melanogaster* has dedicated optic flow sensing neurons, such as horizontal system (HS) cells, that respond to specific optic flow patterns. While the response characteristics of these cells are well described, their role in behavior is not yet fully understood. Experimental evidence, however, strongly suggests that HS cells are involved in visually guided behaviors. In this thesis, I investigated the contribution of HS cells to walking behavior in *Drosophila melanogaster*. Specifically, I explored the application of a novel anion channelrhodopsin as an optogenetic silencer within the visual system and subsequently manipulated the neural activity of HS cells during tethered walking behavior. Based on my experiments, I described novel functions of these cells, thus broadening the current knowledge of the implications of HS cells for behavior.

The remainder of this chapter introduces the concept of optic flow and its potential importance for course control. Furthermore, the visual system of *Drosophila melanogaster* and evidence for the behavioral importance of optic flow neurons are presented. The second chapter provides an overview of methods and genetic tools in *Drosophila*. The third chapter contains the main findings that have been published in two peer reviewed articles. Finally, the last chapter provides a discussion on optogenetic tools and their application within visual systems, as well as the importance of HS cells for behavior.

1.1 THE RELEVANCE OF VISUAL FEEDBACK FOR COURSE CONTROL

1.1.1 Control of Self-Motion by Sensory Feedback

Animals perform voluntary movements to navigate through the environment. However, some factors can introduce involuntary motion components that push the animal off-course, such as external influences or internal noise in neural circuits. Accordingly, the animal must constantly use sensory feedback to detect and counteract deviations.

Drosophila melanogaster has several sensory systems that provide information about its own body pose and the environment. Importantly, signals from more than one sensory system can simultaneously serve as feedback during self-motion. This is supported by studies demonstrating that *Drosophila* not only relies on vision, but also incorporates other sensory modalities and internal signals to control its motion (Bender and Dickinson, 2006; Bartussek and Lehmann, 2016; Kim et al., 2017).

One of these sensory modalities is proprioception, which provides feedback on the execution of self-motion. Proprioceptive information is generated by mechanosensory neurons located in muscles, joints or tendons and signals the current position of body parts of an animal. It informs the brain about movement and velocity of limbs or wings, vibrations, maximum positions (limits), and the current load on a limb (Bartussek and Lehmann, 2016; Mamiya et al., 2018).

Another mechanosensory feedback is provided by the so-called halteres, which indicate body rotations during flight (Bender and Dickinson, 2006; Bartussek and Lehmann, 2016). Halteres are evolutionary adapted hind-wings that function similarly to gyroscopes (Pringle and Gray, 1948). They beat in anti-phase with respect to the wings and respond linearly with the angular velocity (Dickinson, 1999). It has been recently shown that signals from halteres are also being used during walking behavior (Hall et al., 2015).

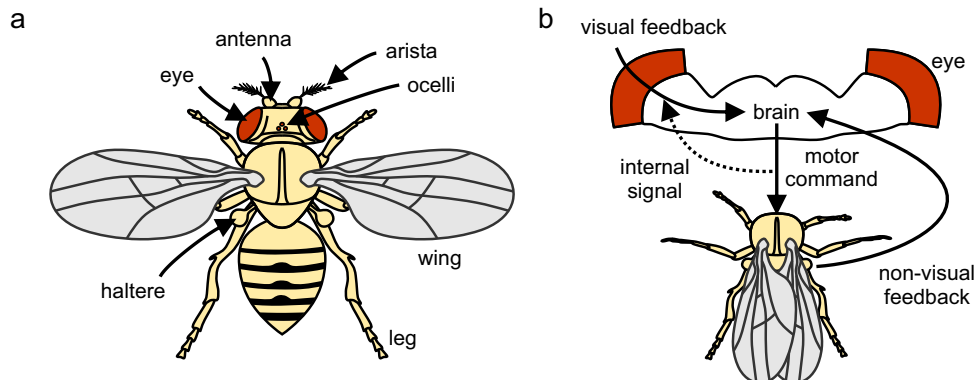


Figure 1: Illustration of *Drosophila melanogaster* and its feedback signals during self-motion. **a** Illustration of *Drosophila melanogaster*. **b** Visual and non-visual feedback signals during self-motion. Motor commands are sent to the legs and/or wings, generating motion in an environment. This creates visual and non-visual feedback that can be used for course control. Non-visual feedback can be provided, for example, by proprioceptive signals from the wings/legs or signals from the halteres. Moreover, internal signals are sent to silence self-motion evoked sensory feedback.

Besides non-visual feedback signals, visual feedback and internal signals also provide important information about self-motion. These will be introduced in more detail below.

1.1.2 The Necessity of Computing Visual Feedback

While visual systems capture many aspects of the environment, a simple point-by-point description does not yield meaningful information by itself.

Additional computations are required to extract important features. The complexity of this computation is such that we as humans recognize an object, for example a chair, regardless of its pose, color, or texture; but researchers have only achieved good object recognition based on camera images in recent years.

Biological visual systems are specialized sensory systems that capture and interpret light, enabling an animal to perceive the world. They emerged by evolution and are generally considered to be adapted to the niche in which an animal lives (Vallerga, 1994). Therefore, they are optimized for specific visual processing tasks in the animal's natural environment (Webster, 2015). Furthermore, they often have integrated and learned *a priori* information about expected visual inputs, such as formulated in the theory of *unconscious inference* (Von Helmholtz, 1867). Thus, biological visual systems can be matched to the statistical properties of the environment.

The computation of visual information to provide meaningful feedback during locomotion can be very demanding. However, it is possible to exploit the spatial arrangement of a population of receptors to match certain aspects of a computational problem (Wehner, 1987). These so-called *matched filters* can simplify computations considerably. However, they greatly limit the amount of information accessible to subsequent neuronal structures. While originally proposed at the receptor level, the concept of matched filters can also be applied to processing stages within the brain.

1.1.3 Optic Flow

Sighted animals constantly perceive coherent retinal image shifts during locomotion, which are considered to be a rich source of information about self-motion (Gibson, 1950; Krapp and Hengstenberg, 1996). These image shifts are known as optic flow.

Optic flow, containing translational and rotation information, describes the change of structured patterns of light caused by the relative motion between an animal (as observer) and its environment (Gibson, 1950). Its overall structure is decisively shaped by two factors (Lappe et al., 1999): the pattern of motion and the structure of the environment. While optic flow fields of pure rotations or translations within a stationary environment are rather simple, optic flow patterns of natural behavior are composed out of the linear sum of the underlying translational and rotational flow fields (Koenderink and van Doorn, 1987). Thus, their overall structure is more complex.

Optic flow can be visualized by vector fields with distributed vectors of a specific length and orientation (see figure 2). The length of a vector describes the velocity of the image shift at the depicted point and the orientation represents the direction.

1.1.4 Self-Motion Information from Rotational and Translational Optic Flow

As previously described, optic flow has a translational and a rotational element. Translational flow fields depend on the distance between an observer

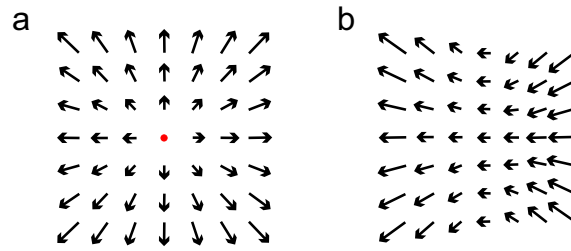


Figure 2: Exemplary illustration of optic flow as vector fields. **a** Optic flow generated by forward motion. The red point indicates the focus of expansion. **b** Optic flow generated by rotation to the right. Modified from [Sunkara et al., 2015](#).

and the objects within its environment, the angular position of the objects with respect to the direction of the motion, and the speed of the motion ([Egelhaaf et al., 2012](#)). Additionally, translational flow fields contain a focus of expansion and a focus of contraction. These focus points are opposite with respect to each other and indicate the direction of self-motion (see figure 2). Furthermore, the strength of translational flow provides relative information about the movement speed.

Since translational flow fields are dependent on the environmental structure, animals can use optic flow generated by active behavior to extract spatial information ([Egelhaaf et al., 2012](#)). This information can be useful during locomotion where environmental objects within the trajectory have to be bypassed.

Rotational flow fields do not depend on the distance between an observer and the objects within its environment. Therefore, they do not contain spatial information. However, rotational flow fields evoked by self-rotation contain information about the direction, mode (roll, pitch, yaw), and velocity of rotation.

Overall, rotational flow fields are well suited to provide feedback on self-rotation, while translational flow fields are well suited to provide feedback on self-motion in x , y , z (see figure 3).

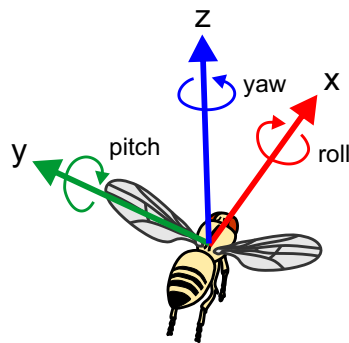


Figure 3: Schematic overview of rotations (roll, pitch, yaw) and translations (x , y , z).

1.1.5 Visual Feedback from Voluntary and Involuntary Movements

The distinction between visual sensory feedback derived from voluntary self-motion and involuntary displacements is frequently non-trivial. The *reafference principle*, describing the relationship between self-motion and sensory feedback using internal signaling, assumes that the brain has access to neural signals controlling actuators, i.e. signals that are used to execute self-motion (von Holst and Mittelstaedt, 1950). Thus, copies of these signals, referred to as efference copies, are used to inform corresponding sensory systems about the execution of self-motion. For instance, the brain could send efference copies to inform the visual system about the execution of self-motion. These signals can be used to subtract the expected visual feedback caused by the self-motion from the overall visual feedback, resulting in the perception of solely involuntary motion components.

1.2 REQUIREMENTS FOR OPTIC FLOW DETECTION

For animals to use optic flow as feedback signal for course control, they must be able to extract it from visual inputs. To this end, and given the fact that the photoreceptors only capture local luminescence values, the visual systems must first compute local motion information before computing global optic flow fields.

The computation of local motion from non-motion directive inputs has been investigated in many species (Barlow and Hill, 1963; Briggman et al., 2011; Albright, 1984). As a result, several models have been developed, including the *Hassenstein-Reichardt* detector (Hassenstein and Reichardt, 1956), the *Barlow-Levick* detector (Barlow and Levick, 1965), the *gradient detector* (Fennema and Thompson, 1979), and the *energy model* (Adelson and Bergen, 1985) (for further models see Thorson, 1966; van Santen and Sperling, 1985). Amongst those, the class of correlation-based detectors, which extract motion by temporal filtering and correlation of luminance values of neighboring points in space, is of particular importance for motion perception in flies and other invertebrates. Correlation detectors have successfully been used to describe behavioral responses (Hassenstein and Reichardt, 1956; Götz, 1964) as well as neural activity within motion-vision pathways (Joesch et al., 2008; Borst et al., 2010).

1.2.1 General Requirements for Local Motion Detection

There is strong evidence that many animals, including *Drosophila*, extract motion information from low-level luminance signals (Adelson and Bergen, 1985). As a consequence, there are three general requirements that elementary direction-selective motion detectors have to fulfill (Borst and Egelhaaf, 1989):

- **Two input channels:** Information from a single spatial position is not sufficient to compute the axis of motion. At least two spatially separated input signals are required.

- **Asymmetric temporal processing:** Required to extract the direction of motion. Without such an asymmetry, motion along both directions of the axis of motion would result in the same output response.
- **Non-linear interaction:** Direction selectivity requires non-linear interaction between the input channels. Otherwise, the time-averaged output would be indistinguishable from the time-averaged input signals.

In the following, motion detectors that fulfill these general requirements are presented.

1.2.2 Local Motion Detectors

Hassenstein and Reichardt Detector

The *Hassenstein and Reichardt* (HR) detector, further referred to as *Hassenstein and Reichardt correlator* (HRC) or simply *Reichardt detector*, has been described based on research on the optomotor response of the beetle *Chlorophanus* in the 1950s ([Hassenstein, 1951](#); [Hassenstein and Reichardt, 1956](#)). The HR detector comprises two mirror-symmetric half-detectors. Each half-detector consists of two spatially separated input channels (receptors), which sample the luminance of the environment at neighboring points. The signal of one of these input channels is delayed by linear low-pass filtering before both signals are subsequently multiplied with each other. Therefore, a visual stimulus for motion in the preferred direction (PD) first stimulates the input channel with subsequent filter, which introduces an increased transmission time towards the multiplication stage. Depending on the filter properties, the delayed signal arrives at the multiplication stage simultaneously with the signal from the second input, leading to a strong response. In contrast, a visual stimulus in the opposite or null direction (ND) will have an additional delay in the input channel stimulated last. Consequently, the input signals arrive with little temporal overlap at the multiplication stage, which results in a very weak output signal. Direction selectivity in the HR detector is therefore computed by non-linear amplification of signals in preferred direction, also referred to as *preferred direction enhancement*.

Finally, a full HR detector is constructed by subtracting the output of two half-detectors (see figure 4). This results in a direction-opponent signal: motion in the preferred direction (PD) leads to positive signals, while motion in the null direction (ND) leads to negative signals.

Barlow-Levick Detector

The *Barlow-Levick* (BL) detector represents an alternative model to the Reichardt detector, mainly differing in the non-linear interaction stage. While the overall structure between both models is similar, the Barlow-Levick detector is based on the suppression of motion stimuli in the null direction. It was originally proposed by Barlow and Lewick to account for direction-selectivity of retinal ganglion cells in the rabbit retina ([Barlow and Levick, 1965](#)). Similarly to the Reichardt detector, it consists of two spatially separated input channels, a temporal delay, and a non-linear interaction stage.

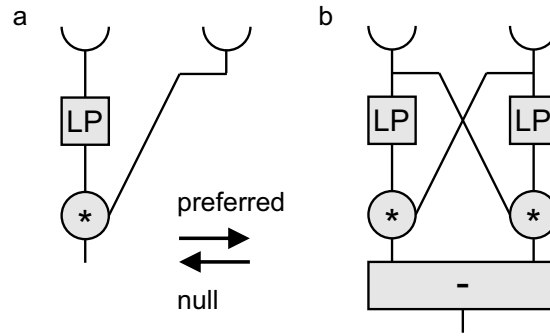


Figure 4: Architecture of the *Hassenstein and Reichardt* (HR) detector. **a** HR half-detector illustrated with low-pass (LP) filter and multiplication stage. **b** Full HR detector composed out of two mirror symmetric half-detectors as illustrated in *a* with additional subtraction stage.

In that case, however, the second input channel in the preferred direction is delayed, which results in a temporal overlap between the two input signals for null direction stimulation. The following suppressive non-linear stage will therefore actively suppress visual signals in null direction. However, signals evoked by visual stimuli in preferred direction arrive with little temporal overlap, i.e. the excitatory input is not suppressed. In contrast to the Reichardt detector, the direction selectivity in the Barlow-Levick model is computed by non-linear suppression of signals in null direction, also referred to as *null direction suppression*.

Hybrid Detector

While the HR and the BL detector have long been seen as rival models, more recent findings have shown that direction-selective T₄/T₅ cells in *Drosophila* implement both in different parts of their dendrites (Haag et al., 2016, 2017). However, the exact biophysical basis and the contribution of individual neurons is currently under investigation.

The simultaneous implementation of the HR and BL detector can be described using a model with three input channels. HR and BL share the central input channel, which does not have a temporal delay. Additionally, the subsequent non-linear interaction stage includes the enhancing and suppressing non-linearity (see figure 5). While the HR and BL detectors alone produce a weak direction selective signal, their combination has a strong direction selectivity.

Further Motion Detector Models

There are other types of motion detectors besides the correlation-type. Two of them, the *gradient detector* and the *motion energy model*, are briefly introduced below.

The gradient detector was developed within the field of computer vision (Limb and Murphy, 1975; Fennema and Thompson, 1979). It computes motion information based on changes of brightness. Essential for the gradient detector is the approximation of the spatial gradient $\partial I / \partial x$ by the bright-

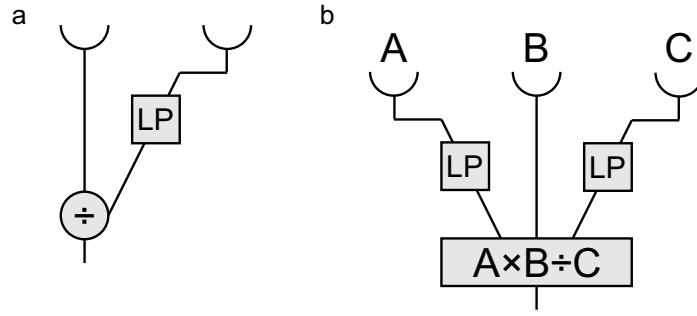


Figure 5: Three-arm hybrid detector. **a** BL half-detector with low-pass (LP) filter and division as non-linear stage. **b** Three-arm hybrid detector, consisting of the combination of a HR half-detector with a BL half-detector.

ness difference ∂I of a visual pattern I , which is sampled at two neighboring points in space separated by the distance ∂x . The division of the temporal gradient $\partial I / \partial t$ by the spatial gradient $\partial I / \partial x$ results in the stimulus velocity v . v is independent of the structure of the pattern, such as its wavelength and contrast. Overall, the gradient detector is an appealing model for motion vision and has successfully been used to study biological systems (Hildreth and Koch, 1987; Borst, 2007). Its implementation in biological systems, however, is rather unlikely, since it requires the computation of local derivatives. Furthermore, gradient detectors are outperformed by correlation-based detectors in noisy signal conditions (Potters and Bialek, 1994; Borst, 2007).

$$\frac{\partial I}{\partial t} = v \cdot \frac{\partial I}{\partial x} \quad (1)$$

$$v = \frac{\partial I}{\partial t} \div \frac{\partial I}{\partial x} = \frac{\partial x}{\partial t} \quad (2)$$

The *motion energy model* (van Santen and Sperling, 1984; Adelson and Bergen, 1985) arose from research on vertebrate vision as well as human psycho-physics. Its underlying approach to generate direction selective signals is the convolution between the space-time representations of the stimulus with a spatio-temporally tilted linear filter. Subsequently, a non-linearity is applied, such as computing the square or a threshold. Even though the motion energy model has a different internal structure in comparison to the Reichardt detector, both models produce equivalent output signals (van Santen and Sperling, 1985).

1.2.3 Wide-Field Integration of Local Motion Signals

Local motion information by itself is not enough to distinguish between different optic flow patterns evoked by self-motion. This problem can nevertheless be resolved by the spatial integration of the output of local motion detectors that resemble the corresponding optical flow pattern (Krapp and Hengstenberg, 1996; Krapp et al., 1998). The realization of this approach within a visual system would place three demands on a hypothetical inte-

grating neuron (Krapp and Hengstenberg, 1996). If fulfilled, such a neuron would respond most strongly for one mode of self-motion.

- The receptive field would have to be large enough to ensure specificity.
- The response would have to be motion-sensitive and direction-selective.
- Local preferred directions within the receptive field would have to resemble the optic flow field evoked by the corresponding self-motion.

It is striking that neurons with these properties, such as *lobula plate tangential cells* (see section 1.3.4), exist in the visual system of flies. Moreover, the integrating nature of the spatially arranged local motion detector signals reflects the concept of matched filters. These neurons seem to be perfectly matched to detect specific optic flow fields of self-motion.

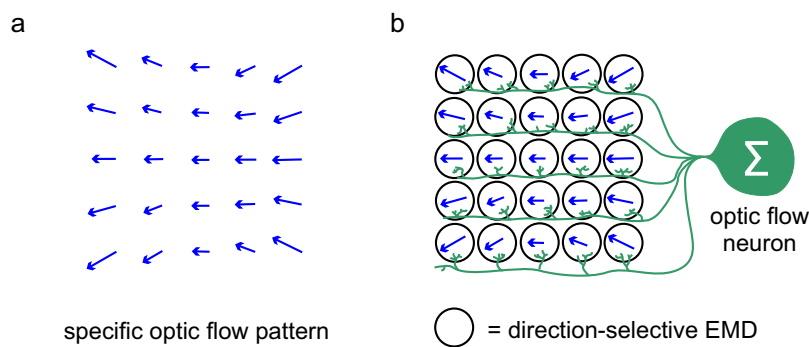


Figure 6: Illustration of the architecture of an optic flow selective neuron. **a** Specific optic flow pattern. **b** Architecture of an optic flow selective neuron, which sums the input of spatially distributed elementary motion detectors (EMD) with corresponding preferred directions. Figure adapted from Krapp et al., 1998.

1.3 VISUAL PROCESSING IN DROSOPHILA

Flies have proven to be a rewarding model organisms for visual information processing. Their visual system has been extensively studied through the application of neurogenetic methods, anatomical studies, physiological experiments, and behavior. Therefore, their visual system is well described.

1.3.1 The Compound Eye

Drosophila melanogaster has two compound eyes, consisting of around 750 ommatidia each (Ready et al., 1976; Hardie, 1985). The ommatidia of each eye are arranged in a regular spaced lattice with an inter-ommatidia angle of around 5° (Götz, 1965; Land, 1997). Thus, *Drosophila melanogaster* has a rather low visual resolution (Land, 1997). However, it can sample almost the entire visual panorama, excluding just a small blind band of about 40° width directly behind the head (Buchner, 1971; Heisenberg and Wolf, 1984;

Hardie, 1985). The binocular overlap of *Drosophila* is less extensive than in other species, consisting of only two to three ommatidial rows in the frontal visual field (Hardie, 1985).

Neural Superposition

As the spatial distribution of the photoreceptors R1-R6 inside one ommatidium results in slightly different optical axes, they sample different locations in space. Pooling of these signals would therefore reduce visual acuity. Intriguingly, however, axons of photoreceptors of the same ommatidium are connected to different lamina cartridges. Photoreceptors of neighboring ommatidia, which share the same optical axis, converge on the same cartridge. This principle, which is termed *neural superposition*, provides higher sensitivity without sacrificing spatial acuity (Kirschfeld, 1967).

Optic Lobes

Drosophila devotes a significant amount of neural substrate to process visual information, i.e. 120.000 out of the 250.000 neurons that the brain has are located in the optic lobes (Morante and Desplan, 2004; Chiang et al., 2011; Néric and Desplan, 2016; Heisenberg and Wolf, 1984). Each optic lobe can be subdivided into four distinct neuropils: lamina, medulla, lobula and lobula plate. Incoming visual stimuli are detected by the retina, but most visual processing happens within the optic lobes underneath the ommatidia. After visual information has been processed, signals are conveyed via the central brain to motor circuits in the thorax.

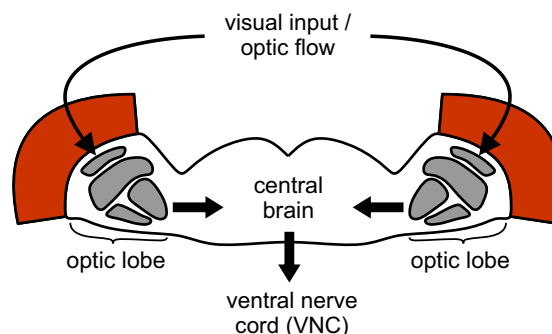


Figure 7: Schematic overview of the visual information flow. Arrows indicate the flow of visual information, neglecting feedback connections. Visual information first reaches the retina and is then processed in the optic lobes. Next, it is transmitted to the central brain and finally sent to the ventral nerve cord (VNC).

1.3.2 Retina

Photoreceptors

Each ommatidium can be seen as an optical system, including a small lens, photoreceptors, and pigment cells. The incoming light is focused by the lens

onto eight photoreceptors that can be subdivided into two types: the outer six (R1-R6) and the inner two photoreceptors (R7 and R8). Photoreceptors R1-R6 contain the Rhodopsin1 (Rh1), a broadband photopigment with two spectral sensitivity peaks. They provide achromatic visual information and are involved in motion vision and orientation responses (Heisenberg and Buchner, 1977; Rister et al., 2007). The inner two photoreceptors R7 and R8 are stacked on top of each other in the center of each ommatidium (R7 on top of R8). Based on the inner photoreceptors, three ommatidial subtypes can be distinguished (Wernet and Desplan, 2004).

First, there are two stochastically distributed subtypes: pale (p) and yellow (y), with a proportion of approximately 3 : 7, respectively (Chou et al., 1996; Wardill et al., 2012; Wernet and Desplan, 2004). p-type ommatidia express rhodopsin Rh3 in R7 and Rh5 in R8. y-type ommatidia contain rhodopsin Rh4 in R7 and Rh6 in R8. It was initially thought that these two subtypes are mainly used for color discrimination without contributing to the motion detection system (Heisenberg and Buchner, 1977; Melnattur et al., 2014; Yamaguchi et al., 2008). However, recent studies have shown that *Drosophila melanogaster* incorporates signals from color vision pathways to improve motion discrimination (Wardill et al., 2012). Conversely, signals from outer photoreceptors contribute to color vision (Schnaitmann et al., 2013). Further information about color vision can be found in (Schnaitmann et al., 2013; Gao et al., 2008; Karuppudurai et al., 2014).

A third subtype with enlarged rhabdomeres is located at the dorsal rim area, expressing rhodopsin Rh3 in both R7 and R8 (Fortini and Rubin, 1990; Feiler et al., 1992; Wernet et al., 2003, 2012). Information provided by this subtype allows *Drosophila* the detection of the e-vector from polarized skylight (Wernet et al., 2012; Behnia and Desplan, 2015). Interestingly, it has been shown that photoreceptors of the third subtype are used to maintain a stable heading during flight (Weir and Dickinson, 2012).

Phototransduction

Phototransduction describes the process of converting visual information transmitted by photons into electrical signals. Similar to most invertebrates, phototransduction in *Drosophila melanogaster* is based on a G-protein-coupled signaling cascade (Hardie and Juusola, 2015; Hardie, 2011; Hardie and Raghu, 2001; Hardie, 2001). It takes place in the light-guiding rhabdomeres, which contain approximately 30.000 microvilli (Hardie and Raghu, 2001). Each microvillus contains all components of the signaling cascade, including around thousand membrane-bound visual pigments called rhodopsins. These G-protein-coupled-receptors are covalently bound to the chromophore 11-*cis* 3-hydroxy-retinal (Vogt and Kirschfeld, 1984; Hardie, 2001). Upon photon absorption, the chromophore is converted into all-*trans* retinal. This conversion triggers a conformational change from rhodopsin into the active meta-rhodopsin state, which functions as a catalyst for heterotrimeric G-protein activation. Consequently, phospholipase C (PLC) is activated, which leads to the activation of cation-permeable channels via various potential mechanisms and causes photoreceptors to depolarize (Hardie, 2001).

Reisomerization, i.e. the transformation from the active metarhodopsin state (all-*trans* retinal) to rhodopsin (11-*cis* 3-hydroxy-retinal), is induced by light with longer wavelengths (Hardie, 2011). These wavelengths are not blocked by the screening pigments of the compound eye, as they are transparent in the red spectrum (Stavenga, 1995; Hardie, 2011). Thus, red light enters and scatters inside the eye, resulting in an efficient and fast reset of the phototransduction cascade.

Overall, *Drosophila*'s visual system has a significant faster signaling cascade than mammalian visual systems (between 10 – 100 times faster). As a result, it has a flicker fusion frequency of around 200Hz (Heisenberg and Wolf, 1984; Cosens and LeBlanc, 1980). Additionally, it is important to note that mutations within the signaling cascade can lead to significant visual deficits and blindness (Hardie, 2011).

1.3.3 Lamina, Medulla and Lobula

Lamina

Axons of the photoreceptors R1-R6 terminate in the lamina, the first neuropil of the optic lobe. The lamina is composed of retinotopically arranged cartridges, also referred to as columns. Each cartridge corresponds to a single point in visual space and contains 12 cell types (Fischbach and Dittrich, 1989): eight columnar neurons and four multi-columnar neurons. The columnar neurons are lamina monopolar cells (L1-L5), two centrifugal neurons (C2, C3), and T1 neurons; and the multi-columnar neurons are the lamina intrinsic neuron (Lai), the lamina tangential neuron (Lat), and lamina wide-field neurons (Lawf1 and Lawf2). All of these cells receive either direct or indirect inputs from the photoreceptors R1-R6 (Meinertzhagen and O'Neil, 1991; Borst, 2014).

The primary input cells for motion vision are the lamina output neurons L1 and L2 (Zhu, 2013). The simultaneous blocking of both cell types renders *Drosophila* motion-blind, abolishes the optomotor response (Rister et al., 2007; Tuthill et al., 2013) (see section 1.4.1), and eliminates direction-selective responses in lobula plate tangential cells (LPTC) (Joesch et al., 2010). The block of either L1 or L2 abolishes LPTC responses to one polarity of edge-motion. Blocking L1 results in responses solely to moving dark-edges (OFF), while blocking L2 results in responses solely to moving bright-edges (ON) (Joesch et al., 2010; Zhu, 2013; Borst, 2014). These findings show the early split of motion processing into two independent pathways: ON and OFF. Furthermore, additional blocking experiments showed that most lamina cells have subtle effects on visual guided behavior (Tuthill et al., 2013).

Medulla

The second neuropil within the optic lobe is the medulla, which receives input projections from lamina cells. Similar to the lamina, the medulla consists of columns in register with the hexagonal grid of the compound eye. Accordingly, the mapping between lamina and medulla remains retinotopic.

However, the fibers connecting lamina and medulla form a chiasm, i.e. posterior medulla cartridges receive input from anterior lamina cartridges.

The medulla has ten synaptic layers (M1 to M10) and contains over 60 different cell types (Fischbach and Dittrich, 1989; Takemura et al., 2008; Zhu, 2013). Based on projections, these cell types can be divided in four distinct groups (Borst, 2014). First, medulla intrinsic (Mi) neurons with dendrites in distal layers and axons in the proximal medulla. Second, trans-medulla (Tm) neurons, which connect specific layers from the medulla with the lobula. Third, y-shaped trans-medulla (TmY) neurons, connecting specific layers from the medulla with the lobula and the lobula plate. Finally, columnar bushy T cells (T2-T4), which connect to different layers of the lobula.

There are many neural connections and various cell types within the medulla, which makes it challenging to gain a complete functional understanding. Nonetheless, there has been significant progress over the past years, such as electron microscopy studies that have shown two clusters of connected neurons inside the medulla, which correspond to ON and OFF motion pathways (Takemura et al., 2013; Shinomiya et al., 2014). Furthermore, several cell types within the medulla have been characterized by whole-cell patch clamp recordings (Behnia et al., 2014), calcium imaging (Meier et al., 2014; Serbe et al., 2016), and voltage imaging (Yang et al., 2016).

Lobula

The lobula can be divided into at least six layers (Fischbach and Dittrich, 1989). The most prominent cell type within the lobula are lobula columnar (LC) neurons, which receive their major inputs from the medulla. There are multiple types of LC neurons with similar morphology that span the complete visual field in a retinotopic fashion (Otsuna and Ito, 2006). Overall, these neurons can be subdivided into more than twenty distinct subtypes, which convey information about different visual features (Wu et al., 2016).

1.3.4 Optic Flow Detectors in the Lobula Plate

The lobula plate can be divided into four layers, each containing lobula plate tangential cells (LPTCs). Due to the relatively large size of LPTCs and the methods available in the past, LPTCs are well described in terms of their physiological and anatomical characteristics (Borst and Haag, 2002; Borst et al., 2010).

Lobula Plate Tangential Cells

LPTCs within layer 1 of the lobula plate can be subdivided into horizontal system (HS) cells and centrifugal horizontal (CH) cells (Boergens et al., 2018). *Drosophila* has three HS cells with significant dendritic overlap per hemisphere (see figure 8). These cells are named based on their anatomical location: northern HS cell (HSN, dorsal), equatorial HS cell (HSE, middle), and southern HS cell (HSS, ventral). In general, all three HS cells depolarize for motion in their preferred direction (front-to-back) and hyperpolarize for motion in the opposite direction (their null-direction, back-to-front) (Schnell

et al., 2010). In contrast to HS cells, CH cells are only described regarding their anatomy in *Drosophila*, but not according to their functionality. However, they match known cells from blow flies (Eckert and Dvorak, 1983).

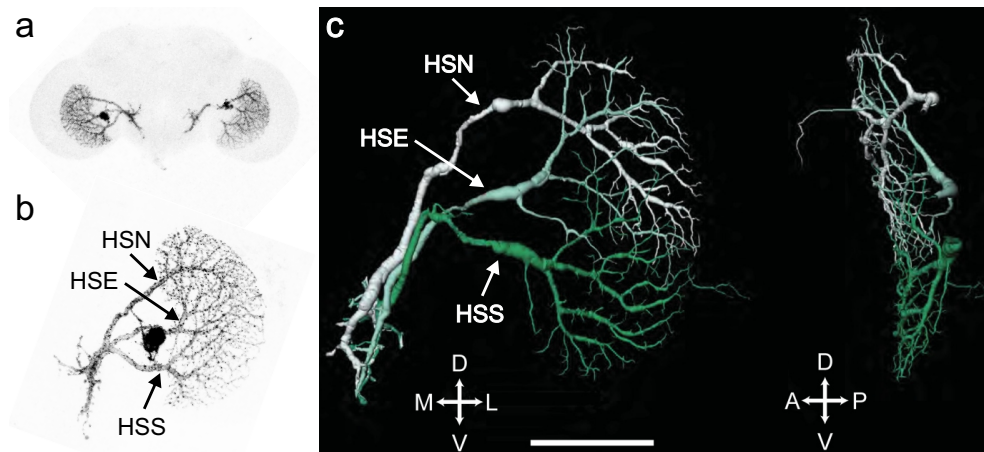


Figure 8: Horizontal system (HS) cells. **a** Visualization of HS cells in the brain of *Drosophila*. **b** Enlarged view of the three HS cells: HSN, HSE and HSS. **c** Reconstructions of the three HS cells. Scale bar 50 μ m (from Boergens et al., 2018).

Lobula plate tangential cells within layer 2 are less well described in comparison to layer 1. Nevertheless, three neurons with large arborizations have been discovered in layer 2 (Levy and Larsen, 2013). Two of these cells project their axons to the ipsilateral and contralateral hemisphere of the brain. The third cell has a rather short neurite to the ipsilateral *posterior lateral protocerebrum* (PLPR) (Levy and Larsen, 2013). While studies on these cells are limited, it has been shown that the so-called Hx cell depolarizes for back-to-front motion and hyperpolarizes for front-to-back motion (Wasserman et al., 2015; Cruz et al., 2019). Additionally, knowledge about layer 2 cells is often transferred from studies in *Callipora*, as they present anatomical similarities (Levy and Larsen, 2013; Egelhaaf, 1985; Gauck and Borst, 1999; Wasserman et al., 2015; Krapp et al., 1998).

The description of tangential cells within layer 3 of *Drosophila* is virtually nonexistent, but LPTCs within layer 4 have been described with greater detail. Layer 4 LPTCs are part of the vertical system (VS), thus referred to as VS cells. They can be separated into two subtypes: six VS tangential cells (VS1-VS6) and three VS like cells (VSlike1-VSlike3) (Boergens et al., 2018). Both cell types have narrow band-like dendrites that span the lobula plate from the dorsal to the ventral end. VS cells depolarize for downward motion (preferred-direction) and hyperpolarize for upward motion (null-direction) (Joesch et al., 2008). Most of VS cells' dendrites are located in layer 4, however, some branches extend partially to other layers (Hopp et al., 2014; Boergens et al., 2018).

Excitatory Visual Input

Lobula plate tangential cells receive direct excitatory cholinergic input from T4 and T5 cells (Mauss et al., 2014). While T4 cells project from the medulla into the lobula plate, T5 cells project from the lobula to the lobula plate.

Thus, information from the ON- and OFF-pathway converge at the level of the lobula plate. T₄ and T₅ cells can be subdivided into four subtypes each: T_{4a}, T_{4b}, T_{4c}, T_{4d} and T_{5a}, T_{5b}, T_{5c}, T_{5d} (see figure 9). These subtypes respond to motion in one of the four cardinal directions and projects to a specific layer within the lobula plate (Maisak et al., 2013). T_{4a} and T_{5a} respond to front-to-back motion and send their axons to layer 1. T_{4b} and T_{5b} respond to back-to-front motion and project to layer 2, and T_{4c} and T_{5c} respond to upward motion, projecting to layer 3. Finally, T_{4d} and T_{5d} respond to downward motion, projecting to layer 4. Based on these projections, two important observations for potential synaptic connections between T₄/T₅ cells and LPTCs can be made. First, LPTCs located in different layers have access to different T₄/T₅ subtypes. Second, local motion signals provided by the corresponding T₄ and T₅ projections exhibit retinotopic organization. Together with the extensive dendritic arborizations of LPTCs, which capture large parts of the visual field, tangential cells are able to integrate local motion information across large areas of the visual field. Therefore, LPTCs are well suited to compute and respond to specific optic flow patterns.

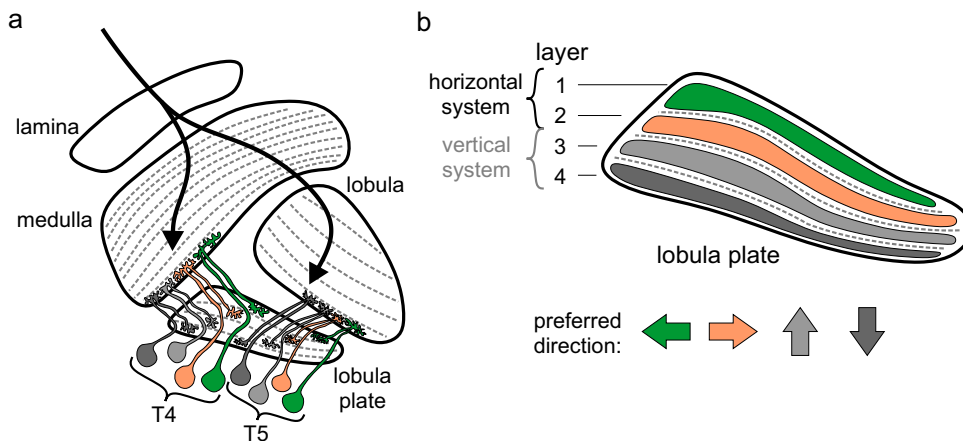


Figure 9: Layered structure of the lobula plate. **a** Illustration of the lobula plate within the optic lobe. Signals from the ON- and OFF-pathway are transmitted via the four subtypes of T₄ and T₅ cells into the lobula plate. **b** Illustration of the layered structure of the lobula plate, including the separation into vertical and horizontal system. T₄ and T₅ cells have subtype specific projections into specific layers (see color code).

Lobula Plate Interneurons

LPTCs within layer 4 receive indirect inhibitory input from the adjacent layer via glutamatergic *lobula plate interneurons* (LPi) (Mauss et al., 2015). Silencing these bi-stratified cells resulted in the loss of null-direction hyperpolarization responses of postsynaptic LPTCs. Furthermore, additional blocking experiments have shown that these inhibitory signals are important to shape the optic flow field selectivity of LPTCs, ensuring well defined responses to specific motion cues (Mauss et al., 2015). While there is no direct evidence for lobula plate interneurons between lobula plates 1 and 2, their existence is strongly anticipated as HS cells in layer 1 have similar response properties to VS cells, besides directional tuning.

State Dependent Modulation

In the past, visual processing by neural circuits has mainly been considered as a static feed-forward computation. This view is currently discarded for many organisms due to evidence supporting substantially altered visual processing with respect to different behavioral states (Longden and Krapp, 2009; Chiappe et al., 2010; Niell and Stryker, 2010). Especially when considering that visual inputs can be highly variable, adaption and state dependent modulation of neural circuits can be beneficial. For example, the speed of visual motion can vary across orders of magnitude depending on the behavior and environmental structure.

State dependent modulations in LPTCs can be observed between resting state and active behavior, such as walking and flying. Hereby, the frequency optimum of LPTCs differs by almost one order of magnitude (Joesch et al., 2008). Furthermore, it has been shown that VS cells show enhanced preferred direction responses during tethered flight in comparison to non-flight (Maimon et al., 2010; Suver et al., 2012). Genetic activation and silencing experiments of octopaminergic projection neurons effected the state dependent modulation, suggesting a critical function of octopamine (Suver et al., 2012). In addition, similar modulation effects have been reported further upstream, at the level of T4 and T5 cells (Arenz et al., 2017; Strother et al., 2018).

Besides state dependent modulation during flight, modulations related to tethered walking versus non-walking have also been reported (Chiappe et al., 2010). The usage of calcium imaging facilitated the measuring of an increased gain in response strength, which was most prominent at higher frequencies (Chiappe et al., 2010). Moreover, a shift of the temporal frequency optimum towards higher motion speeds in HS cells was observed. Finally, also non-visual signals are present in HS cells during walking, which have been correlated to angular velocity, forward velocity, and a behavioral state component (Fujiwara et al., 2016).

Efference Copy and Feedback Signals

Drosophila melanogaster is able to perform extremely fast body turns, referred to as saccades. During a saccade, flies turn approximately 90° in the order of thousands of degrees per second (~ 2000°/s). This results in an extremely fast sweep of the visual scene over the retina. Investigations in visual processing during saccades showed that LPTCs receive motor-related inputs perfectly timed with the execution of saccades (Kim et al., 2015). In alignment with the reafference principle, these signals seemed to completely suppress the perception of visual motion during the turn. However, a subsequent study showed that the suppressive effect is well matched to the saccade itself (Kim et al., 2017). This indicates that only visual responses caused by the voluntary self-motion are suppressed, while other response aspects are preserved. Thus, the visual system cancels out expected visual inputs, but does not go completely blind.

Non-visual feedback signals similar to efference copies have also been discovered during tethered walking experiments (Fujiwara and Chiappe, 2017). However, the observed feedback has the same sign as visual reafference signals and therefore does not cancel out self-evoked visual responses. Instead,

it amplifies self-evoked visual HS cell responses. This amplification hampers the differentiation between self-motion and externally evoked responses based on the HS cell activity. Thus, if the amplified HS signals would be interpreted as externally evoked motion signals, a positive feedback loop would be created. The reason for using non-visual feedback signals to amplify visual reafference signals is still unclear.

1.4 PROBING THE MECHANISMS UNDERLYING VISUALLY GUIDED COURSE CONTROL

Drosophila exhibits a number of visually elicited behaviors, many of which are well suited for its investigation. Of particular relevance for this thesis is the so-called optomotor response.

1.4.1 Optomotor Response

When placing a fly in the center of a rotating textured cylinder, it rotates in the same direction as the cylinder. This behavior is called the *optomotor response* (Blondeau and Heisenberg, 1982). Clockwise rotation of the cylinder evokes clockwise turning of the fly, while counter-clockwise rotation evokes counter-clockwise turning. In addition to the full body rotation, the head also turns according to the stimulus (Hengstenberg, 1988).

The stimulus dependencies impacting the optomotor response are well described and summarized in the following (Borst et al., 2010). First, the rotation behavior is syndirectional with the rotation direction of the pattern. Second, an increase in the pattern contrast evokes stronger responses. Third, the optomotor response has a velocity optimum, which can be observed when flies are presented with sinusoidal gratings of increasing velocity (v), i.e. turning responses decrease after the optimum velocity of 3 – 10Hz has been reached (Götz and Wenking, 1973; Duistermars et al., 2007). Fourth, the strength of the response depends on the temporal frequency $f = v/\lambda$, which is defined by the pattern velocity v and the pattern wavelength λ . Thus, the optomotor response to a given stimulus velocity is pattern-dependent. Finally, spatial aliasing can be observed for pattern wavelengths λ that do not fulfill the nyquist criterium (Götz, 1964). If λ is smaller than twice the receptor distance, the pattern is under sampled, which can result in inverted responses.

Early studies exploited the optomotor response of the beetle *Chlorophanus viridis* to investigate course control mechanisms (Hassenstein, 1951; Hassenstein and Reichardt, 1956). By doing so, some of the mentioned stimulus dependencies were observed, which led to the formulation of the *Hassenstein and Reichardt correlator* (HRC) (see section 1.2.2).

In general, the optomotor response is considered to be a course stabilization mechanism coping with involuntary deviations from an intended course. It is a behavioral readout frequently used for the investigation of motion vision. Since the optomotor response depends on the perception of motion, manipulations of neurons within the motion vision pathway can

lead to altered behavioral responses, which provide information about the contribution of these neurons to the computation of motion. Finally, the optomotor response is not limited to freely moving flies, but can also be measured robustly in tethered preparations.

1.4.2 Tethered Walking Setup

One of the first open loop setups to investigate walking behavior of *Drosophila melanogaster* consisted of a tread compensator developed by [Götz and Wenking \(1973\)](#). A fly was attached to a small metal sledge that prevented it to fly away and placed on top of a controllable sphere with a large diameter. By tracking the displacement of the fly's walking behavior, it was possible to balance the fly on top of the sphere. While this setup allowed to perform experiments in semi-freely walking flies, it posed an engineering challenge to build.

An alternative approach to measure walking behavior was introduced in 1976. Instead of compensating the motion of walking flies, [Buchner, 1976](#) attached flies to a holder and placed them on top of an air-suspended freely rotating ball. On that setting, the movement of the fly correspondingly rotates the ball. By measuring the rotation of the ball, the walking behavior of the tethered fly can be reconstructed as if it would be walking freely. This type of experimental setup is still in use today ([Lott et al., 2007](#); [Seelig et al., 2010](#); [Bahl et al., 2013](#)).

Tethered walking experiments within this work have been performed using the previously described air-suspended ball approach. However, additional parts besides the ball tracking mechanism were added. Initially, a visual stimulation arena comprised out of three high frame-rate monitors was placed around the fly. In combination with a graphic engine, arbitrary visual stimuli could be presented to the fly. Furthermore, a precise temperature regulation system as well as several cameras have been added ([Bahl et al., 2013](#)). The most important addition, however, was the integration of two independent optogenetic stimulation devices. As the fly remains stationary on top of the ball, it is possible to target optogenetic light precisely onto localized areas of the head. The overall setup is depicted in [figure 10](#) and has been described with more detail in ([Mauss et al., 2017](#); [Busch et al., 2018](#)) (see [chapter 3](#)).

1.5 EVIDENCE FOR BEHAVIORAL ROLES OF OPTIC FLOW NEURONS

While there is plenty of evidence supporting the use of visual information by flies during active locomotion behavior ([Robie et al., 2010](#); [Collett and Land, 1975](#); [Collett, 1980](#); [Mronz and Lehmann, 2008](#)), the underlying mechanisms of course stabilization are not yet fully understood. The currently prevailing idea is that optic flow plays a central role in the overall steering behavior ([Hausen and Wehrhahn, 1990](#)). This idea strongly suggests the involvement

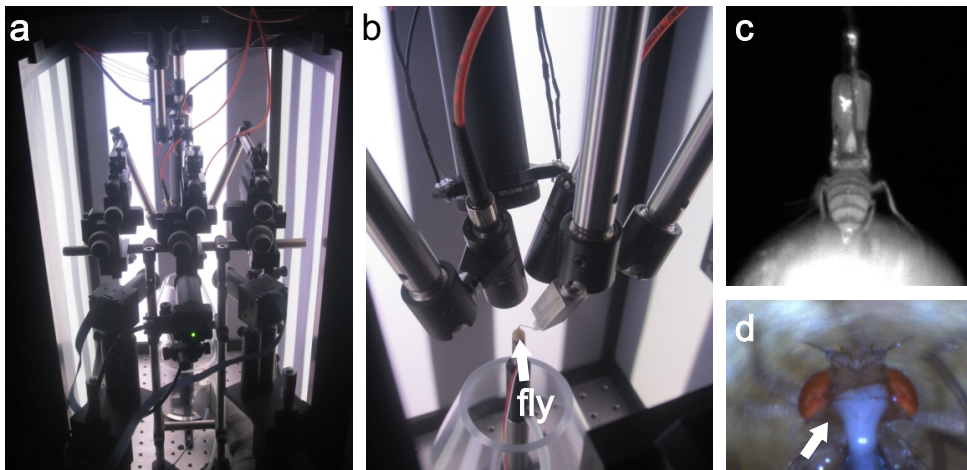


Figure 10: Tethered walking setup. **a** Overview of the used walking setup. **b** Central area of the setup. The position of the fly is annotated. **c** View of the back camera, which allows to position the fly on top of the ball. **d** View of the top camera, which allows to position optogenetic stimulation. The white arrow annotates the targeted area in order to stimulate HS cells.

of lobula plate tangential cells (LPTCs), which is further supported by several studies.

Anatomical studies have shown that horizontal and vertical system cells of flies are connected via descending neurons to motor centers controlling flight (Strausfeld, 1976, 1989; Suver et al., 2016). Furthermore, connections to neck motor neurons have been described (Gronenberg et al., 1995; Gronenberg and Strausfeld, 1990). Optic flow information is therefore transmitted to motor areas that influence or control behavior.

Moreover, flies with missing or defective LPTCs have impaired optomotor responses. The attenuated turning to global motion has been demonstrated in walking and flying experiments with mutant flies, such as the *omb*_{H31} mutant (Heisenberg et al., 1978).

Next, Geiger and Nässel, 1981 used laser beams to ablate tangential cell progenitors in the brain of housefly larvae. Unilateral ablations of large horizontal and vertical cells had no influence on visually guided orientation behavior towards single objects. However, responses to globally moving gratings on the ablated side were reduced, indicating the contribution of tangential cells to optomotor behavior. Similar findings have been obtained with microsurgical lesions on horizontal cells (Hausen and Wehrhahn, 1983). Unilateral lesions led to altered responses to bilateral full-field stimuli that corresponded to the response characteristics for the intact side. These findings indicate that horizontal cells of each optic lobe control horizontal rotation in a way that unilateral depolarization of HS cells leads to ipsilateral turning behavior.

Further evidence for the importance of LPTCs for steering behavior derives from electrical stimulations in the lobula plate in *C. erythrocephala* (Blondeau, 1981). These stimulations at three different locations evoked movements that were seamlessly integrated into the behavior of flies. Hereby, the location of the stimulation defined the behavior response. Electrical stimula-

tions in the frontal third of the ganglion evoked polarity dependent behavior: negative stimulations resulted in contralateral rotations, while positive stimulations resulted in ipsilateral rotations. However, the exact interpretation of these kind of experiments is rather complex, as it is generally not known which cells were stimulated.

Recent advances in genetic tools and methods made it possible to perform more precise experiments in which the manipulated neurons are known. For instance, by using a bistable channelrhodopsin-2 variant (ChR2-C128S), it was possible to activate and deactivate HS cells repeatedly. These experiments showed that optogenetic activation of HS cells induces robust yaw rotation for head and steering during tethered flight (Haikala et al., 2013). Similar to earlier studies, unilateral stimulation of HS cells evoked turning to the stimulated side. Overall, these findings provided strong evidence for the behavioral importance of HS cell activity for steering behavior and suggested that HS cell activity is sufficient to elicit optomotor behavior in *Drosophila*.

Furthermore, the existence of efference copies and feedback signals indicates that LPTCs are involved in course control. It has been discovered that self-motion induced visual responses of HS and VS cells are actively suppressed during rapid flight turns (Kim et al., 2015). Moreover, HS and VS4-6 cells receive precisely matched motor-related inputs, which cancel out expected rotational components (Kim et al., 2017). These findings suggest the neural implementation of the reafference principle, in which visual self-motion feedback is suppressed at the level of LPTCs. Thus, it can be assumed that LPTCs are part of a course stabilization mechanism.

Finally, it has been shown that HS cells are influenced by three additional non-visual signals (Fujiwara et al., 2016). First, HS cells are slightly depolarized shortly before the onset of different behaviors, such as grooming, walking or jumping. This depolarization is constant and stays active during the complete behavior, even outlasting it. Second, HS cells are modulated by turning as well as forward walking. Third, a complementary turning correlated signal is added to HS cell responses, which provides additional de- or hyperpolarization (Fujiwara et al., 2016). Taken together, these findings provide additional evidence that HS cell signals are used for walking behavior.

1.6 AIM OF THESIS AND OVERVIEW OF PUBLISHED WORK

While the encoding of optic flow is well described in insects, further studies are required to understand how and if associated neural activity is used during locomotion behavior. Based on the above-presented evidence, LPTCs are strongly suggested to play a key role in locomotion behavior.

Drosophila has two groups of optic flow sensing neurons that respond to horizontal motion. The first group are HS cells, which depolarize for front-to-back motion and hyperpolarize for motion in the opposite direction. The second group, LPTCs in layer 2 of the lobula plate, has mirror-symmetrical response characteristics, thus depolarizing for back-to-front motion and hyperpolarizing for front-to-back motion.

While it has been shown that unilateral artificial depolarizations of HS cells cause ipsilateral rotations, the possible contribution of unilateral hyperpolarizations to turning behavior has not yet been investigated. Furthermore, the importance of HS cell signals for walking speed is not fully understood. Together with my colleagues, I addressed these open questions by using optogenetics in tethered walking experiments in *Drosophila melanogaster*.

Drosophila is well suited to investigate the contribution of HS cells to locomotion behavior. Importantly, it offers a comprehensive genetic toolkit, a detailed description of the visual system, various investigation methods, and robust visually mediated behaviors. Hereof, the optomotor response represents a reliable readout to investigate responses to horizontal optic flow patterns. The optomotor response can be measured in tethered preparations, allowing visual stimulation to be controlled with high accuracy. Furthermore, tethered preparations facilitate the integration of optogenetics into experiments, as the required light can be locally focused on the cells of interest.

The findings of this work can be divided into two main parts, each resulting in one publication (see chapter 3). The first part focuses on the application of a novel optogenetic silencing tool in *Drosophila*. The motivation for performing this work was the current lack of potent optogenetic tools and the recent discovery of the anion channel GtACR₁ as a promising neural silencer. Specifically, I set out to test the usability and function of GtACR₁ within the visual system of *Drosophila*. The second part describes the role of HS cells for walking behavior by introducing acute artificial de- and hyperpolarization within HS cells.

2

METHODS AND TOOLS IN CIRCUITS NEUROSCIENCE

The rapid progress in the development of genetic tools and techniques has made *Drosophila melanogaster* an appealing model organism for circuits neuroscience. This chapter provides an overview of the currently existing tools and methods.

2.1 ACCESS TO NEURAL POPULATIONS

Genetic access to single neurons or defined neural populations provides powerful opportunities to gain understanding of neural circuits. Cell-specific genetic manipulations allow to link functional consequences to specific neurons. While earlier research on *Drosophila* was predominantly based on mutant analysis with rather poor cellular specificity and wide-spread undefined implications for the entire organism, many areas of nowadays' research are defined by neuron-centric techniques.

2.1.1 The Binary Expression System GAL4-UAS

A major step towards targeted circuit analysis in *Drosophila melanogaster* was the development of binary expression systems, such as the GAL4-UAS system. Binary expression systems provide the means to target the expression of arbitrary genes to specific neurons. In general, they consist out of two components, one defining *where* the expression occurs and the other *what* is expressed.

The GAL4-UAS system is based on the yeast transcription factor GAL4, which binds to the genomic *Upstream Activating Sequence* (UAS) and consequently leads to the expression of the gene downstream of UAS (Brand and Perrimon, 1993). It requires two transgenic lines, the driver (GAL4) and the effector (UAS) line. Driver lines express GAL4 under the control of an endogenous enhancer specific for certain cells, leading to the expression of GAL4 in some subset of *Drosophila*'s tissues. As *Drosophila* does not have endogenous UAS, GAL4 by itself has no effect. However, UAS is present in the effector line and its activation will mediate the transcription of the downstream gene, which normally is a reporter gene. Therefore, when driver and effector lines are combined, both UAS as well as GAL4 are present and consequently the reporting gene will be expressed uniquely in the cells that produce GAL4 (see figure 11).

An important parameter in the GAL4-UAS system is the location of insertion of the exogenous GAL4 and UAS elements. Different techniques allow to insert these elements either in a random or in a specific manner. Initially, transposable P-elements were used to insert the corresponding constructs into the fly's genome (Rubin and Spradling, 1982). Due to the lack of con-

control over the insertion location when using transposable P-elements to create transgenic lines, however, inserted elements could interfere and destroy important coding areas of the fly genome. This resulted in unwanted side effects or death. Furthermore, it made the process of generating transgenic lines inefficient, leading to variable expression levels and broad expression patterns. To address this issue, the so-called ϕ C31 integrase system was developed (Groth et al., 2004; Bischof et al., 2007). The ϕ C31 integrase system allows for site-specific insertion of transgenes in the fly genome, which resulted in more stable expression levels and increased specificity of driver lines. Transgene expression can further be boosted by chaining multiple UAS sequences (Pfeiffer et al., 2012).

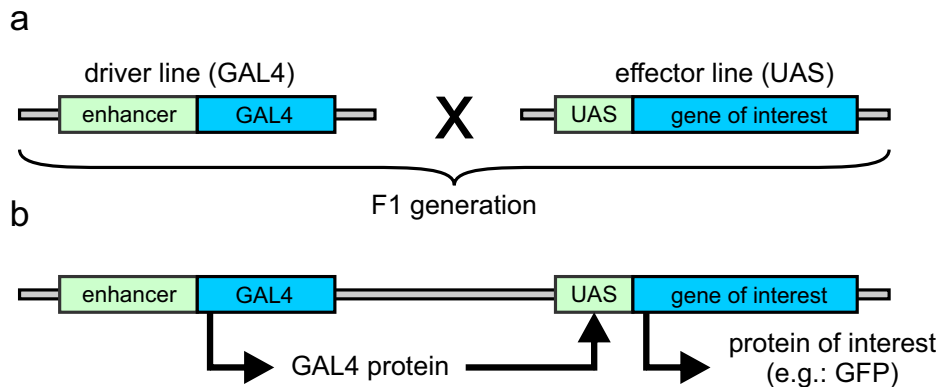


Figure 11: Illustration of the working principle of the GAL4-UAS system. **a** Driver and effector line of choice are crossed. **b** The offspring (F1 generation) of such a cross has both: GAL4 and UAS, allowing the expression of the gene of interest.

Finally, it has been observed that expression levels are slightly temperature dependent. Increased temperatures ($\sim 29^\circ\text{C}$) boost expression levels, while reduced temperatures ($\sim 16^\circ\text{C}$) decrease them (Duffy, 2002). This temperature dependency might be caused by heat shock elements present in the promoter (Mondal et al., 2007).

2.1.2 Split-GAL4 and GAL80

While the GAL4-UAS system has proven to be efficient in targeting neural populations, its expression patterns are often not specific enough. Phenotypes can therefore not be reliably assigned to specific cells.

Intersectional strategies allow to enhance the specificity of the GAL4-UAS system (Venken et al., 2011). A prominent combinatorial approach for *Drosophila* is called split-GAL4 system, pioneered by Luan et al., 2006 and further optimized by Pfeiffer et al., 2010. The split-GAL4 system is based on the division of the GAL4 protein into two hemidrivers: the DNA-binding domain (DBD-part) and the transcription-activation domain (AD-part). Both functionally important parts are expressed under control of different promoters. Thus, transgene expression is restricted to areas where the two expression domains overlap. In those areas, the AD- and the DBD-parts heterodimerize, ultimately leading to functional GAL4 (Luan et al., 2006).

Furthermore, it is possible to suppress transgene expression in certain neural subpopulations for an increased specificity. This can be achieved by another yeast protein, GAL80, which is a repressor of GAL4. GAL80 binds to the carboxy-terminal 30 amino acids of GAL4 and thereby prevents GAL4-mediated transcriptional activation (Ma and Ptashne, 1987; Duffy, 2002). Thus, the combination of different GAL4 driver lines with GAL80 lines can result in an increased specificity by preventing the expression of GAL4 in defined neural populations.

Additionally, different GAL80 variants with temperature dependent efficacy were described to gain temporal control over the GAL80 induced suppression. Such a thermo-unstable variant of GAL80 can be expressed in a pan-neuronal manner by e.g. placing it downstream the ubiquitous tubulin promoter. An increase in temperature will inactivate GAL80 and therefore avoid the suppression of GAL4 (McGuire et al., 2003). This kind of temporal control can be used to avoid transgene expression during development. Alternative strategies to gain temporal control over expression rely on GAL4 variants, which are activated by drugs (Han et al., 2000; Osterwalder et al., 2001; Roman et al., 2001; Venken et al., 2011). While these approaches tend to have slow GAL4 activation, they do not require strict temperature control.

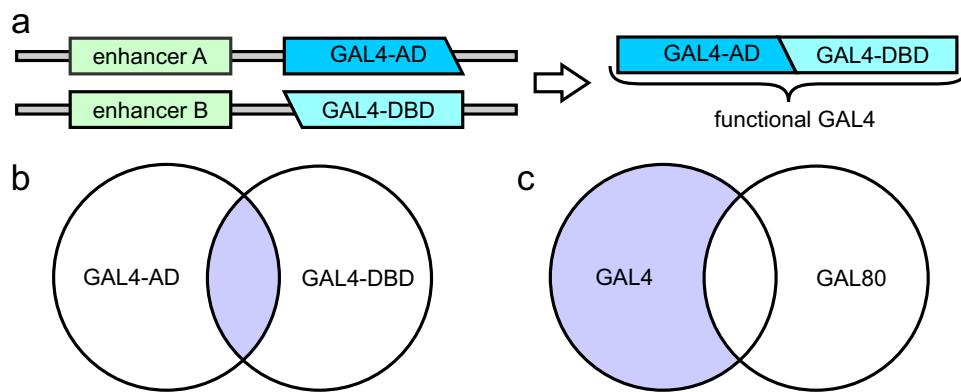


Figure 12: Split-GAL4 and GAL80. **a** Working principle of the split-GAL4 system. GAL4 is split into two parts which are expressed under the control of different enhancers. **b** As both GAL4-AD and GAL4-DBD parts are required in order to create functional GAL4, functional GAL4 will only be present in the overlap of both expression patterns. **c** GAL80 suppresses GAL4 within overlapping neural populations.

2.1.3 Other Binary Systems and Techniques

There are several other binary expression systems besides the GAL4-UAS system (Venken et al., 2011), including the *LexA* system (Lai and Lee, 2006), the Q system (Potter et al., 2010), the improved Q system (Riabinina et al., 2015), as well as the *Tet-On* (Bieschke et al., 1998; Stebbins et al., 2001) and *Tet-Off* system (Bello et al., 1998; Stebbins et al., 2001; Stebbins and Yin, 2001). These systems can be useful in combination with the GAL4-UAS system to target two distinct neural populations at once. For example, the GAL4-UAS system can be used to express an optogenetic tool in a specific neural pop-

ulation, while the *LexA* system can be used to express a functional reporter in a second neural population. This configuration enables the manipulation of neural activity in the first neural population to observe the effects in the second population.

2.1.4 Libraries of Driver Lines

While binary expression systems use driver lines with temporally- and spatially-defined expression patterns to manipulate specific neurons, there is no method to create a driver line with predefined expression pattern. Therefore, the success of these systems relies on the availability of large driver line libraries that contain lines with different cell specific expression patterns (Jenett et al., 2012; Tirian and Dickson, 2017; Dionne et al., 2018). In order to perform a specific experiment, a suited driver line should be already available within these libraries.

The creation of such collections can be achieved, for example, by generating driver lines based on selected DNA fragments that contain one or more enhancers. These enhancer fragments can be used to generate constructs, which allow to produce transgenic fly lines (for further details see e.g. Jenett et al., 2012). While the expression pattern of driver lines is defined by the corresponding enhancer, it is currently not possible to predict the final pattern. Once a driver line is created, its expression pattern can be visualized by fluorescent proteins.

2.2 EFFECTORS AND REPORTERS

Drosophila offers one of the most extensive toolkits to investigate neural circuits (Venken et al., 2011). This section provides an overview of the most used effectors and reporters.

2.2.1 Fluorescence Proteins

Visualization of neurons is a prerequisite to understand neural circuitry. To this end, fluorescent proteins (FPs), such as the jellyfish-derived *green fluorescent protein* (GFP), can be expressed in the cytosol (Chalfie et al., 1994). FPs are fluorescent when excited with light of specific wavelength. Nowadays, there are many different genetically engineered variations of fluorescent proteins with different properties, e.g. emitted wavelength and intensity. Further information on FPs is summarized in (Shaner et al., 2005; Kremers et al., 2011; Rodriguez et al., 2017).

2.2.2 Functional Reporters

Fluorescent proteins have further been engineered to work as functional reporters of neural activity. For this purpose, the fluorescence intensity of FP has been coupled directly or indirectly to the activity of neurons. Functional reporters enable the observation of neural signals from large sets of neurons

in vivo using light microscopy techniques. Furthermore, these tools allow the investigation of neurons that are not accessible by electrophysiological methods due to their position or small size.

One of the most frequently used functional reporters is the calcium indicator *GCaMP* (Nakai et al., 2001). *GCaMP* is created from a fusion of the green fluorescence protein (GFP), the M13 domain of a myosin light chain kinase, and the calcium-binding protein calmodulin. Binding of calcium to the calmodulin domain changes the conformation of *GCaMP*. This conformational change promotes de-protonation of the chromophore, which leads to an increased fluorescence. Over the past years, *GCaMP* has been genetically optimized, resulting in significant improvements of the signal-to-noise ratio and temporal resolution (Chen et al., 2013; Dana et al., 2018).

Several limitations should be considered when using calcium as a proxy for neural activity. First, calcium concentration in neurons is not directly related to membrane voltage. Calcium indicators, however, can only report membrane voltage changes that lead to significant calcium fluxes. Since voltage-gated calcium channels are normally only activated when neurons are depolarized, hyperpolarization and sub-threshold depolarization are generally not detected (Chamberland et al., 2017). Thus, reported signals of calcium indicators are basically half-wave rectified. Second, calcium indicators function based on the binding of calcium and therefore further act as calcium buffer, which influences the concentration of free calcium in the cytosol. High calcium indicator concentrations can have significant impact on the calcium dynamics in cells, which can even lead to nonlinear perturbations (Borst and Abarbanel, 2007). Furthermore, binding as well as release of calcium to and from the indicator occurs at certain rates, which limit the temporal response dynamics of indicators, making the reported signal slower in comparison to membrane voltage changes. Finally, when using calcium as a proxy for neural activity, it is often assumed that neural activity is the only source of calcium change within cells. However, this assumption does not hold true for every cell type (Sepehri Rad et al., 2017).

Additionally, efforts have been done to develop voltage indicators that directly report the membrane voltage of neurons (Xu et al., 2017). In general, such indicators consist of a transmembrane voltage sensing domain fused to a reporter, e.g. a fluorescent protein (Lin and Schnitzer, 2016). However, current voltage reporters are still in their early stages of development (Platisa and Pieribone, 2018). In comparison to calcium indicators, they suffer from lower signal-to-noise ratio and faster photobleaching (Lin and Schnitzer, 2016). Nevertheless, voltage indicators remain a promising tool and have already been successfully used in *Drosophila* (Cao et al., 2013; Chamberland et al., 2017).

Besides functional reporters that are engineered to report neural activity, it is also possible to visualize other neural signals. For instance, pH-sensitive reporters and tools linked to neurotransmitter release are existing: GluSnFR (Marvin et al., 2013), SynaptopHluorin (Miesenböck et al., 1998), and dVMAT-pHluorin (Freyberg et al., 2016).

2.2.3 Ablation

Another approach to understand the functional implication of certain neurons is the usage of genetically programmed cell death. Cell death can be induced by apoptotic genes, such as *reaper* (White et al., 1994, 1996; Zhou et al., 1997), *hid* (Grether et al., 1995), and *grim* (Wing et al., 1998). Alternatively, it is possible to take advantage of cell toxins, e.g. *ricin* (Hidalgo et al., 1995). Nonetheless, it should be considered that the removal of single neurons or even complete populations can cause major changes in neural structures and therefore it is important to control for both off-target damage and developmental abnormalities in order to draw meaningful conclusions.

2.2.4 Silencing

Silencing can be achieved by targeted interference with cellular synaptic transmission mechanisms or by ion channel manipulations. There are three frequently used tools in *Drosophila* to interfere with synaptic transmission.

First, synaptic transmission can be blocked by expression of tetanus toxin light chain (TNT). TNT cleaves the synaptic vesicle protein synaptobrevin and hereby blocks synaptic vesicle release (Sweeney et al., 1995). This interrupts the synaptic connection to the postsynaptic cell, which effectively silences TNT expressing neurons.

Second, neurons can be silenced by introducing an artificial constant hyperpolarization. This can be achieved through the expression of the inwardly rectified potassium channel *Kir2.1* (Baines et al., 2001). When expressed in neurons, *Kir2.1* leads to a reduction in action potential firing and suppresses neurotransmitter release (Johns et al., 1999). Overall, it reduces neuronal excitability and is suited for chronic, irreversible silencing (Wiegert et al., 2017).

Finally, it is possible to silence neurons by *shibire^{ts}*, a dominant-negative temperature-sensitive allele of dynamin (Kitamoto, 2000). *Shibire^{ts}* allows for temperature controlled blocking, since its expression within neurons has no effect at temperatures below $\sim 29^{\circ}\text{C}$. However, it will effectively stop the vesicle recycling machinery within targeted neurons for temperatures above $\sim 29^{\circ}\text{C}$. This kind of interruption will lead to neurotransmitter depletion, which results in blocked synaptic transmission.

2.2.5 Activation

Besides neuronal silencing, it is also possible to introduce artificial neuronal activation. Most of the approaches are based on the expression of additional ion channels within targeted neurons.

The bacterial depolarization-activated sodium channel *NaCh-Bac* can be used to increase the membrane excitability of targeted neurons. Therefore, any kind of membrane depolarization will trigger a positive feedback loop, which results in hyper electrical excitability (Nitabach et al., 2006). While *NaCh-Bac* does not increase neuronal activity by itself, it shifts neurons in a state that leads to prolonged periods of depolarization.

In addition, it is possible to evoke neuronal activation by introducing the temperature dependent cation channel *TrpA1*. *TrpA1* reversely opens for temperatures above 26°C, thus causing strong depolarization in targeted neurons (Hamada et al., 2008; Rosenzweig et al., 2005). It is often the tool of choice to introduce neuronal activation in freely behaving fly assays or activation screens (Inagaki et al., 2014; von Philipsborn et al., 2011; Robie et al., 2017).

Finally, the cation channel P2X₂ can also be used to evoke neuronal activation (Lima and Miesenböck, 2005). P2X₂ is activated via ATP binding, provides better temporal control than *TrpA1* and has large single-channel conductance. Therefore, it is an ideal tool for experiments where strong cellular depolarization is required (Honjo et al., 2012). While initially designed as an optogenetic tool triggered via photoreleased ATP, it was rarely used as one. This is because P2X₂ requires caged ATP injections, thus making its usage cumbersome (Lima and Miesenböck, 2005; Inagaki et al., 2014). Nevertheless, it is sometimes used in electrophysiological preparations to control neuronal activation by exposure to ATP via pressure-injection (Fujiwara and Chiappe, 2017).

2.3 OPTOGENETICS

Optogenetics refers to all techniques combining genetic and optical methods to gain exogenous control of specific cellular functions (Riemensperger et al., 2016). Often, optogenetic tools are based on light activated proteins, such as ion channels and pumps. Starting with the description of *Channelrhodopsin-2*, optogenetics has revolutionized many biological fields (AzimiHashemi et al., 2014; Fenno et al., 2011; Rein and Deussing, 2012; Fiala et al., 2010). Its success is owed to the several advantages that optogenetic methods present. For instance, optogenetics enables high temporal resolution of stimulation, noninvasive access to deeper located neurons, and reversible manipulations within the same animal.

2.3.1 Intrinsic Parameters of Optogenetic Tools

The usage of optogenetics requires the selection of the right tool for the specific experimental needs. Therefore, many parameters should be considered and compared between different tools. Often, however, existing tools are not sufficiently characterized in the experimental system under investigation, which makes this comparison challenging. Thus, it is advised to test several candidates in order to find the most suitable tool.

Key properties of optogenetic channels are ion selectivity, ion conductance, light sensitivity, activation spectrum, and kinetics. Ion conductance and ion selectivity determine how many ions are exchanged per unit time across the membrane. They provide important information about the general light sensitivity of a tool. While high light sensitivity is often desired to reduce the required intensity of the activation light, very high light sensitivity can complicate the control of tools.

The activation spectrum provides information about the suitable wavelengths required to activate an optogenetic tool. It can be important in preparations where the activation light must not interfere with other light sensitive systems, such as when using optogenetics within the fly visual system. Furthermore, knowledge of the activation spectrum is useful to avoid unintended activation of the optogenetic tool by other light sources and allows to minimize the required light intensity by selecting efficient wavelengths that activate the tool the most.

Kinetics of optogenetic tools define their temporal response profiles. Upon activation, tools can exhibit a transient peak response that transitions into a smaller steady-state response. Alternatively, they can directly transition into a steady-state response where they remain until the stimulation stops. Eventually, optogenetic tools will show some form of decay after the optogenetic light has ended. The temporal dynamics of the overall response can vary significantly between tools. For some tools, its temporal dynamics is one of the most important properties. As such, tools based on step-function opsins take advantage of the slow inactivation dynamics of certain opsins and therefore remain active long after the optogenetic light has stopped (see section 2.3.6). Furthermore, the overall kinetics of an optogenetic tool can also depend on other properties, such as the activation wavelength.

Finally, other properties of optogenetic tools, such as pH-dependence and the recovery time from desensitization, may also need to be considered for specific experiments.

2.3.2 Opsins

Light-gated ion channels or pumps of the opsin type provide the basis for many optogenetic tools (Guru et al., 2015). Opsins are present in different kinds of organisms and can be subdivided in two main classes: type I and II. Type I opsins are composed of single membrane-bound protein components and can be found in prokaryotic and eukaryotic microbial organisms, including bacteria, archaea, and most importantly algae. Type II opsins exist only in higher eukaryotes.

Both opsin classes require retinal, a form of vitamin A, to function properly. Retinal binds to opsins and functions as a light-absorbing chromophore. Upon photon absorption, a conformational change in the opsin is triggered by photoisomerization of the retinal. This leads to the activation of underlying channels or pumps, which causes a redistribution of ion concentrations. While sufficient retinal is present within mammalian neural structures, invertebrates like *Drosophila* have to be externally supplied with retinal.

2.3.3 Neuronal Activators

Channelrhodopsin-2 (ChR2), which originates from the alga *Chlamydomonas reinhardtii* (Nagel et al., 2003), is one of the most prominent optogenetic activators (Simpson and Looger, 2018). ChR2 is a non-selective cation channel with an activation sensitivity peak at around 470nm (blue light). It is well suited to evoke action potentials and tonic depolarization. The exchange

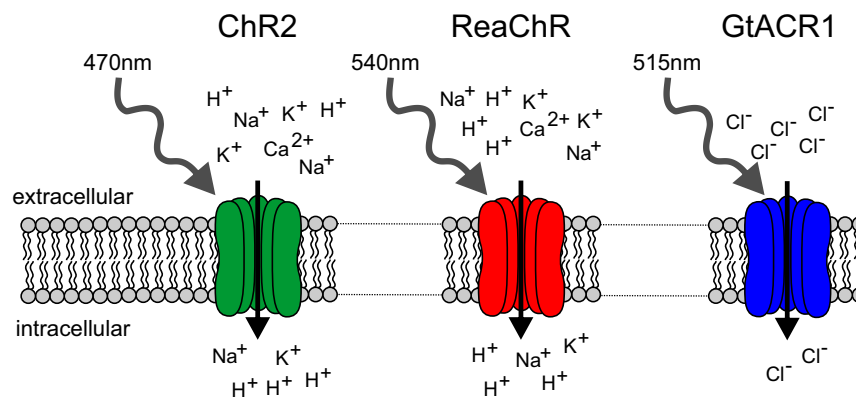


Figure 13: Illustration of selected optogenetic channels. Individual channels have different peak absorption wavelengths and allow defined anions or cations to pass through.

of several aminoacids in ChR2 has led to further improvements of various properties such as cation selectivity, photocurrent amplitude, and kinetics. Variants based on ChR2 include: CatCh (Kleinlogel et al., 2011), ChIEF (Lin et al., 2009), ChR2-XXL (Dawydow et al., 2014), ChR2-TC (Berndt et al., 2011), ChETA (Gunaydin et al., 2010), and Chronos (Klapoetke et al., 2014).

The blue light used to activate ChR2 is at the peak activation wavelength of Rh1 of *Drosophila*. Thus, optogenetic stimulation will interfere with the visual system and cause unwanted artifacts or even prolonged blinding. Red-shifted optogenetic tools strongly reduce this interference. Optogenetic tools with red-shifted activation spectrum include the chimeric opsins C1V1 and the red-activatable ChR (ReaChR) (Yizhar et al., 2011; Lin et al., 2013; Inagaki et al., 2014). Both variants have their absorption peak at around 540nm, thus around 70nm shifted towards long wavelengths with respect to ChR2. When comparing ReaChR and C1V1, ReaChR shows better membrane trafficking, more robust responses for higher wavelengths, and enhanced steady-state activation (Lin et al., 2013). Thus, ReaChR seemed to be the tool of choice for optogenetic activation experiments presented within this work (see section 3.2).

Another far red-shifted optogenetic activation tool is called CsChrimson. It originated from the yellow-peaked channelrhodopsin *CnChR1*, which was found in the algae species *Chloromonas subdivisa* (Klapoetke et al., 2014). While CsChrimson has its activation peak at 570nm, longer wavelengths (over 600nm) are sufficient to drive activity, being almost completely out of the visual range of *Drosophila*. However, when I tested CsChrimson in T4/T5 cells, optogenetic activation led to prolonged side effects up to several minutes after optogenetic light offset. Furthermore, unilateral HS cell activation using CsChrimson did not evoke the previously described turning responses (Fujiwara et al., 2016).

2.3.4 Neuronal Inhibitors

Acute neuronal silencing can be critical to understand neural circuits, since it enables to show the necessity and contribution of individual circuit components. The discovery of halorhodopsin (NpHR) was key for the development of initial optogenetic silencing tools. Halorhodopsin is a light-sensitive anion pump derived from the archaeobacteria *Natronobacterium pharaonis*, with an absorption peak at 570nm. Upon activation, NpHR pumps chloride ions into targeted cells, thus causing hyperpolarization. Most of the early optogenetic silencing tools were based on engineered variants of halorhodopsin (NpHR), such as the enhanced NpHR (eNpHR) (Gradinaru et al., 2008), which is successfully used within adult *Drosophila* and *Drosophila* larvae (Inada et al., 2011).

While chloride pumps evoke hyperpolarization by pumping chloride into cells, proton pumps achieve hyperpolarization by pumping protons out of cells. Despite the similar effect on the membrane potential, both pumps differ in their overall characteristics. Proton pumps show faster recovery from inactivation as well as higher light-driven currents, which makes them promising alternatives to chloride pumps (Guru et al., 2015). Known proton pumps include archaerhodopsin-3 (Arch) (Chow et al., 2010), a proton pump derived from the fungus *Leptosphaeria maculans* (Mac) (Waschuk et al., 2005), archaerhodopsin from the *Halorubrum* strain TP009 (ArchT) (Han et al., 2011), and an enhanced version of *bacteriorhodopsin* (eBR) (Gradinaru et al., 2010).

Since proton pumps require high light intensities and engineered chloride-conducting ChRs have small ion conductance, both are not ideally suited for optogenetic studies in the visual system of *Drosophila*. This was disrupted by the recent discovery of a novel family of light-gated anion channels (ACRs), including GtACR1 and GtACR2 (Govorunova et al., 2015), which was critical to this work. These channels are derived from the cryptophyte algae species *Guillardia theta* and exhibit a strong light-gated chloride conduction. They are very light sensitive (around three orders of magnitude higher than eNpHR), evoke efficient membrane hyperpolarization, and have fast kinetics. GtACR1 has its peak sensitivity at 515nm, whereas GtACR2 peaks at 470nm. Together with my colleagues, I could show that GtACR1 induces neuronal silencing within the visual system of *Drosophila* without significant interference of visual processing (see chapter 3).

Besides GtACR1 and GtACR2, other optogenetic inhibitors have been recently developed. These include variants of ChR2 designed to conduct chloride (ChloC) (Wietek et al., 2014), improved ChloC (iChloC) (Wietek et al., 2015), and the chimeric light-activated chloride channel iC++ (Berndt et al., 2016).

Finally, light-gated potassium channels can evoke strong shunting inhibition without major ion gradient changes (Sierra et al., 2018). However, the development of light gated potassium channels is within its early stages. Reported tools include the blue-light-induced K⁺ channel 1 (BLINK1) (Cosentino et al., 2015), its optimized version BLINK2 (Alberio et al., 2018), the optical silencing system PAC-K (Sierra et al., 2018), and the recently reported cyclic nucleotide-gated based channel SthK (Beck et al., 2018).

2.3.5 Synthetic Retinal Analogues

It is also possible to change the properties of optogenetic tools by using synthetic retinal analogues. This approach has already been successfully used to tune color and photocycle characteristics of microbial rhodopsin based tools (AzimiHashemi et al., 2014; Sineshchekov et al., 2012). Furthermore, synthetic retinal analogues can modulate spectral properties and pump activity of proteorhodopsins (Ganapathy et al., 2015). In combination with directed evolution, more drastic changes can be introduced (Herwig et al., 2017).

2.3.6 Step-Function Opsins

The previously introduced optogenetic tools require constant light stimulation in order to work. However, depending on the experimental setup or research question, it might not be possible to provide constant optogenetic light. The so-called step function or bi-stable opsins (SFOs) can be switched between open and closed state using short light pulses and are useful alternatives in these situations.

First step function opsins were engineered by introducing specific point mutations into ChR2, see e.g. ChR2(C128A), ChR2(C128S), or ChR2(C128T) (Berndt et al., 2008). These point mutations resulted in substantially slower closing kinetics and therefore prolonged depolarization after brief light illumination. Further mutations of ChR2 led to different variants with even slower closing time constants (in the order of minutes), such as ChR2/D156A. The subsequent combination of both types of mutations produced the step function opsin ChR2(C128S/D156A) that remains in open conformation for around half an hour (Yizhar et al., 2011). Moreover, there is also a step-function inhibitory channelrhodopsin called SwiChR++ (Berndt et al., 2016), which is a bi-stable light-activated chloride channel.

2.4 PHYSIOLOGICAL TECHNIQUES

The recording of neural activity is essential to understand electrical signaling and signal propagation between neurons. There are two methods that are commonly used in *Drosophila melanogaster*: whole-cell patch clamp recording and two-photon imaging.

2.4.1 Whole-Cell Patch Clamp Recording

Electrophysiological recordings can directly measure the neural activity with high temporal resolution *in vivo*. There are different recording techniques that have been well established for *Calliphora*, such as extracellular recordings or sharp electrode intracellular recordings (Bishop and Keehn, 1967; Laughlin and Osorio, 1989; Haag and Borst, 2001). However, electrophysiological recordings for *Drosophila melanogaster* have only been established within the last two decades. This was mainly due to the small size of many neurons, which prevented a direct technology transfer from larger flies. In-

stead, a slightly different method was developed, which is referred to as whole-cell patch-clamp recording (Sakmann and Neher, 1984). Detailed information on how to perform whole-cell patch-clamp recordings within the visual system of *Drosophila* can be found in Mauss and Borst, 2016; Joesch et al., 2008.

Whole-cell patch clamp recordings are mainly limited by two factors: soma size and anatomical accessibility of neurons. Nevertheless, recordings were successfully performed in different brain regions (Wilson et al., 2004; Murthy et al., 2008; Joesch et al., 2008; Behnia et al., 2014). Furthermore, it is possible to record from head-fixed walking and flying flies (Fujiwara et al., 2016; Maimon et al., 2010). Even recordings from small neurons with soma size of $\sim 2\text{-}3\mu\text{m}$ are currently becoming feasible (Gruntman et al., 2018).

2.4.2 Two-Photon Imaging

The successful implementation of two-photon imaging has been a milestone for many fields within natural science, including neuroscience (Denk et al., 1990). While electrophysiological methods allow to collect high-resolution data ($\sim 10\text{kHz}$), they lack the ability to record from large neural populations. In such cases, two-photon imaging can be the method of choice.

Two-photon imaging combines two-photon laser-scanning fluorescence microscopy and functional reporters (see section 2.2.2). It is based on a femtosecond-pulsed laser ($\sim 900\text{nm}$), which is used to stimulate fluorescence proteins. While a single photon lacks the required energy to excite the fluorophore, two coinciding photons are sufficient to overcome the excitation threshold. Thus, fluorescence is spatially restricted to the focus point of the laser stimulation. Furthermore, the high wavelength of the laser is outside of the visual range of the photoreceptors of *Drosophila*. As a result, this makes two-photon imaging well suited to investigate the response properties of neurons within the visual system (Reiff et al., 2010; Maisak et al., 2013). Similar to patch clamp recordings, two-photon imaging can be used during head fixed walking and flying behavior (Seelig et al., 2010; Schnell et al., 2017).

2.5 METHODS FOR STRUCTURAL ANALYSIS

Targeted manipulations of neural circuits are heavily depending on knowledge of the underlying anatomical structure. Only with information about location, morphology and neural connections is it possible to identify neurons of interest. These neurons can then be tested for their contribution to behavior.

Early studies used Camillo Golgi's silver staining to gain anatomical knowledge about neural structures within the fly's brain (Ramón y Cajal et al., 1915). Systematic and comprehensive application of such techniques led to the first neural atlases for *Calliphora* (Ramón y Cajal et al., 1915; Strausfeld, 1976) and later on for *Drosophila* (Fischbach and Dittrich, 1989; Bausenwein

et al., 1992). While these resources have proven to be very useful and are still frequently used, modern techniques provide a more directed approach.

2.5.1 Effector Based Anatomical Analysis

The large number of existing driver lines builds a solid foundation to gain anatomical insight into neural circuits of interest. Suited driver lines can be used to analyze labeled neurons based on fluorescence. However, it is not unusual that these driver lines have expression in groups of neurons near each other, which hinders single-cell reconstruction.

One approach commonly used to disentangle nearby neurons, is the stochastic reduction of labeled neurons within driver lines. This can be achieved with *flip-out* techniques, which often rely on FLP recombinase. Depending on the used tool, it is possible to obtain flies with stochastic labeled mosaic like expression patterns, which are usually tuned by heat shocks. Hereby, the severity of the applied heat shock as well as the developmental stage of the organism define the gain or loss frequencies of expression (Golic and Lindquist, 1989; Struhl and Basler, 1993; Bohm et al., 2010).

While classical flip-out techniques facilitate anatomical analysis by reducing the number of neurons expressing the same fluorescence proteins, it is further possible to introduce discriminability with stochastic distributed colors. Depending on the density and position of neurons, it is possible to gain full separation. Techniques based on color separation include: Flybow (Hadjieconomou et al., 2011), Brainbow (Hampel et al., 2011), and MultiColor FlipOut (MCFO) (Nern et al., 2015).

Besides anatomical information, it is also important to know the connectivity between neurons in order to understand neural circuits. While separated neurons are clearly not directly connected, neurons with overlapping processes may form synaptic connections with each other. Therefore, it might be necessary to probe for connectivity. A technique referred to GFP Reconstitution Across Synaptic Partners (GRASP) allows to label membrane contacts and synaptic connections between cells by splitting a functional fluorescence protein (FP) in two parts, each of which is expressed in distinct sets of neurons (Feinberg et al., 2008). Only if both parts of the FP are in very close proximity to each other, the reassembly of functional FP occurs. Thus, it is possible to make a confident statement of connectivity based on the observation of fluorescence.

Furthermore, it is possible to show connectivity based on neuronal tracing. Published methods include trans-TANGO (Talay et al., 2017) and TRACT (TRANsneuronal Control of Transcription) (Huang et al., 2017). Both approaches are based on ligand-induced intramembrane proteolysis, which subsequently leads to membrane anchored transcription factor release (Huang et al., 2017).

2.5.2 Electron Microscopy

The resolution of light microscopy is often not sufficient to resolve synaptic connections (Shih et al., 2015). Therefore, if a detailed reconstruction of neu-

rons with synaptic connections is required, a method with higher resolution has to be used, such as electron microscopy (EM) (Knoll and Ruska, 1932).

Electron microscopy uses accelerated electrons as the source of illuminating radiation. Due to the short wavelength of accelerated electrons, it is possible to achieve resolutions within the ångström range (Smith, 2008). Acquisition and subsequent analysis efforts that aim to understand the nervous system by generating and analyzing comprehensive maps of neural connections, are referred to as connectomics.

The visual system of *Drosophila melanogaster* has been analyzed by several electron microscopy studies (Shinomiya et al., 2019; Takemura et al., 2008, 2013; Shinomiya et al., 2014; Takemura et al., 2015, 2017; Rivera-Alba et al., 2011). Furthermore, an electron microscopy dataset of the entire adult fruit fly brain at synapse resolution has been published recently (Zheng et al., 2018). However, this data has only been partially analyzed.

3 | PUBLICATIONS

3.1 OPTOGENETIC NEURONAL SILENCING IN DROSOPHILA DURING VISUAL PROCESSING

This study demonstrated that GtACR₁ can be used to introduce fast and reversible silencing within the visual system of *Drosophila* during electrophysiological as well as behavioral experiments. The paper was published in *Scientific Reports* in October 2017.

SUMMARY Optogenetic tools are well suited to investigate many aspects of neural circuits, including the functional role of specific neurons for behavior. However, mainly due to the activation wavelength and sensitivity, there was a lack of potent optogenetic tools that could be used within the visual system of *Drosophila*. To address problem, we characterized the anion channelrhodopsins GtACR₁ and GtACR₂, which were recently discovered at this time. Furthermore, we performed patch-clamp recordings from tangential cells expressing GtACR₁, which showed strong and light-sensitive photocurrents. By doing so, we could only observe minor light induced artifacts within the visual system. Finally, by performing additional physiological recordings and behavioral experiments, we could demonstrate that GtACR₁ is well suited to introduce fast and reversible hyperpolarization within the visual system of *Drosophila*.

AUTHORS Alex S. Mauss, **Christian Busch**, and Alexander Borst.

CONTRIBUTIONS A.S.M. and A.B. conceptualized the project. A.S.M., **C.B.** and A.B. conceived the experiments. A.S.M. and **C.B.** conducted the experiments and analyzed the results. A.S.M. wrote the manuscript, with the help of all other authors.

SCIENTIFIC REPORTS

OPEN Optogenetic Neuronal Silencing in *Drosophila* during Visual Processing

Alex S. Mauss , Christian Busch & Alexander Borst

Received: 26 April 2017

Accepted: 6 October 2017

Published online: 23 October 2017

Optogenetic channels and ion pumps have become indispensable tools in neuroscience to manipulate neuronal activity and thus to establish synaptic connectivity and behavioral causality. Inhibitory channels are particularly advantageous to explore signal processing in neural circuits since they permit the functional removal of selected neurons on a trial-by-trial basis. However, applying these tools to study the visual system poses a considerable challenge because the illumination required for their activation usually also stimulates photoreceptors substantially, precluding the simultaneous probing of visual responses. Here, we explore the utility of the recently discovered anion channelrhodopsins GtACR1 and GtACR2 for application in the visual system of *Drosophila*. We first characterized their properties using a larval crawling assay. We further obtained whole-cell recordings from cells expressing GtACR1, which mediated strong and light-sensitive photocurrents. Finally, using physiological recordings and a behavioral readout, we demonstrate that GtACR1 enables the fast and reversible silencing of genetically targeted neurons within circuits engaged in visual processing.

Genetically expressed optogenetic ion channels and pumps confer light sensitivity to neurons of interest, allowing to control their activity on demand^{1,2}. Such techniques have become powerful means to establish neuronal connectivity as well as causal relationships between neuronal activity and behavior. Remote control of neuronal activity by light has many advantages: it is fast, reversible, easy to parameterize and applicable in intact behaving animals. However, it poses challenges for studies in visual systems, since here endogenous light-sensing cells, the photoreceptors, are also activated by light required for optogenetic control. This can lead to prominent visual artifacts or, in extreme cases, even blinding. This disadvantage is particularly prevalent in the fly optic lobe, which has otherwise become a paradigmatic example for visual processing due to identified neurons and large numbers of selective driver lines for their visualization and manipulation^{3,4}.

Ignoring visual artifacts, or indeed performing experiments in genetically blinded flies, depolarizing optogenetic channels have been nonetheless very useful to infer connectivity and behavioral roles upon selective neuronal activation⁵⁻⁹. In principle, selective activation should be possible in conjunction with simultaneous probing of visual circuit function. For instance, red-shifted CsChrimson¹⁰ or bistable Channelrhodopsin^{5,11,12} allow the spectral or temporal separation, respectively, of transgenic and endogenous rhodopsin activation. In contrast, hyperpolarizing tools are much less abundant and usually require strong illumination in spectral ranges incompatible with visual stimulation. Thus, there is a strong necessity for suitable hyperpolarizing channels, for instance, to probe the full transmission range of graded synaptic connections or to silence genetically identified neurons on demand while circuit function is being read out.

Recently, anion channelrhodopsins (ACRs) have been discovered in the cryptophyte algae species *Guillardia theta*¹³ (GtACR1 and GtACR2). These channels are promising versatile inhibitory tools since they impart strong light-gated chloride conductance, which is much more light-sensitive than, for instance, the Halorhodopsin class of chloride pumps^{14,15}. Particularly GtACR1 is of interest for applications in the fly visual system, since its activation spectrum is shifted towards longer wavelengths with respect to five of the six *Drosophila* rhodopsins (except rhodopsin 6), and in particular the main photopigment rhodopsin 1¹⁶⁻¹⁸. A recent study has demonstrated the utility of GtACR1 and GtACR2 for fast and reversible neuronal silencing in behaving flies¹⁹. Here, we first confirmed these findings in a *Drosophila* larval crawling assay. Since intracellular electrophysiology data on GtACRs is not yet available in flies, we performed whole-cell patch-clamp recordings in the adult *Drosophila* optic lobe. We thus obtained response curves revealing strong light-sensitive hyperpolarization mediated by GtACR1. We then explored GtACR1 utility together with electrophysiological and behavioral readouts for probing visual function. Our results demonstrate that optogenetics via GtACR1 permits selective, fast and reversible neuronal silencing in visually active circuits.

Max-Planck-Institute of Neurobiology, Martinsried, 82152, Germany. Correspondence and requests for materials should be addressed to A.S.M. (email: amauss@neuro.mpg.de)

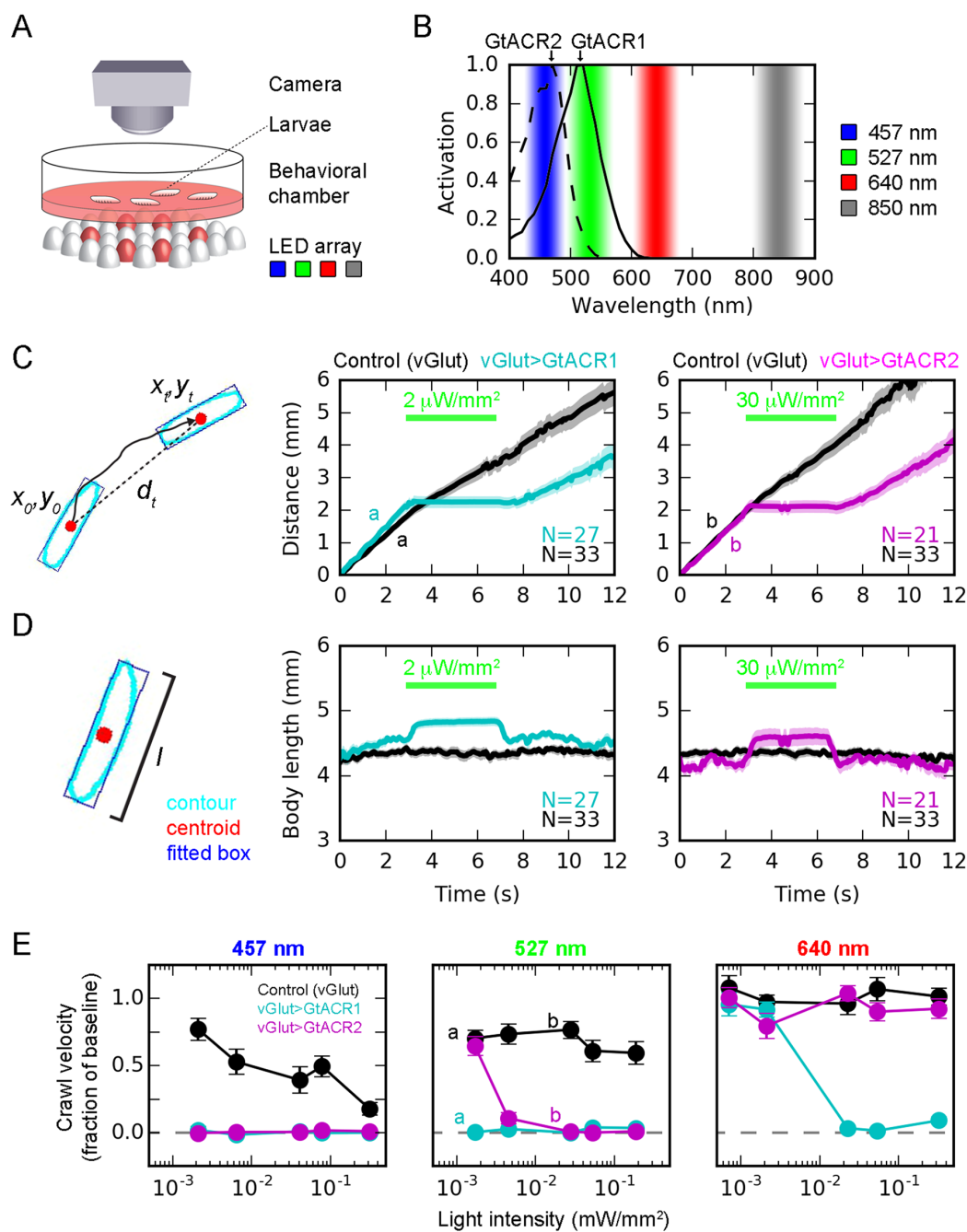


Figure 1. Characterization of GtACR1 and GtACR2 using a larval crawling assay. (A) Larvae were released in an agarose-coated petri dish and their crawling activity video-taped from above. Infra-red background illumination was provided by LED arrays emitting 850 nm light from below. Furthermore, three other LED arrays below emitted 457, 527 and 640 nm illumination for GtACR activation. Only one illumination was used for optogenetic stimulation at a time, here exemplified in red. (B) Relative activation spectra of GtACR1 and GtACR2, replotted from ref.¹³, with LED illumination used in the larval crawling assay indicated. (C) To quantify crawling activity, the measured centroid positions (red dots) were plotted as covered distance over time. The crawling activity of control larvae (vGlut-Gal4 only, no GtACR expression; black trace) was only mildly affected by illumination (527 nm at indicated intensity). In contrast, larvae with GtACR1 (cyan) or GtACR2 (magenta) expression in glutamatergic neurons (including motorneurons) seized crawling immediately with onset of light. Offset of illumination restored crawling activity. Traces labeled with a and b refer to data points in (E). (D) As another behavioral parameter, body length was quantified by fitting

a rectangle to each larva contour and measuring its length. Upon illumination, only larvae with GtACR expression in glutamatergic neurons (vGlut-GtACR) elongated, in agreement with a relaxation of the body wall musculature due to GtACR-mediated motorneuron silencing. (E) Crawling activity (fraction of baseline) for illumination with three different wavelengths as a function of light intensity. Letters a and b indicate data points for which example traces are displayed in (C). All data are presented as mean \pm standard error of the mean.

Results

The recently discovered anion channelrhodopsins GtACR1 and GtACR2¹³ have been shown to be suitable for silencing genetically targeted neurons in intact flies with remarkably low light requirements¹⁹. Here, we tested their utility for silencing neurons of the optic lobe in conjunction with visual stimulation. To be able to express these channels cell-specifically in *Drosophila* using existing Gal4 lines we cloned the two EYFP-tagged coding regions into the UAS expression vector pJFRC7²⁰. With the resulting vectors we generated genomic insertions in defined chromosomal locations using phiC31 integrase²¹ to obtain UAS-GtACR1-EYFP and UAS-GtACR2-EYFP flies (landing sites attP40 on 2nd and VK00005 on 3rd chromosome).

Assessing the efficacy of optogenetic tools using larval crawling as a behavioral readout. In order to assess the efficacy of optogenetic tools in *Drosophila* in a first approach, we devised a high-throughput larval crawling assay. We expressed GtACR1 and GtACR2 using vGlut-Gal4 driving expression in glutamatergic neurons including motorneurons and reasoned that silencing those should manifest in easily quantifiable reduction in crawling activity. For behavioral analysis, we obtained video data from batches of 3rd instar larvae simultaneously crawling in a petridish (batch size \sim 10; for each experiment, on average 26.6 ± 6.2 (S.D.) larvae were tracked) (Fig. 1A). The dish was illuminated from below by LED arrays of different wavelengths: 850 nm as background illumination for image capture and 457 nm (blue), 527 nm (green) and 640 nm (red) for optogenetic stimulation, guided by the two published activation spectra of GtACR1 and GtACR2¹³ (Fig. 1B). Behavioral parameters were extracted offline from video data in an automated fashion (see Methods). We defined locomotor activity as the covered distance over time (Fig. 1C). The example traces show strong effects of illuminating vGlut > GtACR-expressing larvae in that they immediately cease to crawl. This effect is fully reversible and illuminated larvae resume crawling shortly (\sim 1 s) after light offset. We also used body length as another behavioral measure (Fig. 1D). Exposing vGlut-GtACR-larvae with light increases body length as abruptly as it stops crawling, in line with a presumed relaxation of body wall musculature due to motor neuron inactivation.

Next, we quantified the effects of GtACR1 and GtACR2 as a function of wavelength and intensity (Fig. 1E). These experiments revealed different light requirements of GtACR1 and GtACR2, in agreement with their different activation spectra¹³. GtACR1 activation caused a full reduction of crawling activity for both blue and green light at all intensities tested ($2\text{--}300 \mu\text{W}/\text{mm}^2$), while red light required intensities of at least $20 \mu\text{W}/\text{mm}^2$. GtACR2 was most effective with blue light, showing full crawling suppression. However, green light required $> 5 \mu\text{W}/\text{mm}^2$ and red light did not produce any crawling phenotype for intensities below $300 \mu\text{W}/\text{mm}^2$. To conclude, our data are in agreement with the literature^{13,19}. Particularly GtACR1 with an activation peak shifted relative to rhodopsin 1 seemed to be a promising candidate for selective neuronal silencing within visually active circuits. In the following, we therefore focus on the characterization of GtACR1 in the *Drosophila* optic lobe.

Light requirements of neuronal hyperpolarization by GtACR1. GtACRs are expected to hyperpolarize neurons, depending on the chloride reversal potential, which can be rigorously addressed only by intracellular electrophysiological recordings. In order to fully characterize mode of action and light requirements, we aimed to directly measure the GtACR1-mediated physiological effects in single neurons. Tangential cells of the lobula plate lend themselves well for this purpose since whole-cell patch-clamp recordings can be readily obtained from their large cell bodies²² (Fig. 2A). Tangential cells characteristically respond with graded potential changes of about 5–15 mV, depending on the stimulus, to visual wide-field motion: depolarization in response to the preferred direction and hyperpolarization in response to the opposite or null direction²². Using a selective driver line, we expressed GtACR1 in tangential cells (Fig. 2B–B’). To activate GtACR1, we passed light from a Xenon arc lamp through optic band pass filters (resulting wavelengths relative to Rh1 and GtACR1 shown in Fig. 2C) and delivered it to the preparation via the epifluorescent light path of the microscope. Illumination of brains in control flies without GtACR1 expression resulted in transient ON and OFF tangential cell voltage deflections, in line with the light reaching the photoreceptors⁷, but little tonic changes. In stark contrast, GtACR1-expressing tangential cells responded with strong hyperpolarization of up to 22 mV on average (Fig. 2D), which is roughly twice the amplitude of robust visually evoked null direction inhibition²². The hyperpolarization onset latency (see small insets in Fig. 2D, red trace) was in the range of 2–3 ms and therefore much faster than the one of the visual ON transient in the control condition (\sim 15 ms). In line with GtACR1’s spectral response peak, light of 535 nm wavelength was most effective and 615 nm light had to be of considerable higher intensity to reach the same effects. We quantified responses for each tested wavelength as a function of light intensity and fitted sigmoidal functions to the responses. Thus, we obtained light intensities at 50% maximal hyperpolarization of 3.5, 8.2 and $296 \mu\text{W}/\text{mm}^2$ for 535, 565 and 615 nm, respectively (Fig. 2D).

Neuronal silencing using GtACR1 is compatible with simultaneous visual stimulation in a physiological preparation. The light requirements of GtACR1 in terms of wavelength and intensity seemed potentially suitable to silence neurons in the visual pathway without strongly activating photoreceptors. To test this, we took advantage of the fact that the visual pathways impinging on lobula plate tangential cells are characterized in exquisite detail³. Tangential cells receive direct cholinergic input from arrays of local direction-selective

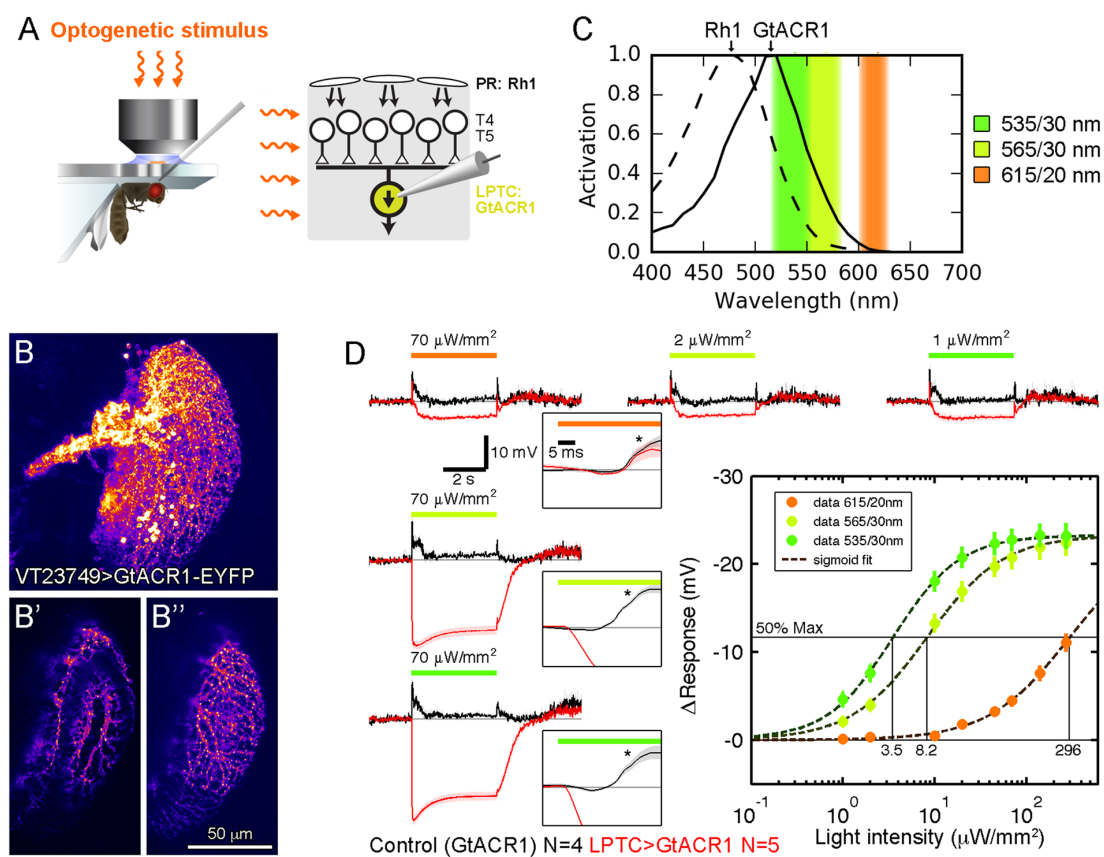


Figure 2. Characterization of GtACR1 in lobula plate tangential cells by whole-cell patch-clamp recordings. (A) Illustration of preparation for tangential cell recordings (left schematic adapted with permission from ref.²²). Lobula plate tangential cells (LPTCs) receive direction-selective visual input from T4/T5 neurons, three synapses downstream of photoreceptors (PR). Illumination for GtACR1 activation in tangential cells is conveyed to the brain via the epi-fluorescent light path of the microscope. (B–B'') Confocal images showing expression of GtACR1-EYFP in tangential cells. **B** depicts a maximal projection and **B'**, **B''** show projections from z-subsections highlighting individual dendritic branches. (C) Relative activation spectra of photoreceptor rhodopsin 1 (replotted from ref.¹⁷) and transgenically expressed GtACR1 (replotted from ref.¹³). Center illumination wavelengths (e.g. 615 nm) and bandwidths (e.g. 20 nm) used for the following experiments are indicated. (D) GtACR1-expressing tangential cell responses (membrane potential) to illumination of indicated wavelengths and intensities over time, averaged across 8 trials and N cells. Different wavelengths of similar intensity cause hyperpolarizations of different amplitudes (traces on the left). The same hyperpolarization in cells can be achieved with different wavelengths at different intensities (traces on top). Voltage traces with an expanded time axis are shown in the insets, showing a ~15 ms delayed depolarizing visual response (asterisk) that is replaced by short-latency (2–3 ms) GtACR1-mediated hyperpolarization using 535 and 565 nm illumination (red trace). The responses are quantified as the baseline-subtracted time-averaged potential during the steady-state (3–4 s after illumination onset minus 1–0 s before illumination onset). For each wavelength, sigmoid functions were fitted to the response amplitudes to obtain the light intensities required to reach 50% of the maximal response. Data are presented as mean \pm standard error of the mean.

T4/T5 neurons, giving rise to preferred direction excitation^{7,23,24}. In addition, tangential cells receive indirect inhibitory input from oppositely tuned T4/T5 cells via glutamatergic interneurons, causing hyperpolarization during null direction motion⁶. Therefore, all visual motion responses in tangential cells require T4/T5 cell activity, providing an ideal test bed for combined visual stimulation and optogenetic silencing (Fig. 3A).

In an initial set of experiments, we explored the suitability of different wavelengths for combined optogenetic and visual stimulation. To this end, we recorded from tangential cells in control flies (no GtACR1 expression) and illuminated the brain with 535, 565 and 615 nm light previously established to produce the same GtACR1-mediated hyperpolarization (1, 2 and 70 $\mu\text{W}/\text{mm}^2$, respectively; see Fig. 2D). Simultaneously probed visual responses were indistinguishable for 565 and 615 nm but reduced for 535 nm (data not shown). This unfavorable effect of 535 nm light is potentially caused by wavelength-dependent relative differences in absorption by

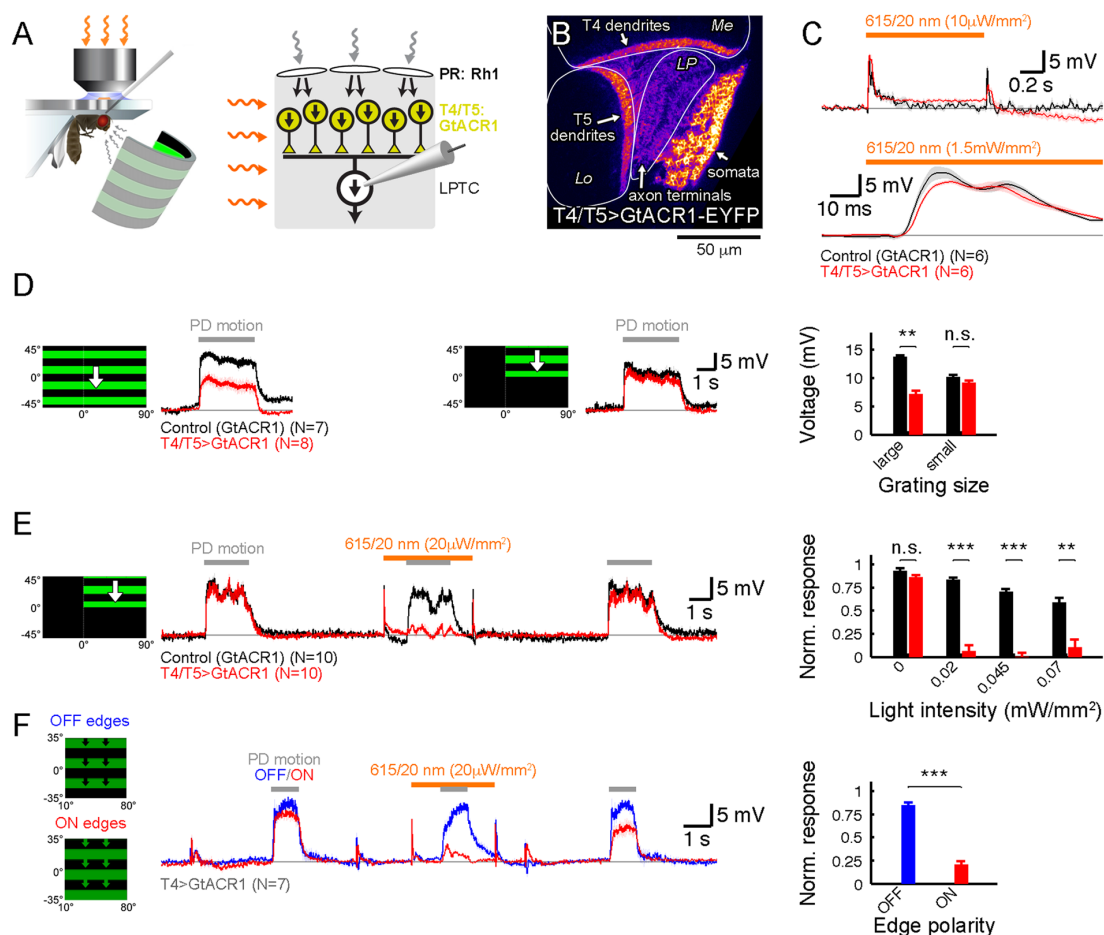


Figure 3. Using GtACR1 for optogenetic silencing of visual motion inputs to tangential cells. (A) Illustration of preparation for tangential cell recordings with GtACR1 expression in upstream direction-selective T4/T5 neurons (left schematic adapted with permission from ref.²²). (B) Confocal image showing expression of GtACR1-EYFP in T4/T5 neurons in a horizontal cross section. Me, medulla; Lo, lobula; LP, lobula plate. (C) Tangential cell responses in control (black traces) and T4/T5 > GtACR1 flies (red traces) to 615 nm illumination of indicated intensities. Note the different time scales. (D) Tangential cell responses in control (black traces) and T4/T5 > GtACR1 flies (red traces) to gratings of different sizes moving in the preferred direction. For the large pattern, cells in T4/T5 > GtACR1 flies show a reduced average response compared to control flies, presumably due to GtACR1 activation by the visual stimulus. Quantifications represent time-averaged and baseline-subtracted membrane potentials. (E) Tangential cell responses in control (black traces) and T4/T5 > GtACR1 flies (red traces) to combined visual and optogenetic stimulation. Visual stimuli were presented three times per trial and the second stimulation combined with 615 nm illumination (average voltage traces shown for 20 μ W/mm²). Responses in control flies become progressively more reduced at increasing illumination intensities yet still reach ~50% at the highest intensity. In contrast, responses in T4/T5 > GtACR1 flies are eliminated already by weak illumination. For quantification, time-averaged membrane potentials were baseline-subtracted for the first and second visual stimulus. A normalized response was obtained by dividing the second by the first response. (F) Tangential cell responses to moving ON (red) and OFF edges (blue) in the same individuals expressing GtACR1 in ON-selective T4 cells. The stimulus is presented three times per trial and the second time combined with 615 nm light illumination. The OFF response is comparable to wild type while the ON response is almost absent. The third visual ON response is slightly reduced for unknown reasons. Quantification as in (E). Traces in C–F represent the membrane potential averaged across 4 trials and N cells. All data are shown as mean \pm standard error of the mean. A two-tailed Wilcoxon ranksum test was performed to establish statistical significance: n.s., not significant; ** $p < 0.01$; *** $p < 0.001$.

Rhodopsin1 or its activated metarhodopsin state and GtACR1. In the following electrophysiological experiments, we therefore used 615 nm light, although a slightly shorter wavelength such as 565 nm also seemed suitable.

To assess direct effects of T4/T5 cell hyperpolarization in absence of visual stimulation, we recorded from tangential cells in control flies carrying only the GtACR1 transgene without the driver, hence termed “Control

(GtACR1)”, and in flies expressing GtACR1 in presynaptic T4/T5 cells, termed “T4/T5 > GtACR1” (Fig. 3B). When illuminating the brain with 615 nm light, expected ON and OFF transients due to photoreceptor activation became apparent in both conditions, with little tonic effects on the membrane potential (Fig. 3C). The time course of the ON transient with an onset latency of 15 ms was virtually indistinguishable between both genotypes. Thus, it appears that only positive T4/T5 signals are transmitted to downstream tangential cells⁷.

Next, to test whether GtACR1-expressing T4/T5 cells retain their normal visual function, we stimulated control and T4/T5 > GtACR1 flies visually with moving gratings, while recording from tangential cells. For large patterns, we measured reduced visual responses in the latter experimental group (Fig. 3D, left traces and quantification). Since GtACR1 is rather light sensitive and the visual stimulus arena emits 565 nm light, well suited to activate GtACR1, we reasoned that the ambient light might already be sufficient to partially silence GtACR1-expressing T4/T5 cells. To test this, we reduced total luminance from the arena by decreasing the pattern size. Now, responses in the two genetic conditions were indistinguishable (Fig. 3D, right traces and quantification), in agreement with cross-activation of GtACR1 from arena light in the large pattern condition.

To determine whether GtACR1 is suitable to conditionally silence T4/T5 neurons in visually active circuits, we combined visual and optogenetic stimulation in control and T4/T5 > GtACR1 flies while recording from tangential cells (Fig. 3E). One stimulus sequence consisted of three identical visual stimulations (grating moving downward, i.e. in the preferred direction of the recorded cells), with the second one combined with optogenetic illumination (615 nm light of varying intensities). Control flies’ visual responses became progressively reduced with increasing light intensities (due to interference of the optogenetic illumination with photoreception) but were still robustly detectable at 70 $\mu\text{W}/\text{mm}^2$ (Fig. 3E). In T4/T5 > GtACR1 flies however, visual responses during illumination were almost entirely absent at light intensities of 20 $\mu\text{W}/\text{mm}^2$ and above. Importantly, the first and third visual response in each trial were not different between T4/T5 > GtACR1 and control flies, demonstrating the normal function of GtACR1-expressing neurons immediately before and after exposure to optogenetic illumination.

Like in the vertebrate retina, visual motion processing in flies is split into an ON- and an OFF-pathway^{3,25} with T4 cells being the first direction-selective neurons in the ON- and T5 cells the first ones in the OFF-pathway^{23,26–28}. To rule out any confounding effects on visual sensitivity due to genetic background we performed another set of experiments with an internal control for visual function. To this end, we expressed GtACR1 in T4 cells only and stimulated flies with moving ON or OFF edges (Fig. 3F). Importantly, moving decrements of light (OFF edges) are processed in the parallel pathway by T5 cells, which do not express GtACR1 in this experiment and should thus retain their normal function. In downstream tangential cells, ON and OFF responses should thus be differentially affected by optogenetic illumination in the same animal. Indeed, OFF edge responses were hardly reduced by illumination, while ON edge responses were almost completely abolished (Fig. 3F). We also noted a slight average decrease in the third visual response amplitude immediately after optogenetic stimulation. However, this response was still markedly larger than the preceding one during optogenetic stimulation (second visual response) and fully recovered until the following trial. Taken together, our experiments unequivocally demonstrate the selective optogenetic silencing in the visual circuit while leaving vision functional.

Neuronal silencing using GtACR1 is compatible with simultaneous visual stimulation in intact behaving animals.

A powerful application for optogenetic tools is to control neuronal activity in intact animals, thus establishing causal relationships between neuronal activity and behavior. We wanted to test the potential of GtACR1 for silencing neuronal activity in fly visual circuits while simultaneously tracking visually controlled behavior. As a readout, we used tethered flies walking on an air-suspended ball allowing us to precisely measure their turning tendency in response to panoramic visual motion (optomotor response²⁹) (Fig. 4A). Permanent blocking of T4 and T5 cells by expressing the temperature-sensitive shibire allele or tetanus toxin light chain had previously been shown to abolish the optomotor response completely and render flies motion-blind^{30,31}. Again, we expressed GtACR1 in T4/T5 neurons, termed “T4/T5 > GtACR1”, and used flies with T4/T5-Gal4 driver or UAS-GtACR1 only as genetic parental controls without GtACR1 expression, termed “Control (T4/T5)” and “Control (GtACR1)”, respectively. We then measured the optomotor response in presence and absence of 565 nm light illumination of varying intensities focused onto a 0.12 mm² spot to the back of the head on the right side (Fig. 4B). Since the optogenetic illumination has to penetrate the cuticle, which is expected to scatter and filter out a considerable proportion of photons, higher light intensities compared to the physiological experiments were used. Control flies exhibited turning responses similar to baseline (no illumination) upon visual stimulation up to light intensities of 50 μW , demonstrating negligible visual interference of the optogenetic light stimulus (Fig. 4C,D). T4/T5 > GtACR1 flies, however, displayed marked reduction in their turning responses upon illumination. As expected, this phenotype was more light-sensitive for visual stimulation on the same side of optogenetic illumination. Visual responses to moving patterns on the contralateral side were also reduced at higher light intensities, probably due to light scattering within the head capsule across hemispheres.

To further demonstrate selective T4/T5 silencing during visual processing, we presented flies with either back-to-front or front-to-back bilateral motion. Control and T4/T5 > GtACR1 flies without illumination showed no average turning response. This was expected, since the opposing motions on both sides as normally perceived during forward or backward translation do not elicit a directed turn (Fig. 4E,F). However, with increasing illumination intensities (5–10 μW), T4/T5 > GtACR1 flies on average increased their turning with the motion direction presented on the contralateral side. This finding is in agreement with optogenetically mediated, ipsilateral motion blindness due to the silencing of T4/T5 cells. At yet higher intensities, average turning decreased to baseline, again most likely due to the contralateral spread of light.

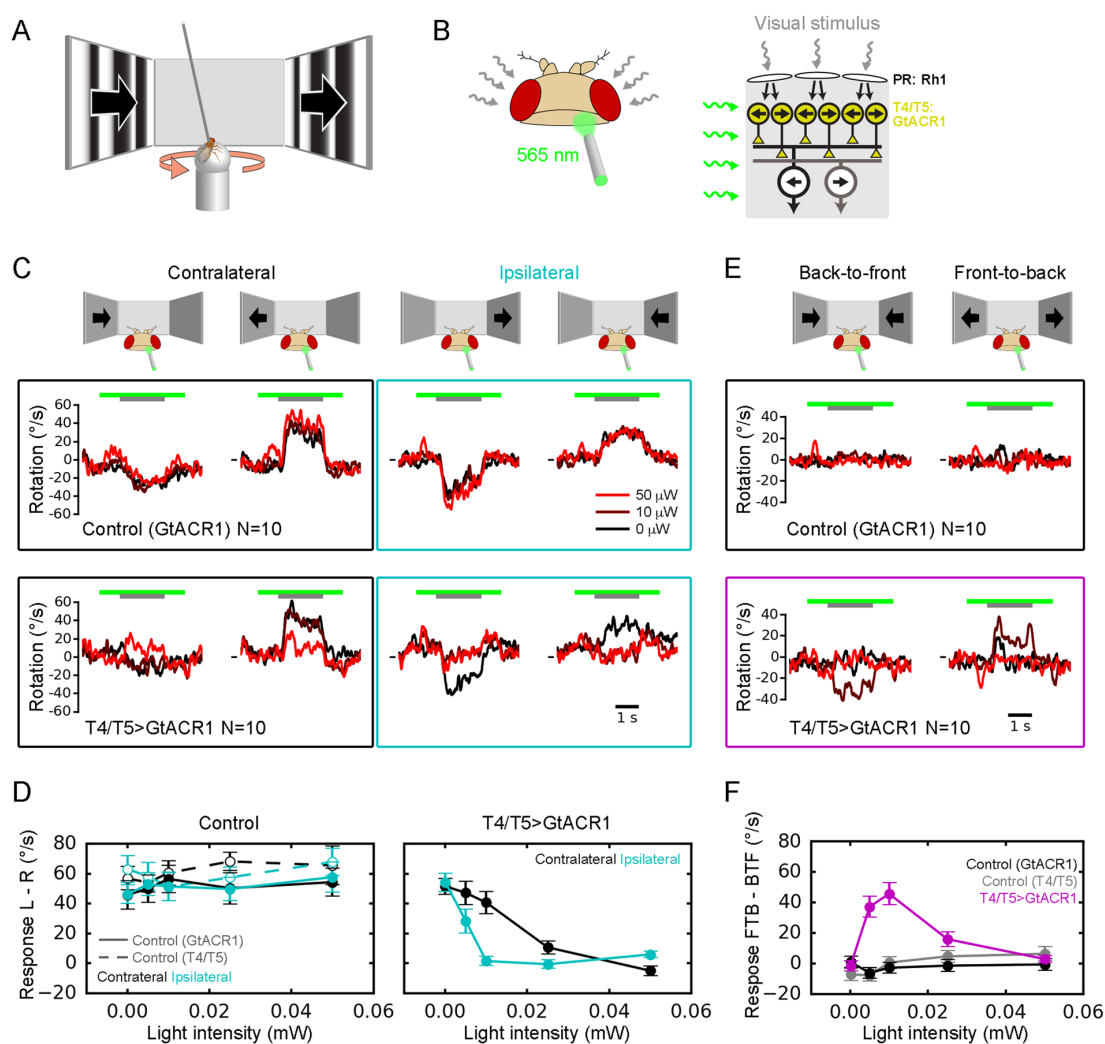


Figure 4. Using GtACR1 for optogenetic silencing of visual motion signals underlying the optomotor response. **(A)** Schematic illustrating the behavioral optomotor assay. A tethered fly is walking on an air-suspended ball whose rotation is measured, allowing to obtain fly turning responses to visual motion. **(B)** To optogenetically silence visual neurons expressing GtACR1, light is focused onto a small spot (0.12 mm^2) on the back of the fly head. **(C)** Fly turning responses (averaged across 20 trials and 10 flies) to visual motion towards left and right, presented either on the same (ipsilateral) or contralateral side of optogenetic illumination. Response traces for three illumination conditions are overlaid (0, 10 and $50 \mu\text{W}$). Control flies (upper row) show no discernible changes in optomotor behavior due to illumination. In contrast, T4/T5 > GtACR1 flies display markedly reduced optomotor turning upon illumination (lower row), particularly in combination with ipsilateral visual stimulation (two plots on the right). The short horizontal lines in front of traces indicate zero turning. **(D)** Quantification of experiment presented in C, with an additional control (T4/T5 driver only, i.e. without expression) and two additional optogenetic light intensities. Baseline-subtracted responses to left- and right-ward motion were combined (L-R) separately for ipsi- and contralateral stimulation. **(E)** Experiment as in C but with simultaneous visual motion in opposite directions on left and right side (back-to-front, shown on the left; front-to-back, shown on the right). Control flies do not display turning on average in any condition. T4/T5 > GtACR1 flies respond with turning to both visual stimuli when combined with illumination of intermediate intensities, in agreement with GtACR1-mediated unilateral motion blindness. The short horizontal lines in front of traces indicate zero turning. **(F)** Quantification of experiment presented in E, with an additional control (T4/T5 driver only, i.e. without expression) and two additional optogenetic light intensities. Baseline-subtracted responses to front-to-back and back-to-front were combined (FTB - BTF). Data in D and F represent the mean \pm standard error of the mean.

Discussion

Targeting light-gated hyperpolarizing ion channels and pumps to genetically defined neuron types is a powerful means to control their activity on demand^{1,2}. However, applying this approach to visual circuits is highly problematic because the required light typically also stimulates endogenous light-sensing photoreceptors, often even beyond saturation. Here, we demonstrate in *Drosophila* that the recently discovered anion channelrhodopsin GtACR1 has the necessary properties to enable optogenetic neuronal silencing in active visual circuits.

Optogenetic control over neuronal activity within visual circuits essentially requires independent gating of endogenous and transgenic rhodopsins by light. Primary visual circuits, such as the mammalian retina or the insect optic lobe, are usually very close to photoreceptors so that spatial restriction of illumination is exceedingly difficult in translucent neural tissue. Instead, different activation spectra of rhodopsins can be exploited for independent control with different wavelengths of light, but only given suitable other properties such as sensitivity and conductance. For instance, the chloride-pumping halorhodopsins^{14,15} exhibit peak activation at ~600 nm quite separated from the main photopigment rhodopsin 1 in *Drosophila* (~480 nm¹⁶). However, their strong light requirements seem inadequate for leaving photoreceptors functional. The anion channel rhodopsins GtACR1 and GtACR2 in turn mediate large photocurrents that are orders of magnitude more sensitive¹³. GtACR1 is maximally activated by 515 nm light, ~30 nm apart from rhodopsin 1. Here, we have demonstrated that this spectral difference is sufficient for independent control of visually stimulated photoreceptors and GtACR1-expressing visual neurons illuminated from the back of the head. However, not surprisingly, since the activation spectra substantially overlap (Fig. 2C), illumination has to be carefully calibrated in order to keep photoreceptor activation minimal. Cross-activation can also occur in the other direction in that visual stimuli reach and partially silence GtACR1-expressing neurons, adding another parameter to control for. In support of this notion, tangential cell responses on average are reduced in flies with T4/T5 > GtACR1 expression when using the full spatial range and luminance of our visual stimulation arena (Fig. 3D).

The family of excitatory optogenetic channels has undergone considerable technical modifications which exemplify how the above-mentioned issues could be alleviated, either by molecular engineering or genomic screening: 1) slowed kinetics rendering anion channelrhodopsins switchable could be used to maintain inhibitory conductance for some time after offset of illumination^{5,11,12,32}; or 2) anion channelrhodopsins with red-shifted activation spectra more separated from those of endogenous rhodopsins would greatly improve independent spectral control^{10,14,32,33}. Recent work has begun to expand the family of natural and artificial anion conducting channelrhodopsins in this direction to generate variants with altered kinetics and spectral sensitivities^{34,35}.

While GtACR's are rather selective for chloride ions, two studies in rats have found surprising activating effects in axon terminals. GtACR1-expressing thalamocortical terminals exhibited neurotransmitter release and, as a consequence, evoked strong and short-latency excitatory postsynaptic currents in downstream neurons upon light onset³⁶. A similar mode of action was ascribed to GtACR2, which mediated the generation of antidromic action potentials in cortical pyramidal neurons³⁷. These activating effects of GtACR's were suggested to arise by depolarized chloride reversal potentials in axon terminals. Here, in flies, we have found that tangential cells expressing GtACR1 exhibit pure hyperpolarization with a fast onset latency of 2–3 ms, as measured at the soma (Fig. 2D). Furthermore, illumination of GtACR1-expressing presynaptic T4/T5 neurons does not lead to short-latency excitatory potentials in tangential cells (Fig. 3C), as would be expected in case of transient T4/T5 activation⁷. Longer latency transients (~15 ms onset) became apparent but those are almost certainly of visual origin since they also occur in control flies without GtACR1 expression and are absent in blind flies⁷. Therefore, we consider an excitatory action of GtACR1 unlikely in flies, at least in the neuron types considered here.

In the *Drosophila* visual system and beyond, other genetic strategies are available to silence neuronal output^{4,38}. Widely used temperature-sensitive dynamin (shibire-ts³⁹) interferes with synaptic vesicle recycling and thus depletes chemical synaptic transmission. However, applied temperature changes may cause physiological or behavioral phenotypes and are in practice brought about only on slow time scales. This way, permissive and non-permissive conditions are rarely applied within a single experiment. While still useful in many cases, experiments with absent activity in downstream neurons as a consequence of chronic perturbation can be exceedingly difficult to interpret. For instance, 2-photon calcium imaging experiments often require some evoked neuronal activity to target the site of optical recording. The use of synaptic silencers can also be problematic because their efficacy may depend on the cell type and their molecular composition, as for instance indicated by differential phenotypic penetrance between expression of shibire and tetanus toxin light chain^{40,41}. Furthermore, chemical synaptic silencers do not affect transmission across gap junctions, leaving a potential source for phenotypic underestimation. Expression of the potassium channel Kir2.1⁴² circumvents this latter issue but this tool is not inducible.

Two properties of optogenetic inhibitory ion channels can overcome the above-mentioned drawbacks of conventional neurogenetic silencers: first, they are inducible and reversible on fast time scales; and second, their mode of action by opening inhibitory conductances should be applicable to any neuron type, provided a chloride reversal potential below rest, and affect chemical and electrical synaptic output alike. Transgenically expressed GtACR1 as described here makes it possible to effectively hyperpolarize selected neurons on demand in electrophysiological and behavioral preparations without marked interference with visual perception, given a specific and sufficiently strong expressing neuronal driver line. This will be very useful to probe the requirement of identified cell types for visual and other computations by taking neuronal elements out of the circuit on a trial-by-trial basis. The efficacy is dependent on light intensity and thus tunable, allowing to establish dose-response relationships. The fact that the control and experimental conditions are provided in the same individual will greatly facilitate data interpretation and statistics. Furthermore, the temporally precise silencing of neurons could be crucial to investigate the temporal integration of signals in downstream stages. Importantly, many neurons particularly in the optic lobe transmit synaptic signals in a graded fashion. Inducible hyperpolarizing channels such as GtACR's will be very useful to probe their full transmission range and to complement optogenetic depolarization studies

to characterize synaptic connectivity of candidate neurons. Finally, in order to probe behavioral causality in naturalistic contexts, one can now envisage the tantalizing possibility of switching selected neurons repeatedly off and back on again during unrestrained, visually guided behavior.

Methods

Flies. Flies were raised at 25 °C and 60% humidity on standard cornmeal agar medium at a 12 h light/dark cycle. The following fly strains were used: *vGlut-OK371-Gal4* (ref.⁴³; glutamatergic neurons targeted in the larval crawling assay; courtesy of the Bloomington Stock Center), *VT23749-Gal4^{attP2}* (lobula plate tangential cells targeted in electrophysiology; courtesy of Barry Dickson), *R42F06-Gal4^{attP2}* (ref.²⁴; T4/T5 cells targeted in electrophysiology; courtesy of Gerald Rubin), *R59E08-AD^{attP40} + VT16255-DBD^{attP2}* (T4 cells targeted in electrophysiology; previously unpublished Split-Gal4 line, kindly provided by Georg Ammer & Barry Dickson), *R59E08-AD^{attP40} + R42F06-DBD^{attP2}* (ref.³¹; Split-Gal4 line expressing in T4/T5 cells targeted in the optomotor behavior assay).

Generation of transgenic GtACR lines. GtACR1-EYFP and GtACR2-EYFP coding regions were PCR-amplified from the vectors pFUGW-hGtACR1-EYFP and pFUGW-hGtACR2-EYFP (kindly provided by John Spudich, Addgene plasmids #67795 and #67877, respectively), introducing an XbaI restriction site at the 3' end immediately after the stop codon. PCR products were then XbaI-digested and inserted via mixed sticky-blunt end ligation into the pJFRC7-20XUAS backbone (obtained by XhoI digestion, blunting via T4 DNA polymerase and XbaI digestion of pJFRC7-20XUAS-IVS-mCD8::GFP, kindly provided by Gerald Rubin, Addgene plasmid #26220). The resulting vectors pJFRC7-20XUAS-GtACR1-EYFP and pJFRC7-20XUAS-GtACR2-EYFP were sent to the Department of Genetics Fly Facility, University of Cambridge, for injection and phiC31-mediated integration²¹ into landing sites attP40 on 2nd and VK00005 on 3rd chromosome to obtain transgenic UAS fly strains. All experiments presented in this paper were done with 3rd chromosomal VK00005 insertions. However, we have also tested 2nd chromosomal attP40 *UAS-GtACR1* and *UAS-GtACR2* insertions in the larval crawling assay without detecting any discernible difference in performance (data not shown).

Genotypes used for experiments. Figure 1: (1) *w⁻/w⁻*; *vGlut-Gal4/vGlut-Gal4*; + (“Control (vGlut)”, no expression), (2) *w⁻/w⁻*; *vGlut-Gal4/+*; *UAS-GtACR1-EYFP/+* (“vGlut>GtACR1”, GtACR1 expression in glutamatergic neurons), (3) *w⁻/w⁻*; *vGlut-Gal4/+*; *UAS-GtACR2-EYFP/+* (“vGlut>GtACR2”, GtACR2 expression in glutamatergic neurons). Figure 2: (1) *w⁻/w⁻*; +; *UAS-GtACR1-EYFP/UAS-GtACR1-EYFP* (“Control (GtACR1)”, no expression) (2) *w⁻/w⁻*; +; *VT23749-Gal4/UAS-GtACR1-EYFP* (“LPTC>GtACR1”, GtACR1 expression in lobula plate tangential cells). Figure 3: (1) *w⁻/w⁻*; +; *UAS-GtACR1-EYFP/UAS-GtACR1-EYFP* (“Control (GtACR1)”, no expression) (2) *w⁻/w⁻*; +; *R42F06-Gal4/UAS-GtACR1-EYFP* (“T4/T5>GtACR1”, GtACR1 expression in T4/T5 cells) (3) *w⁻/w⁻*; *R59E08-AD/+*; *VT16255-DBD/UAS-GtACR1-EYFP* (“T4>GtACR1”, GtACR1 expression in T4 cells). Figure 4: (1) *w⁺/w⁺*; +; *UAS-GtACR1-EYFP/UAS-GtACR1-EYFP* (“Control (GtACR1)”, no expression) (2) *w⁺/w⁺*; *R59E08-AD/R59E08-AD*; *R42F06-DBD/R42F06-DBD* (“Control (T4/T5)”, no expression) (3) *w⁺/w⁺*; *R59E08-AD/+*; *R42F06-DBD/UAS-GtACR1-EYFP* (“T4/T5>GtACR1”, GtACR1 expression in T4/T5 cells).

Larval crawling assay. Larvae were raised in standard cornmeal agar medium supplemented with 1 mM *all-trans* retinal (ATR, R2500; Sigma Aldrich), a necessary co-factor of channelrhodopsins. 3rd instar larvae were released in batches of ~10 into a petri dish (diameter 3.5 cm) coated with a thin layer of 2% agarose. For each genotype, wavelength and light intensity, a minimum number of 16 and on average 26.6 ± 6.2 (S.D.) larvae were tracked.

Optogenetic stimulation. Larvae were exposed to illumination from blue (457 nm peak), green (527 nm peak) and red (640 nm peak) LUXEON Rebel LEDs below, controlled from Python2.7 via a bus-powered multifunction DAQ USB device (USB-6008/6009, National Instruments).

Image capture. Larvae were filmed from above with a PointGrey USB3.0 camera (FL3-U3-13S2M-CS) equipped with a Fujinon lens (LENS-30F2-V80CS, 2.8-8mm focal length) at 19 frames per second. The petri dish was backlit with infrared light at 850 nm (Vishay Semiconductors, VSMY1850x01). To filter out optogenetic illumination, a 715 nm longpass filter was mounted in front of the camera (Thorlabs, FGL715S). Images were captured using the software Point Grey FlyCapture (in trigger mode) as avi files.

Tracking. Image analysis was performed using the openCV3.1 library in Python3.5. Briefly, the first frame was subtracted from all other frames, positively labeling only changing pixels, i.e. moving larvae. A threshold was applied to segment the images into binary positively and negatively labeled pixels. Contours were fitted to connected pixels using the function `cv2.findContours`. Overlapping contours from multiple larvae were discarded based on a fixed area threshold, avoiding potentially incorrect tracking of larvae within close proximity. The center of mass (centroid) was extracted from each contour (`cv2.moments`) and a rectangle was fitted (`cv2.boxPoints`). Centroids of contours and lengths of rectangles in each frame provided the measures used for quantification. After the initial detection of a moving larvae, a unique identifier was assigned. This identifier was used to track larvae over time, based on the nearest centroid position in the past frames. Larva crawling tracks were discarded, when one of the following and other criteria applied: contours were missing in > 25 consecutive frames or 28 frames in total; average crawling velocity in the time before illumination was below 0.4 mm/s; many or large jumps in position were detected.

Electrophysiology assay. For electrophysiology, freshly hatched female flies were collected and fed for 1 d with yeast paste containing 1 mM ATR. Fly preparation, whole-cell patch-clamp electrophysiology, visual and optogenetic stimulation were performed as described previously^{6,7,44}, briefly outlined below. We recorded exclusively from tangential cells of the vertical system, i.e. VS cells²², tuned to downward motion.

Preparation and recording. Flies were tethered with their thorax to a plexiglass holder with bees wax and mounted below a recording chamber to gain access to the back of the head via a small cut-out in the chamber. The cuticle was removed with a hypodermic needle. Under a microscope equipped with polarized light contrast, the glia sheath covering the brain was ruptured using a pulled and collagenase-filled glass capillary⁴⁵ (~5 μm opening) with a combination of mechanical tearing and enzymatic digestion. Whole-cell patch-clamp recordings (current clamp) were obtained from exposed tangential cell bodies with electrodes of 4–7 M Ω resistance. Signals were amplified via a BA-1S bridge amplifier (npi Electronics), low-pass filtered at 3 kHz, and digitized at 10 kHz using an analog/digital converter (PCI-DAS6025; Measurement Computing). Data were acquired in Matlab (R2010b; Mathworks) using the data acquisition toolbox. Normal external solution contained the following (in mM): 103 NaCl, 3 KCl, 5 TES, 10 trehalose, 10 glucose, 3 sucrose, 26 NaHCO₃, 1 NaH₂PO₄, 1.5 CaCl₂, and 4 MgCl₂, pH 7.3–7.35, ~280 mOsmol/kg. External solution was carboxygenated (95% O₂/5% CO₂) and constantly perfused over the preparation at 2 ml/min. Internal solution, adjusted to pH 7.26 with 1 N KOH, contained the following: 140 K-aspartate, 10 HEPES, 4 Mg-ATP, 0.5 Na-GTP, 1 EGTA, 1 KCl (~265 mOsmol/kg).

Visual stimulation. A custom-built LED arena was used for visual stimulation in electrophysiology experiments. The design is based on ref.⁴⁶. The arena covered approx. 170° and 90° in azimuth and elevation, respectively, and allowed refresh rates of 550 Hz and 16 intensity levels²³. LEDs had an emittance peak at approximately 565 nm and a luminance range from 0 to 51 cd m⁻². The following stimuli were used in electrophysiology experiments: 1) Moving square wave gratings (spatial wavelength of 24°) at full arena contrast displayed across the entire arena or in a smaller region of the arena (~90° azimuth \times ~45° elevation). In between static presentations, the grating was moved in the preferred direction of recorded tangential cells (downward) at a velocity of 24°/s (Fig. 3D) or 19.2°/s (Fig. 3E), corresponding to a temporal frequency of 1 and 0.8 Hz, respectively. 2) An initially static square wave grating (spatial wavelength of 24°) at 30% reduced luminance was presented in a rectangular window of 72° \times 72°. Then either ON or OFF edges were moved downward at a velocity of 12°/s (Fig. 3F).

Optogenetic stimulation. Optogenetic stimulation was performed as previously described⁷. Light pulses were delivered by a Lambda DG-4 Plus wavelength switcher (Sutter Instrument) with a 300 W Xenon Arc lamp via the epifluorescence light path of the microscope through a 40x/0.8 NA water-immersion objective (LUMPlan FI; Olympus). Light was passed through the following band pass filters: HQ535/30 (Chroma), HQ565/30 (Chroma), FF01-615/20-25 (Semrock). Intensities under the objective were measured with a power meter (Thorlabs PM100D) in air to estimate the irradiance per illuminated area in immersion.

Optomotor behavior assay. Female flies were selected 1–2 days after eclosion. They were fed with yeast-paste containing 1 mM ATR and kept for two days at 25 °C, 60% humidity on a 12 h dark, 12 h blue light cycle.

Tethering flies. Flies were cooled down to 2 °C. The tip of a needle was positioned between head and thorax, slightly tilting the head forwards, allowing direct optogenetic stimulation of the back of the head. Using near-ultraviolet bonding glue (Sinfony Opaque Dentin), which was dried by blue LED light (440 nm, curing light, Guilin Woodpecker Medical Instruments Co., Ltd.), head, thorax and wings were tethered to the needle.

Visual stimulation. Behavioral experiments were performed on a locomotion recorder (as described in ref.³⁰), using three 144 Hz Monitors (XL2411Z, BenQ). The panels on the monitors were separated from the casing, covered with diffusion foil and vertically arranged into a U-shape. The resulting visual arena has a dimension of 30.5 \times 33.5 \times 56 cm and a luminance range from 0 to 220 cd m⁻². The coverage of the fly's visual field was \pm 135° horizontally and \pm 61° vertically with a pixel size smaller than 0.09°. All visual patterns were rendered on a virtual, upright cylinder surrounding the fly, which was positioned in the center of the arena. An additional camera (CM3-U3-13S2C-CS, Point Grey Research) was located on top of the fly, which allowed precise positioning of optogenetic stimulation. All experiments were performed at 34 °C to motivate flies to walk. The following two stimuli were used in the behavioral optomotor assay: 1) Initially static vertical stripes with 10° width and random uniformly sampled intensity were presented only on the left or right side of the fly (+135° to +90° or -90° to -135° in azimuth). After optogenetic stimulation was turned on, the visual pattern was rotated for 2 s with an angular velocity of 80°/s clockwise or counter-clockwise. Subsequently, optogenetic stimulation was turned off - still showing the static visual pattern (Fig. 4C,D). 2) Initially static vertical stripes with 10° width and random uniformly sampled intensity were presented on the left and right side of the fly (resp. +135° to +90° and -90° to -135° in azimuth). As in experiment 1, optogenetic stimulation was turned on shortly after the visual pattern was presented. Subsequently, the visual patterns on both sides were rotated simultaneously front-to-back or back-to-front (angular velocity of 80°/s). Finally, optogenetic stimulation was turned off - still showing the static visual pattern again (Fig. 4E,F).

Optogenetic stimulation. Optogenetic illumination was performed using a 565 nm LED (M565F1, Thorlabs), which was coupled into an optical fiber with 105 μm core diameter (M15L01, Thorlabs). A matched achromatic doublet pair (MAP051950-A, Thorlabs) was used to focus the outgoing light from the fiber onto the fly's head, resulting in a spot of 0.12 mm², similar as described in ref.⁵. Light intensity was measured using a power energy meter (PM100D, Thorlabs).

References

- Fenno, L., Yizhar, O. & Deisseroth, K. The development and application of optogenetics. *Annu. Rev. Neurosci.* **34**, 389–412 (2011).
- Zhang, F. *et al.* The microbial opsin family of optogenetic tools. *Cell* **147**, 1446–1457 (2011).
- Borst, A. & Helmstaedter, M. Common circuit design in fly and mammalian motion vision. *Nat. Neurosci.* **18**, 1067–1076 (2015).
- Borst, A. *Drosophila's* view on insect vision. *Curr. Biol.* **19**, R36–47 (2009).
- Haikala, V., Joesch, M., Borst, A. & Mauss, A. S. Optogenetic control of fly optomotor responses. *J. Neurosci.* **33**, 13927–13934 (2013).
- Mauss, A. S. *et al.* Neural circuit to integrate opposing motions in the visual field. *Cell* **162**, 351–362 (2015).
- Mauss, A. S., Meier, M., Serbe, E. & Borst, A. Optogenetic and pharmacologic dissection of feedforward inhibition in *Drosophila* motion vision. *J. Neurosci.* **34**, 2254–2263 (2014).
- Wu, M. *et al.* Visual projection neurons in the *Drosophila* lobula link feature detection to distinct behavioral programs. *Elife* **5**, e21022 (2016).
- de Vries, S. E. J. & Clandinin, T. R. Loom-sensitive neurons link computation to action in the *Drosophila* visual system. *Curr. Biol.* **22**, 353–362 (2012).
- Klapoetke, N. C. *et al.* Independent optical excitation of distinct neural populations. *Nat. Meth.* **11**, 338–346 (2014).
- Berndt, A., Yizhar, O., Gunaydin, L. A., Hegemann, P. & Deisseroth, K. Bi-stable neural state switches. *Nature Neuroscience* **12**, 229–234 (2009).
- Yizhar, O. *et al.* Neocortical excitation/inhibition balance in information processing and social dysfunction. *Nature* **477**, 171–178 (2011).
- Govorunova, E. G., Sineshchekov, O. A., Janz, R., Liu, X. & Spudich, J. L. Natural light-gated anion channels: A family of microbial rhodopsins for advanced optogenetics. *Science* **349**, 647–650 (2015).
- Chuong, A. S. *et al.* Noninvasive optical inhibition with a red-shifted microbial rhodopsin. *Nature Neuroscience* **17**, 1123–1129 (2014).
- Gradinaru, V. *et al.* Molecular and cellular approaches for diversifying and extending optogenetics. *Cell* **141**, 154–165 (2010).
- Britt, S. G., Feiler, R., Kirschfeld, K. & Zuker, C. S. Spectral tuning of rhodopsin and metarhodopsin *in vivo*. *Neuron* **11**, 29–39 (1993).
- Salcedo, E. *et al.* Blue- and green-absorbing visual pigments of *Drosophila*: ectopic expression and physiological characterization of the R8 photoreceptor cell-specific Rh5 and Rh6 rhodopsins. *J. Neurosci.* **19**, 10716–10726 (1999).
- Wardill, T. J. *et al.* Multiple spectral inputs improve motion discrimination in the *Drosophila* visual system. *Science* **336**, 925–931 (2012).
- Mohammad, F. *et al.* Optogenetic inhibition of behavior with anion channelrhodopsins. *Nat. Meth.* **14**, 271–274 (2017).
- Pfeiffer, B. D. *et al.* Refinement of tools for targeted gene expression in *Drosophila*. *Genetics* **186**, 735–755 (2010).
- Groth, A. C., Fish, M., Nusse, R. & Calos, M. P. Construction of transgenic *Drosophila* by using the site-specific integrase from phage ϕ C31. *Genetics* **166**, 1775–1782 (2004).
- Joesch, M., Plett, J., Borst, A. & Reiff, D. F. Response properties of motion-sensitive visual interneurons in the lobula plate of *Drosophila melanogaster*. *Curr. Biol.* **18**, 368–374 (2008).
- Maisak, M. S. *et al.* A directional tuning map of *Drosophila* elementary motion detectors. *Nature* **500**, 212–216 (2013).
- Schnell, B., Raghu, S. V., Nern, A. & Borst, A. Columnar cells necessary for motion responses of wide-field visual interneurons in *Drosophila*. *J. Comp. Physiol. A* **198**, 389–395 (2012).
- Joesch, M., Schnell, B., Raghu, S. V., Reiff, D. F. & Borst, A. ON and OFF pathways in *Drosophila* motion vision. *Nature* **468**, 300–304 (2010).
- Arenz, A., Drews, M. S., Richter, F. G., Ammer, G. & Borst, A. The temporal tuning of the *Drosophila* motion detectors is determined by the dynamics of their input elements. *Curr. Biol.* **27**, 929–944 (2017).
- Serbe, E., Meier, M., Leonhardt, A. & Borst, A. Comprehensive characterization of the major presynaptic elements to the *Drosophila* OFF motion detector. *Neuron* **89**, 829–841 (2016).
- Strother, J. A. *et al.* The emergence of directional selectivity in the visual motion pathway of *Drosophila*. *Neuron* **94**, 168–182.e10 (2017).
- Borst, A. Fly visual course control: behaviour, algorithms and circuits. *Nat. Rev. Neurosci.* **15**, 590–599 (2014).
- Bahl, A., Ammer, G., Schilling, T. & Borst, A. Object tracking in motion-blind flies. *Nat. Neurosci.* **16**, 730–738 (2013).
- Schilling, T. & Borst, A. Local motion detectors are required for the computation of expansion flow-fields. *Biol. Open* **4**, 1105–1108 (2015).
- Mattis, J. *et al.* Principles for applying optogenetic tools derived from direct comparative analysis of microbial opsins. *Nat. Meth.* **9**, 159–172 (2012).
- Zhang, F. *et al.* Red-shifted optogenetic excitation: a tool for fast neural control derived from *Volvox carterii*. *Nat. Neurosci.* **11**, 631–633 (2008).
- Govorunova, E. G. *et al.* The expanding family of natural anion Channelrhodopsins reveals large variations in kinetics, conductance, and spectral sensitivity. *Sci. Rep.* **7**, 43358 (2017).
- Wietek, J. *et al.* Anion-conducting channelrhodopsins with tuned spectra and modified kinetics engineered for optogenetic manipulation of behavior. *Sci. Rep.* (in press).
- Mahn, M., Prigge, M., Ron, S., Levy, R. & Yizhar, O. Biophysical constraints of optogenetic inhibition at presynaptic terminals. *Nat. Neurosci.* **19**, 554–556 (2016).
- Malyshev, A. Y. *et al.* Chloride conducting light activated channel GtACR2 can produce both cessation of firing and generation of action potentials in cortical neurons in response to light. *Neurosci. Lett.* **640**, 76–80 (2017).
- Venken, K. J. T., Simpson, J. H. & Bellen, H. J. Genetic manipulation of genes and cells in the nervous system of the fruit fly. *Neuron* **72**, 202–230 (2011).
- Kitamoto, T. Conditional modification of behavior in *Drosophila* by targeted expression of a temperature-sensitive shibire allele in defined neurons. *J. Neurobiol.* **47**, 81–92 (2001).
- Sweeney, S. T., Broadie, K., Keane, J., Niemann, H. & O’Kane, C. J. Targeted expression of tetanus toxin light chain in *Drosophila* specifically eliminates synaptic transmission and causes behavioral defects. *Neuron* **14**, 341–351 (1995).
- Thum, A. S. *et al.* Differential potencies of effector genes in adult *Drosophila*. *J. Comp. Neurol.* **498**, 194–203 (2006).
- Baines, R. A., Uhler, J. P., Thompson, A., Sweeney, S. T. & Bate, M. Altered electrical properties in *Drosophila* neurons developing without synaptic transmission. *J. Neurosci.* **21**, 1523–1531 (2001).
- Mahr, A. & Aberle, H. The expression pattern of the *Drosophila* vesicular glutamate transporter: a marker protein for motoneurons and glutamatergic centers in the brain. *Gene Expr. Patterns* **6**, 299–309 (2006).
- Mauss, A. S. & Borst, A. Electrophysiological recordings from lobula plate tangential cells in *Drosophila*. *Methods Mol. Biol.* **1478**, 321–332 (2016).
- Maimon, G., Straw, A. D. & Dickinson, M. H. Active flight increases the gain of visual motion processing in *Drosophila*. *Nat. Neurosci.* **13**, 393–399 (2010).
- Reiser, M. B. & Dickinson, M. H. A modular display system for insect behavioral neuroscience. *J. Neurosci. Methods* **167**, 127–139 (2008).

Acknowledgements

We are very grateful to Wolfgang Essbauer (molecular cloning), Michael Sauter (larva behavioral experiments), and Stefan Prech (larva behavioral LED arena) for excellent technical assistance. Fly lines were kindly provided by Gerald Rubin, Georg Ammer, Barry Dickson and Bloomington. Constructs for generating UAS-GtACR1 and UAS-GtACR2 flies were obtained from Addgene, generously supplied by Gerald Rubin and John Spudich. We further acknowledge 'The University of Cambridge Department of Genetics Fly Facility' for microinjection services. We greatly appreciate helpful feedback on the manuscript from Alexander Arenz, Matthias Meier and Aljoscha Leonhardt. Funding was provided by the Max-Planck-Society and the SFB 870 of the German Science Foundation.

Author Contributions

A.S.M. and A.B. conceptualized the project. A.S.M., C.B. and A.B. conceived the experiments. A.S.M. and C.B. conducted the experiments and analyzed the results. A.S.M. wrote the manuscript, with the help of all other authors.

Additional Information

Competing Interests: The authors declare that they have no competing interests.

Publisher's note: Springer Nature remains neutral with regard to jurisdictional claims in published maps and institutional affiliations.



Open Access This article is licensed under a Creative Commons Attribution 4.0 International License, which permits use, sharing, adaptation, distribution and reproduction in any medium or format, as long as you give appropriate credit to the original author(s) and the source, provide a link to the Creative Commons license, and indicate if changes were made. The images or other third party material in this article are included in the article's Creative Commons license, unless indicated otherwise in a credit line to the material. If material is not included in the article's Creative Commons license and your intended use is not permitted by statutory regulation or exceeds the permitted use, you will need to obtain permission directly from the copyright holder. To view a copy of this license, visit <http://creativecommons.org/licenses/by/4.0/>.

© The Author(s) 2017

3.2 BI-DIRECTIONAL CONTROL OF WALKING BEHAVIOR BY HORIZONTAL OPTIC FLOW SENSORS

This study investigated the behavioral effects of optogenetic induced de- and hyperpolarization of HS cells in tethered walking *Drosophila*. Such manipulations, mimicking visual responses, evoked syndirectional turning and therefore showed that the sign of HS cell responses encodes two steering signals. The study was published in *Current Biology* in December 2018.

SUMMARY For many sighted animals, including flies, optic flow is thought to provide important feedback information about self-motion. *Drosophila* has dedicated neurons that respond to specific optic flow patterns. Hereof, horizontal system (HS) cells respond to horizontal motion: depolarizing for front-to-back motion, hyperpolarizing for back-to-front motion. Within this work, we studied the functional importance of HS cells for steering behavior in a tethered walking assay. Using optogenetic tools, we introduced unilateral de- and hyperpolarizations on the level of HS cells, which evoked turning in opposite directions. Thus, both signals are transmitted to downstream pathways. Furthermore, bilateral induced de- and hyperpolarization evoked a reduction in walking velocity. This indicates a functional architecture where HS cell signals are split into two decelerating pathways.

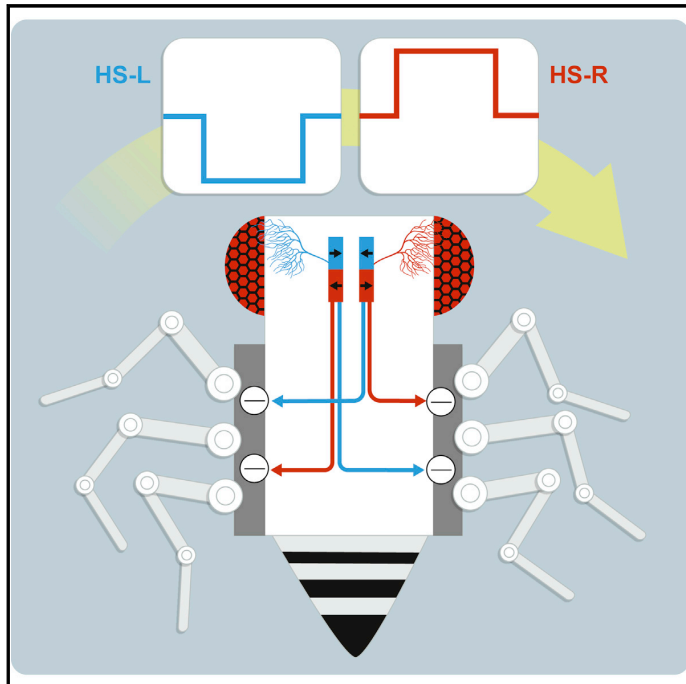
AUTHORS Christian Busch, Alexander Borst, and Alex S. Mauss.

CONTRIBUTIONS Conceptualization, A.S.M., C.B., and A.B.; Methodology, A.S.M., C.B., and A.B.; Formal Analysis, A.S.M. and C.B.; Investigation, A.S.M. and C.B.; Writing – Original Draft, A.S.M.; Writing – Review & Editing, A.S.M., C.B., and A.B.; Supervision, A.S.M. and A.B.; Funding Acquisition, A.S.M. and A.B..

Current Biology

Bi-directional Control of Walking Behavior by Horizontal Optic Flow Sensors

Graphical Abstract



Authors

Christian Busch, Alexander Borst,
Alex S. Mauss

Correspondence

amauss@neuro.mpg.de

In Brief

Busch et al. study the behavioral effects of manipulating optic flow-sensing HS cells in tethered walking *Drosophila*. Both de- and hyperpolarization elicit turning syndirectional with the mimicked visual motion. Therefore, two steering signals are encoded in the HS cell-response sign, likely mediating the fly's tendency to follow a rotating pattern.

Highlights

- Horizontal optic flow detectors (HS cells) affect turning in walking flies
- De- and hyperpolarization evoke opposite turning
- Both signals negatively influence walking speed
- HS cells thus mediate bi-directional turning via asymmetric deceleration

Busch et al., 2018, Current Biology 28, 1–9
December 17, 2018 © 2018 Elsevier Ltd.
<https://doi.org/10.1016/j.cub.2018.11.010>

CellPress

Bi-directional Control of Walking Behavior by Horizontal Optic Flow Sensors

Christian Busch,¹ Alexander Borst,¹ and Alex S. Mauss^{1,2,*}

¹Circuits - Computation - Models, Max Planck Institute of Neurobiology, Am Klopferspitz 18, Martinsried 82152, Germany

²Lead Contact

*Correspondence: amauss@neuro.mpg.de

<https://doi.org/10.1016/j.cub.2018.11.010>

SUMMARY

Moving animals experience constant sensory feedback, such as panoramic image shifts on the retina, termed optic flow. Underlying neuronal signals are thought to be important for exploratory behavior by signaling unintended course deviations and by providing spatial information about the environment [1, 2]. Particularly in insects, the encoding of self-motion-related optic flow is well understood [1–5]. However, a gap remains in understanding how the associated neuronal activity controls locomotor trajectories. In flies, visual projection neurons belonging to two groups encode panoramic horizontal motion: horizontal system (HS) cells respond with depolarization to front-to-back motion and hyperpolarization to the opposite direction [6, 7], and other neurons have the mirror-symmetrical response profile [6, 8, 9]. With primarily monocular sensitivity, the neurons' responses are ambiguous for different rotational and translational self-movement components. Such ambiguities can be greatly reduced by combining signals from both eyes [10–12] to determine turning and movement speed [13–16]. Here, we explore the underlying functional logic by optogenetic HS cell manipulation in tethered walking *Drosophila*. We show that de- and hyperpolarization evoke opposite turning behavior, indicating that both direction-selective signals are transmitted to descending pathways for course control. Further experiments reveal a negative effect of bilaterally symmetric de- and hyperpolarization on walking velocity. Our results are therefore consistent with a functional architecture in which the HS cells' membrane potential influences walking behavior bi-directionally via two decelerating pathways.

RESULTS

In the fly optic lobe, optic flow-sensing tangential cells can be found in the lobula plate, four synapses downstream of photoreceptors (Figure 1A). They receive excitatory input from local motion detectors, T4/T5 cells [17, 18], and inhibitory input from

bi-stratified relay neurons, termed LPi [19] (Figure 1B). T4/T5 terminals are sorted according to their directional preference into four layers such that opposite directions of motion are represented side by side [18, 21]. As a consequence, predominantly mono-stratified tangential cells respond with depolarization to motion along their preferred direction (PD) and hyperpolarization to motion along the opposite or null direction (ND) motion [6, 7]. Because tangential cells in layer 1 and 2 exhibit mirror-symmetrical motion preferences, any horizontal motion (front-to-back or back-to-front) is simultaneously represented in layer 1 and 2 cells by responses with opposite signs (Figure 1C). Here, we explore how such signals control walking behavior by conceptualizing a fly as a Braitenberg vehicle [20], with left and right motors representing the fly walking apparatus (Figures 1D–1G). Each horizontal motion detector comprises a PD and an ND channel that convey direction-selective signals. Those are negatively or positively connected to left and right motors such that the connectivity supports turning syndirectional with horizontal motion. For instance, activating front-to-back-selective signals on the left side can either accelerate the right motor (Figures 1D and 1F) or decelerate the left motor (Figures 1E and 1G) to mediate syndirectional leftward turning. We ask (1) whether only PD signals (carried by depolarizations) are conveyed to downstream neurons to affect locomotor behavior (Figures 1D and 1E) or whether ND signals (carried by hyperpolarizations) also contribute (Figures 1F and 1G) and (2) whether the signals act positively (Figures 1D and 1F) or negatively (Figures 1E and 1G) on the propulsive forces underlying walking [13].

Visual and Optogenetic Control over Horizontal System Cell Activity

To address the functional logic underlying steering by horizontal PD and ND signals, we expressed two different light-activatable channels in horizontal system (HS) cells, which allowed us to induce PD- and ND-like activities: depolarizing cation-conducting ReaChR [22, 23] and hyperpolarizing chloride-conducting GtACR1 [24, 25]. We characterized visual and optogenetic effects of illumination on the HS cells' membrane potential by *in vivo* patch-clamp recordings (Figure 2A). HS cells in control flies (without expression) exhibited depolarizing ON and OFF transients and subtle tonic depolarization in response to 565 nm light, indicating that the light pulse delivered through the microscope is visually perceived by flies (Figure 2B, black trace). This is expected, given the large dynamic range in which visual systems operate. The responses of ReaChR- and GtACR1-expressing HS cells were markedly different in that

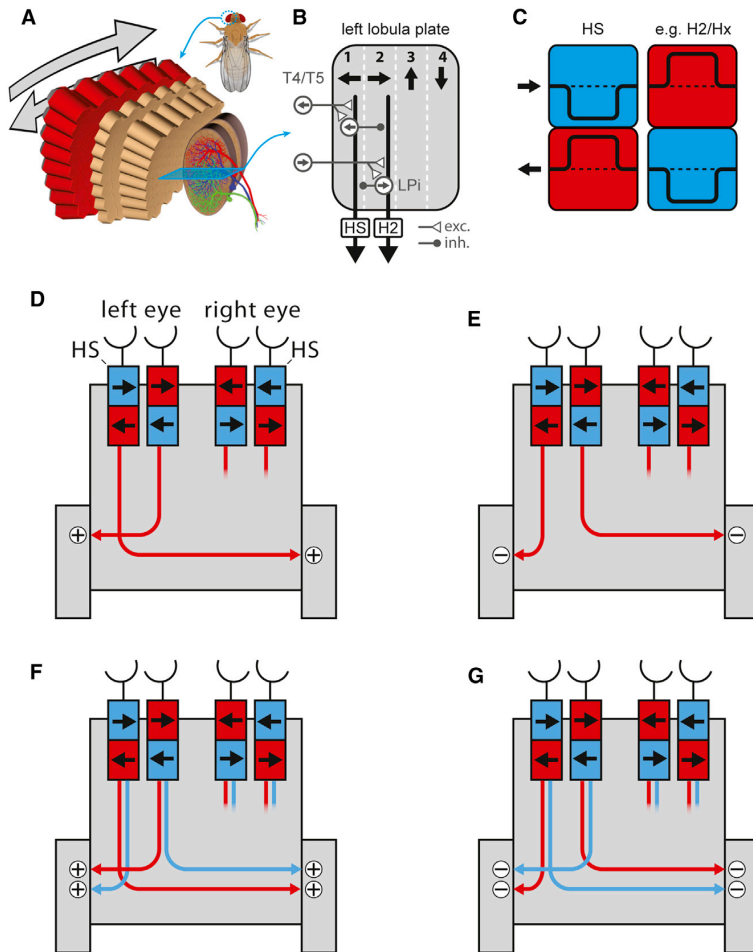


Figure 1. Course Control by Horizontal Optic Flow Sensors

(A) The fly optic lobe (left side) in schematic form, with HS cells of the lobula plate shown.

(B) The functional organization of the lobula plate. T4/T5 terminals provide excitatory inputs [17], sorted into 4 layers according to their directional preference [18]. Mono-stratified tangential cells are thus excited for motion in their preferred direction (PD). Opposite, null direction (ND) inhibition presumably arises by sign-inverting feedforward connections across motion-opponent layers via LPi neurons, as shown for layer 4 tangential cells [19]. Note that the focus here lies on HS cells, with H2 given as one layer 2 example.

(C) Tangential cells of layer 1 (HS cells) and 2 (e.g., H2 or Hx cells) exhibit mirror-symmetrical PD (red) and ND (blue) motion responses.

(D–G) Different versions of a fly conceived as a Braitenberg vehicle [20]. Inputs represent the mirror-symmetrical layer 1 (HS) and 2 lobula plate tangential cells each comprising a PD (red) and ND channel (blue). Signals carried by these channels impinge on left and right motors with positive (+) or negative (–) effect but in all cases supporting turning syndirectional with the perceived horizontal motion direction.

(D and E) Only PD signals are connected to motors, either with a positive (D) or negative (E) effect.

(F and G) Additional ND signals are connected, again either with a positive (F) or negative (G) effect.

they tonically de- and hyperpolarized, respectively, with amplitudes depending on log light intensity with a sigmoidal relationship (Figures 2B and 2C). Above 10 and $2.5 \mu\text{W}/\text{mm}^2$, respectively, visual ON and OFF transients were masked by these robust responses. Apart from the sign, both channels mediated large maximal potential changes of comparable amplitudes (~ 20 mV). However, GtACR1 responses were slightly more light sensitive (50% response at $6.5 \mu\text{W}/\text{mm}^2$ for GtACR1 as opposed to $24.8 \mu\text{W}/\text{mm}^2$ for ReaChR; Figure 2C). Furthermore, imparted HS cell potential changes differed in the time course for the two channels: for responses of comparable amplitudes, ReaChR-mediated depolarization had ON and OFF time constants of 31 and 172 ms, respectively, and GtACR1-mediated hyperpolarization exhibited ON and OFF time constants of 9 and 609 ms (Figures 2B and S1).

We then combined optogenetic HS cell manipulation with visual stimulation (Figure 2D). A preferred direction motion stimulus on its own depolarized HS cells and a null direction motion stimulus led to hyperpolarization. In control flies, with increasing optogenetic light intensity, visually mediated responses were only affected at high illumination intensities, presumably due

to photoreceptor activation, leading to a reduced perceived grating contrast. This shows that dimmer optogenetic illumination leaves visual photoreceptor signals intact. Repeating this protocol in flies expressing ReaChR and GtACR1 in the recorded HS cells led to robust potential changes superimposed on the visual response. PD depolarization was enhanced by ReaChR and reduced by GtACR1 (Figures 2D and 2E). The opposite was true for visually mediated ND hyperpolarization, which was enhanced by GtACR1 and reduced by ReaChR. Therefore, ReaChR and GtACR1 are suitable tools to fast and reversibly control HS cell activity in either response direction, without compromising visual signals in photoreceptors.

Monocular HS Cell De- and Hyperpolarization Elicit Opposite Turning Responses

Next, we explored the effects of monocular HS cell activity manipulations in tethered walking flies (Figure 3A). We performed experiments with five different lines, all sharing expression of optogenetic tools in HS cells (R27B03, R24E09, R81G07, VT023749, and VT058487) [26] at various degrees of strength and selectivity. This way, we reduced the risk of misinterpreting phenotypes arising from off-target expression. Initially, we expressed ReaChR using all five driver lines and tested optomotor responses to a monocular visual stimulus moving front to back (results for one line shown in Figure 3B). Flies of three out of the five genotypes showed normal optomotor response behavior

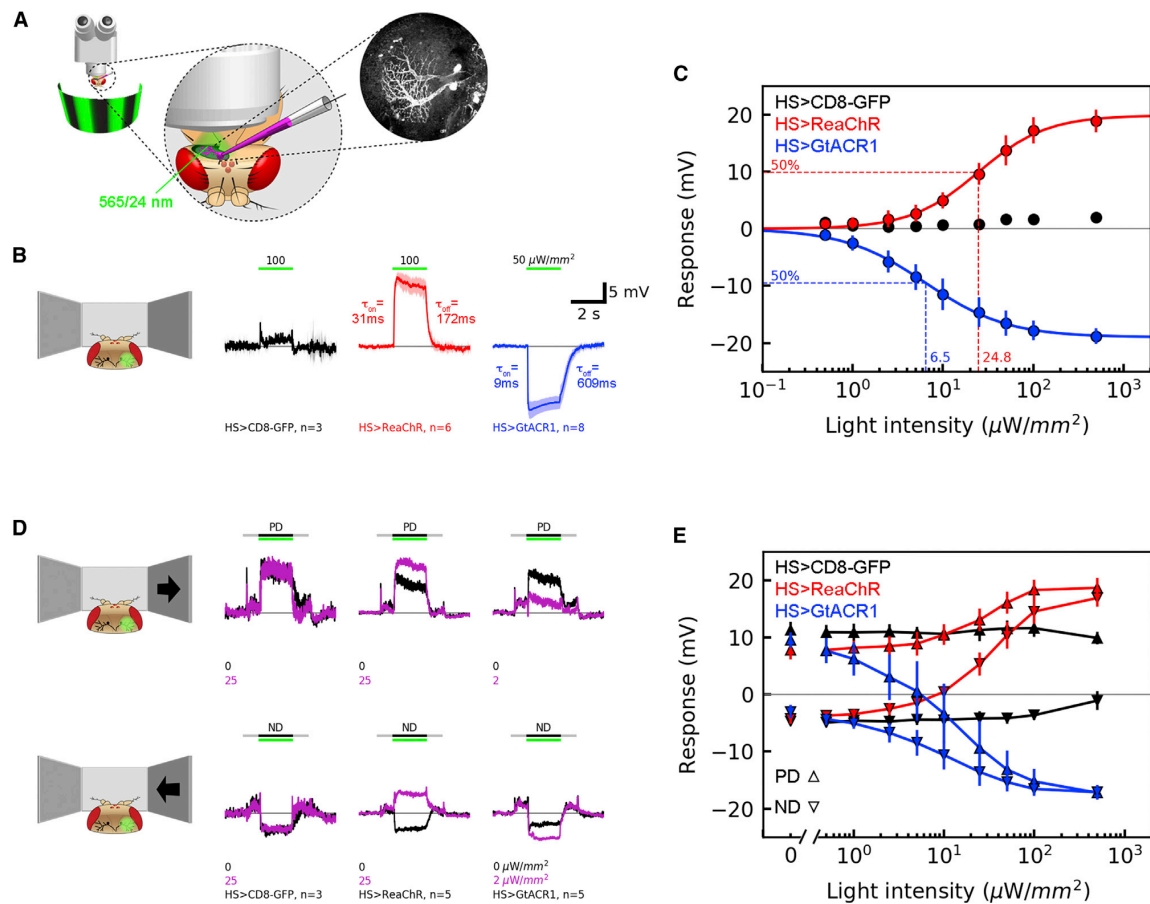


Figure 2. Optogenetic Manipulation of HS Cell Activity

(A) Illustration of recording setup. HS cell membrane potential is obtained via whole-cell patch-clamp recording. Optogenetic illumination is delivered via the microscope objective by passing light through an optical filter with 565 nm center wavelength and 24 nm bandwidth. Visual motion stimulation is provided by a light-emitting diode (LED) screen in front of the fly.

(B) HS cell recording traces averaged across trials and cells. 2 s illumination of control flies (without expression) has modest and mostly transient visual effects on membrane potential. In contrast, ReaChR- and GtACR1-expressing HS cells exhibit robust de- and hyperpolarization, respectively. To assess optogenetic response dynamics, an exponential decay function was fit to response onset and offset to obtain the time constants τ_{ON} and τ_{OFF} (see STAR Methods and Figure S1).

(C) Quantification of experiment shown in (B) for nine light intensities. Data are presented as baseline subtracted light responses. A sigmoid function (see STAR Methods) was fit to the ReaChR and GtACR1 data points and used to determine the light intensity for evoking 50% of the maximal response.

(D) Same as (B) but with simultaneous PD and ND visual motion stimulation. 1 s before and after grating motion, the grating was stationary (gray bars), causing ON and OFF transients upon appearance and disappearance. Potential changes during grating motion are a combination of visual and optogenetic responses.

(E) Quantification as in (C). Note that visual responses in control flies (without expression) are compromised only at the highest light intensity ($500 \mu\text{W}/\text{mm}^2$; close to optogenetic channel saturation), due to photoreceptor activation presumably reducing the perceived visual contrast. Data are presented as mean \pm SD (omitted in D) across 2 trials and n flies. See also Figure S1.

(R27B03, VT023749, and VT058487). However, flies of two genotypes exhibited impaired optomotor responses, indicating unspecific visual or motor defects, and were therefore excluded from further optogenetic experiments (R24E09 and R81G07). In the three remaining genotypes, we optogenetically depolarized HS cells on one side of the head, which evoked turning toward the side of illumination (Figures 3B–3D). This response is syndirectional with the mimicked visual motion direction (front to back) and in agreement with published literature [14], where

HS axon depolarization via ATP-gated P2X2 channel activation evoked similar turning. The comparison between visual and optogenetically induced turning (Figure 3C) shows that the initial average turning response to monocular visual stimulation (dashed lines) is comparable to optogenetically induced turning. However, the dynamics are different in that visually evoked turning is tonic and optogenetic responses are more phasic in nature. Furthermore, the optogenetically induced turning response peaked at a certain illumination intensity and then

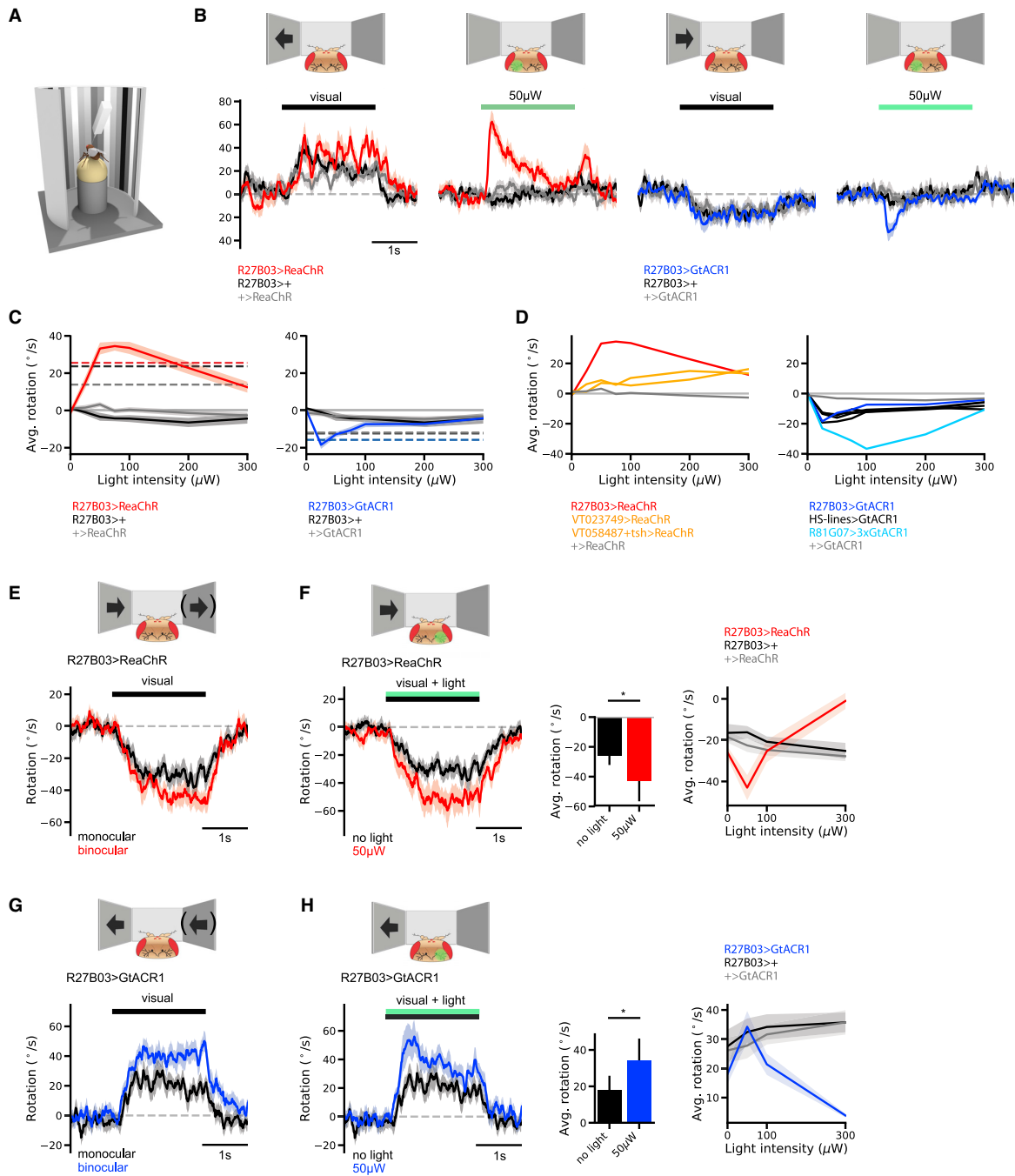


Figure 3. Visually and Optogenetically Evoked Turning Behavior

(A) Illustration of the tethered walking setup (see STAR Methods).

(B) Comparison between monocular visual and optogenetic induced turning, using ReaChR and GtACR1.

(C) Time-averaged turning responses (first second of optogenetic stimulation) of experiments shown in (B), including different light intensities. Dashed lines represent the average monocular visual turning response.

(D) Average turning responses for different driver lines (experiment as illustrated in B; plot as described in C, without visual response).

(legend continued on next page)

declined. This decline might be due to light scattering to the contralateral side [24], activating both left and right HS cells.

We performed a complementary set of experiments using GtACR1 instead of ReaChR to address the question whether HS cell hyperpolarization also affects walking behavior. All five lines expressing GtACR1 showed normal optomotor behavior to visual, monocular back-to-front stimulation; hence, no line was excluded. This time, optogenetic hyperpolarization of HS cells evoked turning in the opposite direction to what we observed during depolarization for all tested lines (Figures 3B–3D) but again syndirectional with the mimicked visual motion direction (back to front). Hence, like depolarization, monocular hyperpolarization of HS cells affects steering behavior. As for ReaChR, GtACR1-mediated turning was phasic in nature, in contrast to more tonic visually evoked responses, and had a response peak at a certain illumination intensity. We then compared expression between all driver lines using fluorescence imaging (enhanced yellow fluorescent protein [EYFP]-tagged optogenetic channels using identical microscopy settings without any amplification step via immunostaining; Figure S2). R81G07 seemed to be the most specific line. However, it mediated often weak and variable expression, sometimes in only one HS cell per hemisphere. This observation matched variable and often modest behavioral effects across flies following illumination. By increasing the expression levels using multiple copies of the optogenetic transgene (Figure S2), the optogenetic turning response could be markedly increased (Figure 3D), highlighting the importance of expression levels for assessing experimental phenotypes.

Increasing Binocular HS Cell Response Asymmetry Enhances Turning Behavior

Yaw rotation usually evokes optic flow on both eyes: front to back on one and back to front on the other side. A corresponding visual stimulus evokes turning in tethered walking flies that is increased with respect to monocular motion (Figures 3E and 3G). Thus, the question arises how the combined left and right HS cell activity affects steering. Because it is technically challenging to express ReaChR and GtACR1 in HS cells on opposite sides, we combined visual and optogenetic HS cell stimulation. To mimic a binocular rotational motion stimulus involving asymmetric left and right HS activity, we presented back-to-front motion on one side and depolarized HS cells via ReaChR on the other side. In a low-light regime, this resulted in an enhanced turning response compared to the visual stimulus alone (Figure 3F). Increasing the light intensity further reduced overall turning, likely due to light scattering to the contralateral side and activating both left and right HS cells [24]. The converse manipulation mimicking binocular rotation in the

other direction—visual front-to-back motion and GtACR1-mediated hyperpolarization on the contralateral side—had equivalent enhancing effects (Figure 3H). These experiments provide further support for the notion that both de- and hyperpolarization from left and right HS cells are integrated downstream to affect turning. They also demonstrate the feasibility of selectively modulating neuronal activity in opposite directions within active visual circuits, representing a powerful experimental system for future studies.

Symmetric Binocular HS Cell Potential Changes Reduce Walking Speed

Considering a walking animal, turning can be brought about by reducing propulsive forces on the inner side of the curve and/or enhancing those on the outer side [13]. The former also reduces forward walking velocity and the latter increases it. Using flies on a tread compensator, Götz and Wenking [13] have found evidence for either, depending on the genotype and condition. However, using a tethered walking assay, Silies et al. [27] measured robust non-directional reductions in walking speed in response to both front-to-back and back-to-front motion. We revisited the effects of both binocular rotating and translating stimuli on walking speed and, in line with the latter study, obtained prominent speed reductions for all stimuli (Figures 4A, 4B, 4D, and 4E). This suggests a predominantly decelerating effect of wide-field horizontal motion detectors, such as HS cells on the motor system. Increasing motion speed of a translational stimulus (200 versus 80°/s) led to stronger deceleration, suggesting a stronger activation of the underlying pathway (Figures 4B and 4E). To probe the influence of HS cells on walking velocity, we de- and hyperpolarized HS cells on both sides simultaneously via ReaChR and GtACR1. Like the corresponding visual stimuli, both binocular manipulations led to a substantial reduction of walking speed (Figures 4B, 4C, 4E, and 4F). In summary, our results are in agreement with a functional architecture in which positive and negative HS cell signals are split into two pathways that both negatively affect left and right propulsive motor forces (Figure 1G).

DISCUSSION

Wide-field motion-sensitive neurons have been extensively studied to elucidate the mechanisms leading to motion detection and flow field selectivity [1–5, 28, 29]. In contrast, how their signals affect steering behavior has only been explored regarding the influence of depolarization on turning [14, 15]. Here, we have used recently characterized de- and hyperpolarizing optogenetic tools [22–25] to indicate further causal links between the activity of HS cells and tethered walking behavior in flies. Our results reveal two

(E) Comparison of the turning response to monocular back-to-front and binocular rotation.

(F) Left: Fly turning response to monocular back-to-front pattern motion with and without simultaneous contralateral optogenetic HS cell activation. (Middle) Quantification of the experiment. (Right) Average rotation response of R27B03 > ReaChR compared to controls for different light intensities.

(G) Comparison of the turning response to monocular front-to-back and binocular rotation.

(H) Left: Fly turning response to monocular front-to-back pattern motion with and without simultaneous contralateral optogenetic HS cell hyperpolarization. (Middle) Quantification of the experiment. (Right) Average rotation response of R27B03 > GtACR1 compared to controls for different light intensities.

Traces represent the mean \pm SEM. Symmetric experimental conditions were pooled by sign inverting the turning response of the mirror-symmetrical condition. In (B), (C), and (D), $n = 10$ with 50 trials per fly; in (E), (F), (G), and (H), $n = 10$ with 40 trials per fly. In (H), the Wilcoxon rank-sum test was used to test for statistically significant differences. In (F), the Wilcoxon signed-rank test was performed. * $p < 0.05$. See also Figure S2.

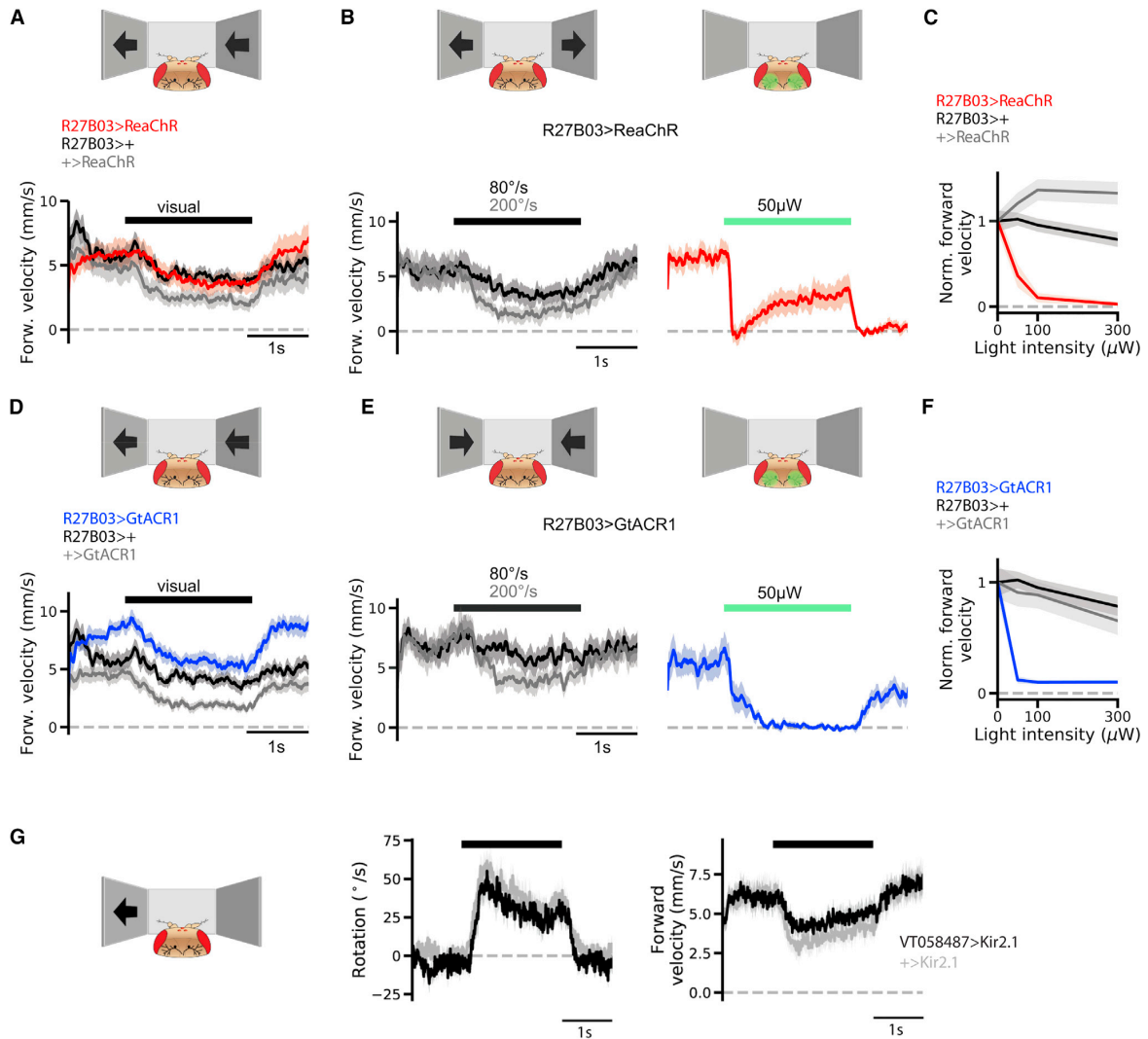


Figure 4. Control of Forward Walking Velocity and Requirement of HS Cells

(A) Forward walking response to binocular visual rotation stimulus ($80^\circ/\text{s}$). Flies slow down during turning.
 (B) Binocular visual stimulation (front-to-back motion with $80^\circ/\text{s}$ in black and $200^\circ/\text{s}$ in gray) in comparison with bilateral optogenetic HS cell depolarization.
 (C) Quantification of bilateral optogenetic stimulation for $R27B03 > \text{ReaChR}$ and controls. Hereby, the forward velocity of each genotype was normalized with respect to its average forward velocity in the dark.
 (D) Experiment as described in (A), with partly different genotypes.
 (E) Binocular visual HS cell hyperpolarization (back-to-front motion with $80^\circ/\text{s}$ in black and $200^\circ/\text{s}$ in gray) in comparison with bilateral optogenetic HS cell hyperpolarization.
 (F) Quantification of bilateral optogenetic stimulation for $R27B03 > \text{GtACR1}$ and controls. The data have been normalized as explained in (C).
 (G) Rotation and forward walking velocity in response to monocular front-to-back motion of control flies ($+ > \text{Kir2.1}$, gray) and flies with HS cells silenced by expression of the K^+ -channel Kir2.1 ($\text{VT058487} > \text{Kir2.1}$, black). Neither visual response component is clearly affected by HS cell silencing. Traces represent the mean \pm SEM. Symmetric experimental conditions were pooled during analysis.
 In (A) and (D), $n = 10$ with 40 trials per fly; in (B), (C), (E), and (F), $n = 10$ with 30 trials per fly. See also [Figure S3](#).

new features: (1) according to their response sign, HS cells can signal two visual motion directions to downstream pathways and (2) these pathways have a predominantly negative effect on the propulsive forces underlying walking ([Figure 1G](#)).

Two Fundamental Functions of ND Input Integration

Motion opponency, i.e., the integration of excitatory PD and inhibitory ND responses, is a widespread phenomenon in wide-field motion-sensitive neurons in animals [30–33]. One

likely purpose is to ensure flow field selectivity. For instance, expanding flow impinges onto fly lobula plate tangential cells via retinotopically organized excitatory T4/T5 and inhibitory LPI connections in different parts of the dendrite. By spatial integration, responses cancel each other, thereby enhancing selectivity to unidirectional optic flow [19]. Furthermore, at least in flies, tangential cells are electrically coupled to each other, allowing transmission of de- and hyperpolarizations. Such coupling has been shown to support robust representation of optic flow parameters averaging out pattern-dependent modulations of local motion detector responses [34]. Here, we demonstrate an additional role of hyperpolarization in response to null direction motion as a direction-selective signal feeding into motor circuits that are involved in controlling heading.

Visually and Optogenetically Evoked Behavioral Responses

In tethered open loop behavior, locomotor responses to horizontal visual wide-field motion are well in line with HS cell activity mediating the behavior. For instance, unilateral motion evokes syndirectional turning, as is also the case for the equivalent optogenetically induced HS cell activity changes, implying a causal relationship (Figures 3B–3D). Regarding the influence of rotating and translating pattern motion on forward walking velocity, we see predominantly negative effects (Figure 4), in line with a previous study [27]. This negative effect is also apparent during bilaterally symmetric optogenetic HS cell stimulation, where flies slow down or stop. In extreme cases, walking velocity may even reverse. This suggests that turning is brought about predominantly by a negative effect—in part mediated by HS cells—on the propulsive forces underlying walking on the inner side of the curve. However, a positive influence on visually evoked walking responses has also been documented [13]. It therefore seems possible that the control system depicted in Figure 1G co-exists with alternative ones, which are differentially weighted depending on the experimental conditions. Although optogenetic HS cell manipulations recapitulate qualitative aspects of visually guided behavior, differences exist regarding the dynamics. For instance, horizontal motion evokes tonic responses both in HS cell activity and turning behavior. Optogenetic HS cell responses have a similar strong tonic component, yet turning behavior is more phasic in nature (Figures 2B, 2D, and 3B). This could indicate the existence of a control mechanism counteracting HS-cell-mediated responses in the absence of activity in other neurons that would normally occur during visual motion.

Requirement of HS Cells for Optomotor Turning

An important question pertains to the requirement of HS cells for optomotor turning. Before the advent of genetically targeted cell-specific manipulations in *Drosophila*, this had been attempted using mutant analysis and surgical interventions [35–37]. Perhaps the most selective manipulation has been conducted by severing the axons of HS cells unilaterally in tethered flying *Calliphora* [37]. This led to a reduction in optomotor turning in response to front-to-back motion on the lesioned side. The residual turning and the caveat that other cells were likely affected by the microsurgical procedures in the intricate network of motion-sensitive cells [38] suggests that other neurons apart from HS cells provide horizontal optic-flow-related information to down-

stream pathways. In agreement with this notion, in *Drosophila*, prolonged hyperpolarization of HS cells via expression of the K⁺ channel Kir2.1 had only a subtle effect on visual-motion-evoked wing steering responses, with normal response amplitudes but a trend toward slower response acceleration at high visual motion speeds [16]. We have tested flies with the same manipulation in the tethered walking assay and did not find a consistent phenotype in the response amplitude or time course (Figures 4G and S3). The outcome that responses to monocular back-to-front and front-to-back motion remained intact further strengthens the conclusion that HS cells are part of a redundant system on each side of the head (Figures 1B, 1C, and 1G). One layer 2 candidate is the H2 cell [6]. Although H2 conveys motion information onto HS cell terminals via contralateral projections (a pathway removed by HS cell silencing) [39], H2 potentially provides synaptic input directly onto descending neurons, a pathway left intact by HS cell silencing. Another layer 2 candidate is the Hx cell [8, 9]. Furthermore, additional yet unidentified lobula plate layer 2 output neurons are likely to exist. The absence of a robust HS loss-of-function phenotype, as opposed to a 50% reduction suggested by the circuit depicted in Figure 1G, could be explained by a potentially saturated steering signal or homeostatic circuit compensation, due to a non-inducible prolonged silencing effect. Furthermore, the existence of other layer 1 output neurons underlying optomotor turning should not be excluded.

Downstream Pathways

Regarding how HS cell signals are conveyed to downstream motor centers, the schematic control circuit depicted in Figure 1G is clearly an oversimplification. For instance, it does not capture any lateral information transfer among tangential cells, which are conveyed via gap junctions or chemical synaptic connectivity, both ipsilaterally and across hemispheres [38, 39]. Any HS cell activity is thus expected to spread through the tangential cell network, likely to impinge on not just one but potentially several descending pathways in parallel. Although first steps have been made to identify those targets [40], many more descending neurons likely remain to be identified [41]. Furthermore, HS and other tangential cells provide input to neck motor neurons [15, 42], thereby likely controlling head movements following panoramic flow [16]. Leg and wing movements underlying steering might thus be implemented more indirectly via a control loop involving proprioceptive feedback from head posture. Despite the yet unknown intricacies, our data support the idea that de- and hyperpolarizing HS cell signals feed into at least two separate pathways. This is because both signals have a decelerating influence on the walking motor, which has to be exerted on opposite sides to support optomotor turning (Figure 1G).

Behavioral Significance of HS Cell Activity

Although it is becoming clear that HS cell activity influences locomotor behavior, the underlying biological significance is a different and more difficult question to address. Our results on asymmetric HS activity manipulations are consistent with the idea that HS cell activity represents an optic flow-based error signal related to self-rotation that counteracts unintended course deviations. However, vision is naturally implemented within action-perception feedback cycles imposing complex dynamics and involving rotational and translational motion

components. Two approaches have been taken in the past to capture naturalistic HS cell responses.

First, using sophisticated technology, the retinal input during unrestrained exploratory behavior of flying *Calliphora* has been reconstructed and HS cells' activity recorded during stimulus replay in order to determine which rotational and translational features they encode. It emerged that HS cell activity—in addition to rotational flow—is substantially modulated by translational motion, particularly in the slow response components. Because translational motion velocity depends on distance, HS activity may be implicated in obtaining spatial environmental information [1, 10, 11]. Indeed, fruit flies are well capable of using motion parallax cues for assessing distance [43–45]. The effect of artificial unilateral activation of HS cells may therefore additionally reflect naturally occurring attraction to a nearby surface or object. Perhaps related to that, binocular front-to-back motion leading to symmetric HS cell activation may indicate expansion as experienced on a collision course and require deceleration. The reverse scenario, binocular back-to-front motion leading to symmetric HS hyperpolarization, in particular during forward walking, may indicate a receding object, leading to deceleration as part of a freezing response [46].

As a second approach, tangential cell signals have been recorded during restrained walking and flight behavior. This showed that lobula plate tangential cells—in addition to visual input—integrate prominent internal motor-related signals. Those were shown to modulate response gain and speed tuning of HS cells [47, 48]. Strikingly, HS and other tangential cells also receive non-visual signals related to turning [14, 16, 49]. In tethered flight, those signals have appropriate signs to silence the expected visual reafference and are thus well suited to serve as efference copies. The remaining visual activity may therefore indicate accidental course deviations, useful for corrective steering [16, 49]. The situation in tethered walking flies is different. There, the visual reafference and non-visual turning signals have the same sign and therefore cooperate to produce larger direction-selective responses in HS cells during turns. Furthermore, HS cells receive depolarizing signals related to walking speed, in addition to the expected depolarizing visual reafference [14]. Why then does optogenetic but not self-generated HS cell activation lead to deceleration? This apparent paradox could be resolved by assuming a processing stage downstream of HS cells, where decelerating error signals are generated by subtracting an expected (via efference copy) from the actual (e.g. optogenetic) response.

Optic flow sensors are thus embedded in sophisticated state-dependent feedback systems, making it non-trivial to infer the role of HS cell activity during natural locomotion. However, as we have done here, an important step is to study the consequences of acute activity manipulations during visually guided behavior. Building on this study, careful analysis of other loss- and gain-of-function phenotypes during restrained and unrestrained behavior will provide further insights into optic-flow-based course control.

STAR★METHODS

Detailed methods are provided in the online version of this paper and include the following:

- **KEY RESOURCES TABLE**

8 *Current Biology* 28, 1–9, December 17, 2018

- **CONTACT FOR REAGENT AND RESOURCE SHARING**
- **EXPERIMENTAL MODEL AND SUBJECT DETAILS**
 - Fly stocks
 - Detailed genotypes of flies used by figures
- **METHOD DETAILS**
 - Electrophysiology
 - Optomotor behavior assay setup
 - Optomotor behavior assay experiments
 - Blocking behavior assays
 - Confocal imaging
- **QUANTIFICATION AND STATISTICAL ANALYSIS**

SUPPLEMENTAL INFORMATION

Supplemental Information includes three figures and can be found with this article online at <https://doi.org/10.1016/j.cub.2018.11.010>.

ACKNOWLEDGMENTS

We are very grateful to Wolfgang Essbauer, Michael Sauter, Renate Gleich, Christian Theile, and Romina Kutlesa for excellent technical assistance. We would also like to thank Julia Kuhl for artwork. Fly lines were obtained from Bloomington, unless stated otherwise. We greatly appreciate helpful feedback on the manuscript from Aljoscha Leonhardt and Ines Ribeiro. Funding was provided from the Max Planck Society and the SFB 870 of the German Research Foundation.

AUTHOR CONTRIBUTIONS

Conceptualization, A.S.M., C.B., and A.B.; Methodology, A.S.M., C.B., and A.B.; Formal Analysis, A.S.M. and C.B.; Investigation, A.S.M. and C.B.; Writing – Original Draft, A.S.M.; Writing – Review & Editing, A.S.M., C.B., and A.B.; Supervision, A.S.M. and A.B.; Funding Acquisition, A.S.M. and A.B.

DECLARATION OF INTERESTS

The authors declare no competing interests.

Received: August 3, 2018
Revised: October 2, 2018
Accepted: November 2, 2018
Published: December 6, 2018

REFERENCES

1. Egelhaaf, M., Kern, R., and Lindemann, J.P. (2014). Motion as a source of environmental information: a fresh view on biological motion computation by insect brains. *Front. Neural Circuits* 8, 127.
2. Borst, A. (2014). Fly visual course control: behaviour, algorithms and circuits. *Nat. Rev. Neurosci.* 15, 590–599.
3. Mauss, A.S., and Borst, A. (2017). Motion vision in arthropods. In *The Oxford Handbook of Invertebrate Neurobiology*, J.H. Byrne, ed. (Oxford University Press).
4. Krapp, H.G. (2000). Neuronal matched filters for optic flow processing in flying insects. *Int. Rev. Neurobiol.* 44, 93–120.
5. Krapp, H.G., and Wicklein, M. (2008). Central processing of visual information in insects. In *The Senses: A Comprehensive Reference*, Volume 1, R.H. Masland, T.D. Albright, P. Dallos, D. Oertel, S. Firestein, G.K. Beauchamp, M.C. Bushnell, A.I. Basbaum, J.H. Kaas, and E.P. Gardner, eds. (Academic Press), pp. 131–203.
6. Hausen, K. (1984). The lobula-complex of the fly: structure, function and significance in visual behaviour. In *In Photoreception and Vision in Invertebrates*, M.A. Ali, ed. (Springer), pp. 523–559.

7. Schnell, B., Joesch, M., Forstner, F., Raghu, S.V., Otsuna, H., Ito, K., Borst, A., and Reiff, D.F. (2010). Processing of horizontal optic flow in three visual interneurons of the *Drosophila* brain. *J. Neurophysiol.* *103*, 1646–1657.
8. Krapp, H.G., and Hengstenberg, R. (1996). Estimation of self-motion by optic flow processing in single visual interneurons. *Nature* *384*, 463–466.
9. Wasserman, S.M., Aptekar, J.W., Lu, P., Nguyen, J., Wang, A.L., Keleş, M.F., Grygoruk, A., Krantz, D.E., Larsen, C., and Frye, M.A. (2015). Olfactory neuromodulation of motion vision circuitry in *Drosophila*. *Curr. Biol.* *25*, 467–472.
10. Karameier, K., van Hateren, J.H., Kern, R., and Egelhaaf, M. (2006). Encoding of naturalistic optic flow by a population of blowfly motion-sensitive neurons. *J. Neurophysiol.* *96*, 1602–1614.
11. Kern, R., van Hateren, J.H., Michaelis, C., Lindemann, J.P., and Egelhaaf, M. (2005). Function of a fly motion-sensitive neuron matches eye movements during free flight. *PLoS Biol.* *3*, e171.
12. Huston, S.J., and Krapp, H.G. (2008). Visuomotor transformation in the fly gaze stabilization system. *PLoS Biol.* *6*, e173.
13. Götz, K.G., and Wenking, H. (1973). Visual control of locomotion in the walking fruit fly *Drosophila*. *J. Comp. Physiol.* *85*, 235–266.
14. Fujiwara, T., Cruz, T.L., Bohnslav, J.P., and Chiappe, M.E. (2017). A faithful internal representation of walking movements in the *Drosophila* visual system. *Nat. Neurosci.* *20*, 72–81.
15. Haikala, V., Joesch, M., Borst, A., and Mauss, A.S. (2013). Optogenetic control of fly optomotor responses. *J. Neurosci.* *33*, 13927–13934.
16. Kim, A.J., Fenk, L.M., Lyu, C., and Maimon, G. (2017). Quantitative predictions orchestrate visual signaling in *Drosophila*. *Cell* *168*, 280–294.e12.
17. Mauss, A.S., Meier, M., Serbe, E., and Borst, A. (2014). Optogenetic and pharmacologic dissection of feedforward inhibition in *Drosophila* motion vision. *J. Neurosci.* *34*, 2254–2263.
18. Maisak, M.S., Haag, J., Ammer, G., Serbe, E., Meier, M., Leonhardt, A., Schilling, T., Bahl, A., Rubin, G.M., Nern, A., et al. (2013). A directional tuning map of *Drosophila* elementary motion detectors. *Nature* *500*, 212–216.
19. Mauss, A.S., Pankova, K., Arenz, A., Nern, A., Rubin, G.M., and Borst, A. (2015). Neural circuit to integrate opposing motions in the visual field. *Cell* *162*, 351–362.
20. Braitenberg, V. (1986). *Vehicles: Experiments in Synthetic Psychology* (MIT Press).
21. Buchner, E., Buchner, S., and Bühlhoff, I. (1984). Deoxyglucose mapping of nervous activity induced in *Drosophila* brain by visual movement. *J. Comp. Physiol.* *155*, 471–483.
22. Inagaki, H.K., Jung, Y., Hoopfer, E.D., Wong, A.M., Mishra, N., Lin, J.Y., Tsien, R.Y., and Anderson, D.J. (2014). Optogenetic control of *Drosophila* using a red-shifted channelrhodopsin reveals experience-dependent influences on courtship. *Nat. Methods* *11*, 325–332.
23. Lin, J.Y., Knutsen, P.M., Muller, A., Kleinfeld, D., and Tsien, R.Y. (2013). ReaChR: a red-shifted variant of channelrhodopsin enables deep transcranial optogenetic excitation. *Nat. Neurosci.* *16*, 1499–1508.
24. Mauss, A.S., Busch, C., and Borst, A. (2017). Optogenetic neuronal silencing in *Drosophila* during visual processing. *Sci. Rep.* *7*, 13823.
25. Govorunova, E.G., Sineshchekov, O.A., Janz, R., Liu, X., and Spudich, J.L. (2015). NEUROSCIENCE. Natural light-gated anion channels: A family of microbial rhodopsins for advanced optogenetics. *Science* *349*, 647–650.
26. Jenett, A., Rubin, G.M., Ngo, T.-T.B., Shepherd, D., Murphy, C., Dionne, H., Pfeiffer, B.D., Cavallaro, A., Hall, D., Jeter, J., et al. (2012). A GAL4-driver line resource for *Drosophila* neurobiology. *Cell Rep.* *2*, 991–1001.
27. Silies, M., Gohl, D.M., Fisher, Y.E., Freifeld, L., Clark, D.A., and Clandinin, T.R. (2013). Modular use of peripheral input channels tunes motion-detecting circuitry. *Neuron* *79*, 111–127.
28. Mauss, A.S., Vlasits, A., Borst, A., and Feller, M. (2017). Visual circuits for direction selectivity. *Annu. Rev. Neurosci.* *40*, 211–230.
29. Borst, A., and Helmstaedter, M. (2015). Common circuit design in fly and mammalian motion vision. *Nat. Neurosci.* *18*, 1067–1076.
30. Wylie, D.R., Bischof, W.F., and Frost, B.J. (1998). Common reference frame for neural coding of translational and rotational optic flow. *Nature* *392*, 278–282.
31. Duffy, C.J., and Wurtz, R.H. (1991). Sensitivity of MST neurons to optic flow stimuli. I. A continuum of response selectivity to large-field stimuli. *J. Neurophysiol.* *65*, 1329–1345.
32. Ibbotson, M.R. (1991). Wide-field motion-sensitive neurons tuned to horizontal movement in the honeybee, *Apis mellifera*. *J. Comp. Physiol. A* *168*, 91–102.
33. Collett, T.S., and Blest, A.D. (1966). Binocular, directionally selective neurons, possibly involved in the optomotor response of insects. *Nature* *212*, 1330–1333.
34. Elyada, Y.M., Haag, J., and Borst, A. (2009). Different receptive fields in axons and dendrites underlie robust coding in motion-sensitive neurons. *Nat. Neurosci.* *12*, 327–332.
35. Heisenberg, M., Wonneberger, R., and Wolf, R. (1978). Optomotor-blind^{H31} – a *Drosophila* mutant of the lobula plate giant neurons. *J. Comp. Physiol.* *124*, 287–296.
36. Geiger, G., and Nässel, D.R. (1981). Visual orientation behaviour of flies after selective laser beam ablation of interneurons. *Nature* *293*, 398–399.
37. Hausen, K., and Wehrhahn, C. (1990). Neural circuits mediating visual flight control in flies. II. Separation of two control systems by microsurgical brain lesions. *J. Neurosci.* *10*, 351–360.
38. Borst, A., and Weber, F. (2011). Neural action fields for optic flow based navigation: a simulation study of the fly lobula plate network. *PLoS ONE* *6*, e16303.
39. Haag, J., and Borst, A. (2001). Recurrent network interactions underlying flow-field selectivity of visual interneurons. *J. Neurosci.* *21*, 5685–5692.
40. Suver, M.P., Huda, A., Iwasaki, N., Safarik, S., and Dickinson, M.H. (2016). An array of descending visual interneurons encoding self-motion in *Drosophila*. *J. Neurosci.* *36*, 11768–11780.
41. Namiki, S., Dickinson, M.H., Wong, A.M., Korff, W., and Card, G.M. (2018). The functional organization of descending sensory-motor pathways in *Drosophila*. *eLife* *7*, e10806.
42. Haag, J., Wertz, A., and Borst, A. (2010). Central gating of fly optomotor response. *Proc. Natl. Acad. Sci. USA* *107*, 20104–20109.
43. Cabrera, S., and Theobald, J.C. (2013). Flying fruit flies correct for visual sideslip depending on relative speed of forward optic flow. *Front. Behav. Neurosci.* *7*, 76.
44. Schuster, S., Strauss, R., and Götz, K.G. (2002). Virtual-reality techniques resolve the visual cues used by fruit flies to evaluate object distances. *Curr. Biol.* *12*, 1591–1594.
45. Pick, S., and Strauss, R. (2005). Goal-driven behavioral adaptations in gap-climbing *Drosophila*. *Curr. Biol.* *15*, 1473–1478.
46. Zabala, F., Polidoro, P., Robie, A., Branson, K., Perona, P., and Dickinson, M.H. (2012). A simple strategy for detecting moving objects during locomotion revealed by animal-robot interactions. *Curr. Biol.* *22*, 1344–1350.
47. Chiappe, M.E., Seelig, J.D., Reiser, M.B., and Jayaraman, V. (2010). Walking modulates speed sensitivity in *Drosophila* motion vision. *Curr. Biol.* *20*, 1470–1475.
48. Maimon, G., Straw, A.D., and Dickinson, M.H. (2010). Active flight increases the gain of visual motion processing in *Drosophila*. *Nat. Neurosci.* *13*, 393–399.
49. Kim, A.J., Fitzgerald, J.K., and Maimon, G. (2015). Cellular evidence for efference copy in *Drosophila* visuomotor processing. *Nat. Neurosci.* *18*, 1247–1255.
50. von Reyn, C.R., Breads, P., Peek, M.Y., Zheng, G.Z., Williamson, W.R., Yee, A.L., Leonardo, A., and Card, G.M. (2014). A spike-timing mechanism for action selection. *Nat. Neurosci.* *17*, 962–970.
51. Mauss, A.S., and Borst, A. (2016). Electrophysiological recordings from lobula plate tangential cells in *Drosophila*. *Methods Mol. Biol.* *1478*, 321–332.
52. Bahl, A., Ammer, G., Schilling, T., and Borst, A. (2013). Object tracking in motion-blind flies. *Nat. Neurosci.* *16*, 730–738.

STAR★METHODS

KEY RESOURCES TABLE

REAGENT or RESOURCE	SOURCE	IDENTIFIER
Chemicals, Peptides, and Recombinant Proteins		
<i>all-trans</i> retinal (ATR)	Sigma Aldrich	R2500
VECTASHIELD Antifade Mounting Medium	Vector Laboratories	Cat#H-1000; RRID: AB_2336789
Experimental Models: Organisms/Strains		
<i>D. melanogaster</i> : R27B03.Gal4 ^{attP2}	[47]	N/A
<i>D. melanogaster</i> : R24E09.Gal4 ^{attP2}	[16], BDSC	BDSC 49083
<i>D. melanogaster</i> : R81G07.Gal4 ^{attP2}	[14, 16], BDSC	BDSC 40122
<i>D. melanogaster</i> : VT023749.Gal4 ^{attP2}	[24]	N/A
<i>D. melanogaster</i> : VT058487.Gal4 ^{attP2}	[16]	N/A
<i>D. melanogaster</i> : tsh.Gal80	N/A	N/A
<i>D. melanogaster</i> : tub.Gal80-ts	Courtesy of Dana Galili & Hiromu Tanimoto	N/A
<i>D. melanogaster</i> : UAS.Kir2.1-GFP	Courtesy of Dana Galili & Hiromu Tanimoto	N/A
<i>D. melanogaster</i> : 10xUAS.Kir2.1-EGFP	[50]	N/A
<i>D. melanogaster</i> : UAS.mCD8-GFP on 2 nd	Courtesy of T. Clandinin	N/A
<i>D. melanogaster</i> : UAS.GtACR1-EYFP ^{attP40}	[24]	N/A
<i>D. melanogaster</i> : UAS.GtACR1-EYFP ^{VK00005}	[24]	N/A
<i>D. melanogaster</i> : UAS.ReaChR-Citrine ^{VK00005}	[22]	BDSC 53749
Software and Algorithms		
MATLAB (R2012b)	The MathWorks	RRID: SCR_001622
Python 3.5.2 (Anaconda)	Anaconda	https://www.anaconda.com
Fiji	NIH	RRID: SCR_002285
Other		
Sinfony Opaque Dentin (Near-ultraviolet bonding glue)	3M Espe	49530
BA OPTIMA 10	BA International	BASES10
Bridge amplifier	npi Electronics	BA-1S
Analog-to-digital converter	Measurement Computing	PCI-DAS6025
Wavelength switcher	Sutter Instrument Company	Lambda DG-4 Plus
Optical band-pass filter (Semrock 565/24 BrightLine HC)	AHF	F37-565
LED (565nm)	Thorlabs	M565F3
Fiber	Thorlabs	M15L01
Matched achromatic doublet pair	Thorlabs	MAP051950-A
Power energy meter	Thorlabs	PM100D
Rotary vane pump	Gardner Denver Thomas GmbH	G6/01-K-EB9L
High-power infrared LED (800nm)	Roithner Electronics	JET series, 90mW
Camera (fly positioning)	FLIR Integrated Imaging Solutions	CM3-U3-13S2M-CS
Monitor panel	BenQ	XL2411Z
Camera (optogenetic positioning)	FLIR Integrated Imaging Solutions	CM3-U3-13S2C-CS

CONTACT FOR REAGENT AND RESOURCE SHARING

Further information and requests for resources and reagents should be directed to and will be fulfilled by the Lead Contact, Alex S. Mauss (amauss@neuro.mpg.de).

EXPERIMENTAL MODEL AND SUBJECT DETAILS

Fly stocks

Flies were raised at 25°C and 60% humidity on standard cornmeal agar medium at a 12 h light/dark cycle. Experiment specific fly preparations and changes from the mentioned conditions are described in the corresponding method details sections. The following transgenic fly strains were used: R27B03.Gal4^{attP2} [47], R24E09.Gal4^{attP2} [16], R81G07.Gal4^{attP2} [14, 16], VT023749.Gal4^{attP2} [24], VT058487.Gal4^{attP2} [16], tsh.Gal80, tub.Gal80-ts and UAS.Kir2.1-GFP (courtesy of Dana Galili & Hiromu Tanimoto), 10xUAS.Kir2.1-EGFP [50], UAS.mCD8-GFP on 2nd (courtesy of T. Clandinin), UAS.GtACR1-EYFP^{attP40} [24], UAS.GtACR1-EYFP^{VK00005} [24], UAS.ReaChR-Citrine^{VK00005} [22].

Detailed genotypes of flies used by figures

Figure 2 and Figure S1

w+ ; UAS.mCD8-GFP/+ ; R27B03.Gal4/+
w+ ; + ; R27B03.Gal4/UAS.GtACR1-EYFP
w+ ; + ; R27B03.Gal4/UAS.ReaChR-Citrine

Figure 3

w+ ; + ; UAS.GtACR1-EYFP/+
w+ ; + ; UAS.ReaChR-Citrine/+
w+ ; + ; R27B03.Gal4/UAS.GtACR1-EYFP
w+ ; + ; R27B03.Gal4/UAS.ReaChR-Citrine
w+ ; + ; R27B03.Gal4/+
w+ ; + ; VT023749.Gal4/UAS.GtACR1-EYFP
w+ ; + ; VT023749.Gal4/UAS.ReaChR-Citrine
w+ ; tsh.Gal80/+ ; VT058487.Gal4/UAS.GtACR1-EYFP
w+ ; tsh.Gal80/+ ; VT058487.Gal4/UAS.ReaChR-Citrine
w+ ; UAS.GtACR1-EYFP ; R81G07.Gal4/UAS.GtACR1-EYFP
w+ ; + ; R81G07.Gal4/UAS.GtACR1-EYFP
w+ ; + ; R24E09.Gal4/UAS.GtACR1-EYFP
w+ ; + ; R24E09.Gal4/UAS.ReaChR-Citrine

Figure 4

w+ ; + ; UAS.GtACR1-EYFP/+
w+ ; + ; UAS.ReaChR-Citrine/+
w+ ; + ; R27B03.Gal4/UAS.GtACR1-EYFP
w+ ; + ; R27B03.Gal4/UAS.ReaChR-Citrine
w+ ; + ; R27B03.Gal4/+
w+ ; + ; 10xUAS.Kir2.1-EGFP/+
w+ ; tsh.Gal80/+ ; VT058487/10xUAS.Kir2.1-EGFP

Figure S2

w+ ; + ; R24E09.Gal4/UAS.GtACR1-EYFP
w+ ; + ; R27B03.Gal4/UAS.GtACR1-EYFP
w+ ; + ; R81G07.Gal4/UAS.GtACR1-EYFP
w+ ; UAS.GtACR1-EYFP ; R81G07.Gal4/UAS.GtACR1-EYFP
w+ ; + ; VT023749.Gal4/UAS.GtACR1-EYFP
w+ ; tsh.Gal80/+ ; VT058487.Gal4/UAS.GtACR1-EYFP

Figure S3

w+ ; + ; 10xUAS.Kir2.1-EGFP/+
w+ ; + ; R24E09/+
w+ ; + ; R24E09/10xUAS.Kir2.1-EGFP
w+ ; tsh.Gal80/+ ; VT058487/10xUAS.Kir2.1-EGFP
w+ ; + ; VT058487/10xUAS.Kir2.1-EGFP

w+ ; tub.Gal80-ts/+ ; R27B03.Gal4/UAS.Kir2.1-GFP
w+ ; tub.Gal80-ts/+ ; R81G07.Gal4/UAS.Kir2.1-GFP
w+ ; tub.Gal80-ts/+ ; VT023749.Gal4/UAS.Kir2.1-GFP

METHOD DETAILS

Electrophysiology

Fly preparation, whole-cell patch-clamp electrophysiology, visual and optogenetic stimulation and data acquisition were performed as described previously [51] and in the following sections. Experiments were performed at room temperature.

Fly preparation

All electrophysiological recordings were performed from 1-2 days old female flies. For optogenetic experiments, freshly eclosed flies were collected and transferred into a vial with yeast paste containing 1mM all-*trans*-retinal (ATR, R2500; Sigma Aldrich). Initially, flies were anesthetized on ice and attached to a custom holder made out of Plexiglas. The head was bend down and fixed in this position by attaching the proboscis to the ventral thorax using a droplet of melted beeswax. The holder was placed underneath a recording chamber with thin foil at the bottom, inserting the fly thorax into a 1 mm cutout, which also provided access to the back of the head. The remaining parts of the fly including the eyes remained below the edges of the cutout. The head was attached to the rim of the cutout using melted bees wax on one side. On the other side, using a hypodermic needle, a window was cut into the head capsule under external solution. Further steps were performed under a Zeiss Axiotech vario microscope which was equipped with polarized light contrast and epifluorescence. Using the polarized light and a cleaning micropipette with around 5 μm opening, a stream of 0.5 mg/ml Collagenase IV (GIBCO) was applied to digest the glia sheath locally.

Whole-cell recordings

Current-clamp recordings were performed with patch electrodes of 5-8 M Ω resistance. The signal was amplified, low pass filtered (3 kHz) and digitized with a sampling frequency of 10 kHz. The following hardware/software has been used: bridge amplifier (BA-1S, npi Electronics), analog-to-digital converter (PCI-DAS6025, Measurement Computing), MATLAB's data acquisition toolbox.

External and internal solutions

External solution contained the following (in mM): 103 NaCl, 3 KCl, 5 TES, 10 trehalose, 10 glucose, 7 sucrose, 26 NaHCO₃, 1 NaH₂PO₄, 1.5 CaCl₂, and 4 MgCl₂, pH 7.3–7.35, 280–290 mOsmol/kg. The external solution was carboxygenated (95% O₂/5% CO₂) and constantly perfused over the preparation at 2 ml/min. The internal solution, adjusted to pH 7.26 with 1N KOH, contained the following: 140 K-aspartate, 10 HEPES, 4 Mg-ATP, 0.5 Na-GTP, 1 EGTA, 1 KCl, and 0.1 Alexa Fluor 488 hydrazide salt (265 mOsmol/kg).

Visual stimulation

Visual stimulation was provided on a custom build LED arena (dimensions: 170° in azimuth and 90° in elevation) with the following properties: max. refresh rate of 600 Hz, max. luminance of 80 cd/m², spatial resolution of 1.4°.

Optogenetic stimulation

For optogenetic stimulation, light pulses were delivered by a Lambda DG-4 Plus wavelength switcher (Sutter Instrument) with a 300W Xenon Arc lamp via the epifluorescence light path of the microscope through a 40x/0.8 NA water-immersion objective (LUMPlan FI; Olympus). Light was passed through an optical filter with 565 nm center wavelength and 24 nm bandwidth (Semrock BrightLine HC). Intensities under the objective were measured with a power meter (Thorlabs PM100D) in air to estimate the irradiance per illuminated area in immersion.

Data analysis

For data representation, recording traces were averaged across trials and then cells to obtain the mean and standard deviation in MATLAB R2012b. For quantification, in each trial baseline and response was obtained by time-averaging the membrane potential 2 s before and after stimulus onset, respectively, and the baseline was then subtracted from the response. This value was then averaged across trials and cells. To obtain a measure for sensitivity of ReaChR and GtACR1, a sigmoid function of the form $y(x) = A / (1 + e^{-k(x-x_0)})$ was fit to the data points as a function of light intensity x . A denotes the maximum response, k determines the steepness of the curve and x_0 indicates the x value of the curve midpoint. To obtain ON and OFF time constants τ , an exponential decay function of the form $y(t) = (N_0 - N)e^{-t/\tau} + N$, with N_0 denoting the initial and N the final value, was fit to the light onset and offset responses as a function of time t . Curve fitting was done using the `curve_fit` tool from the `scipy.optimize` package in Python 3.5.2.

Optomotor behavior assay setup

In general, the experimental setup as well as the preparation used within this work are very similar to [24]. A full description of the fly preparation, tethering as well as the optogenetic and visual stimulation setup is provided in the following sections.

Fly preparation

Freshly hatched female flies were collected during one day. Within the same day, all collected flies were transferred into a vial with yeast-paste containing 1mM ATR. From here on, flies were kept at 25°C, 60% humidity on a 12h dark, 12h blue light cycle for two to three days, until the experiment was performed.

Tethering flies

The tethering procedure was performed while the fly was cooled down to 2°C, hence immobilized. Initially, the tip of a needle was positioned between head and thorax, whereby proper alignment of head and thorax was ensured. By doing so, the head was slightly tilted forward, allowing direct optogenetic stimulation of the back of the head during the experiments. Now, head, thorax and wings were tethered to the needle using near-ultraviolet bonding glue (Sinfony Opaque Dentin) and a blue LED light for drying (440 nm, BA OPTIMA 10, BA International).

Optogenetic stimulation

Unilateral as well as bilateral optogenetic stimulation were performed using the following setup – one for each side. The output of a fiber coupled LED of 565 nm wavelength (LED: M565F3 Thorlabs, Fiber: M15L01, Thorlabs) was focused onto a small point using a matched achromatic doublet pair (MAP051950-A, Thorlabs), which was connected to a micro-manipulator. The focused light point was around 0.12 mm² and could be precisely positioned onto the fly's head. Light intensities used within the experiments were calibrated with the help of a power energy meter (PM100D, Thorlabs).

Locomotion recorder

A locomotion recorder (as described in [52]) was used to record the waking behavior. It consists of an air-suspended polyurethane ball of 6 mm diameter floating in a bowl-shaped holder. The airflow, generated using a rotary vane pump (G6/01-K-EB9L, Gardner Denver Thomas GmbH), is adjusted in strength in such a way, that the ball is able to rotate freely inside the holder without jumping out. The ball is illuminated with the help of a high-power infrared LED (800 nm, JET series, 90mW, Roithner Electronics) and tracked using two optical tracking sensors. A camera (CM3-U3-13S2M-CS, FLIR Integrated Imaging Solutions) is positioned behind the ball in order to enable precise positioning of the fly on top of the ball. The positioning of the tethered fly is done using a micromanipulator.

Visual stimulation

Visual stimulation was provided using three 144 Hz monitor panels (XL2411Z, BenQ) covered with diffusion foil, which have been removed from their casing and vertically arranged into a U-shape. The luminance range of the covered panels ranges from 0 to 220 cd m⁻². The panel arrangement results in a visual arena with 30.5 × 33.5 × 56 cm, allowing to stimulate the fly's visual field within ± 135° horizontally and ± 61° vertically, with a pixel size smaller than 0.09°, whereby the fly was positioned in the center of the arena. All visual patterns were rendered on a virtual, upright cylinder surrounding the fly. Furthermore, an additional camera (CM3-U3-13S2C-CS, FLIR Integrated Imaging Solutions) was located over the fly in order to be able to position the optogenetic stimulation.

Optomotor behavior assay experiments

The following sections provide a detailed description of the optomotor behavior assay experiments. The temperature during all experiments was regulated to 34°C and the sequence of all tested conditions within each set was randomized. Flies which stopped walking before all experiments were performed were excluded from further analysis.

Unilateral optogenetic and visual stimulation

Each stimulus condition lasted five seconds. Unilateral optogenetic stimulation on the left or right side of the head started after one second and lasted two seconds long. Seven different LED intensities were tested (0.0 mW, 0.025 mW, 0.05 mW, 0.075 mW, 0.1 mW, 0.2 mW, 0.3 mW). Hereby, no visual stimulus was presented and the flies were in complete darkness. Visual responses were tested as follows. Initially, static vertical stripes with 10° width and random uniformly sampled intensity were presented only on the left or right side of the fly (+135° to +90° or –90° to –135° in azimuth). After one second, the visual pattern was moved for two seconds with an angular velocity of 80°/s clockwise or counter-clockwise. Subsequently, the pattern stayed one more second static before all monitors turned black.

Combined optogenetic and visual stimulation

Initially static vertical stripes with 10° width and random uniformly sampled intensity were presented only on the left or right side of the fly (+135° to +90° or –90° to –135° in azimuth). After one second, the visual pattern was moved for two seconds with an angular velocity of 80°/s clockwise or counter-clockwise. Simultaneously, the LED contralateral to the visual stimulus was turned on (intensities: 0.0 mW, 0.05 mW, 0.1 mW, 0.3 mW). After these two seconds, the LED turned off and the pattern stopped – being visible one more second before the screens turned black for six seconds.

Bilateral optogenetic or visual stimulation

Each bilateral stimulation condition lasted ten seconds. Optogenetic and visual stimulation were never combined. Bilateral optogenetic stimulation started after one second and lasted two seconds long. The following LED intensities for each channel were used: 0.0 mW, 0.05 mW, 0.1 mW, 0.3 mW. For bilateral visual stimulation, static vertical stripes with 10° width and random intensity taken from a uniform distribution were presented on the left and right side of the fly (+135° to +90° and –90° to –135° in azimuth). After one second, the visual patterns on both sides were rotated for two seconds simultaneously front-to-back or back-to-front (angular velocity of 80°/s or 200°/s). Again, the pattern motion stopped and one second later the screens were turned off.

Blocking behavior assays

The blocking behavior assays were performed on the same setup as the optomotor behavior assays.

Fly preparation and tethering

If possible, young, female flies were selected and kept on 25°C, 60% humidity on a 12h dark, 12h light cycle for two to three days, until the experiment was performed. However, some driver lines in combination with Kir were lethal. For those lines, tubGal80 was included to avoid expression during development. Now, young, female flies were selected and kept on 32°C, 60% humidity on a 12h dark, 12h light cycle for two to three days. The tethering procedure as well as the setup were identical to the optogenetic behavior assays. Again, the temperature during all experiments was set to 34°C and the sequence of all tested conditions within each set was randomized.

Visual stimulation

Each stimulus condition lasted five seconds. Initially static vertical stripes with 10° width and random uniformly sampled intensity were presented only on the left, right, left and right or all monitors of the setup (left: +135° to +90°, right: -90° to -135°, all: +135° to -135° in azimuth). Now, the visual pattern was moved for two seconds with an angular velocity of 80°/s clockwise or counter-clockwise. Subsequently, the pattern stopped, being visible for one more second, before all active screens turned black for one second.

Confocal imaging

Female flies (1-3 days old) were dissected in PBS and fixed at room temperature for 25min in PBS/4% paraformaldehyde (PFA). Subsequently they were washed in PBS and mounted using VECTASHIELD antifade mounting medium (Vector Laboratories). The expression pattern was optically sectioned using a Leica SP5 confocal scanning microscope. Hereby, confocal settings have not been altered between genotypes. Recorded stacks were processed using a maximum z-projection within Fiji.

QUANTIFICATION AND STATISTICAL ANALYSIS

Since experiments were performed and analyzed in a highly automated fashion, experimenters were not blinded to genotypes. Quantification and statistical analysis was performed using Python 3.5.2 (scipy.stats module). Information about the presented data, its quantification and statistical analysis are provided within the corresponding figure legends and within the figure. All behavioral tests were performed in a randomized order. In general, if not stated otherwise, traces represent mean over flies \pm standard error of the mean (shaded envelope around trace or error bars). Behavioral traces were smoothed with a moving average of 50 ms. To test for significance, the data was first tested for normal distribution based on the skewness. For positive outcomes, the Wilcoxon rank-sum test was used to test for statistically significant differences. Otherwise, the Wilcoxon signed-rank test was used. Significance is indicated in figures with *, denoting $p < 0.05$.

Current Biology, Volume 28

Supplemental Information

**Bi-directional Control of Walking Behavior
by Horizontal Optic Flow Sensors**

Christian Busch, Alexander Borst, and Alex S. Mauss

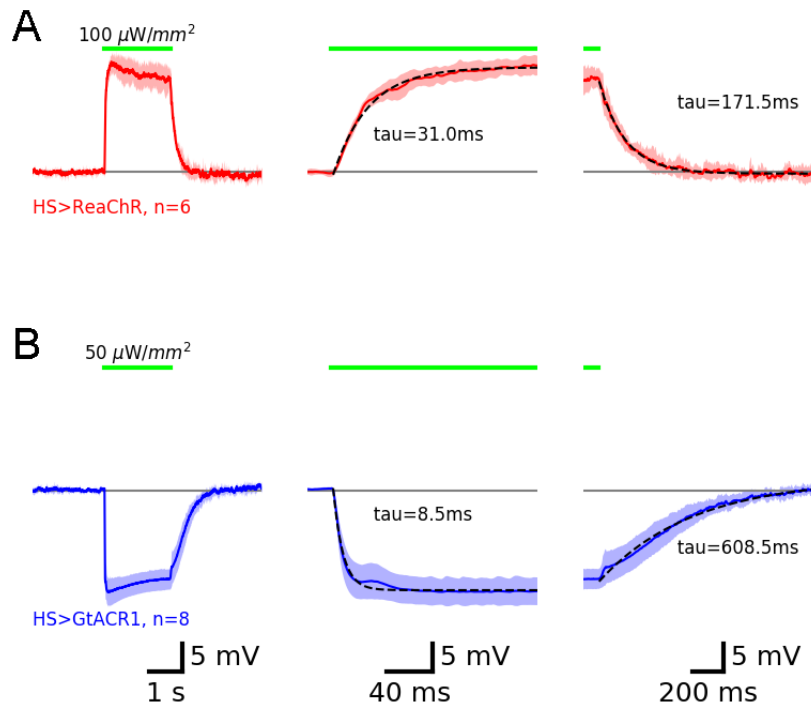


Figure S1. Dynamics of GtACR1- and ReaChR-mediated HS cell membrane potential changes. Related to Figure 2B.

(A) To obtain time constants τ for ReaChR-mediated response onset and offset, an exponential decay function of the form $y(t) = (N_0 - N)e^{-t/\tau} + N$ was fit to the data as a function of time t . N_0 denotes the initial and N the final value. $\tau_{\text{ON}} = 31$ ms; $\tau_{\text{OFF}} = 171.5$ ms.

(B) Time constants for GtACR1-mediated responses were obtained in the same way. $\tau_{\text{ON}} = 8.5$ ms; $\tau_{\text{OFF}} = 608.5$ ms.

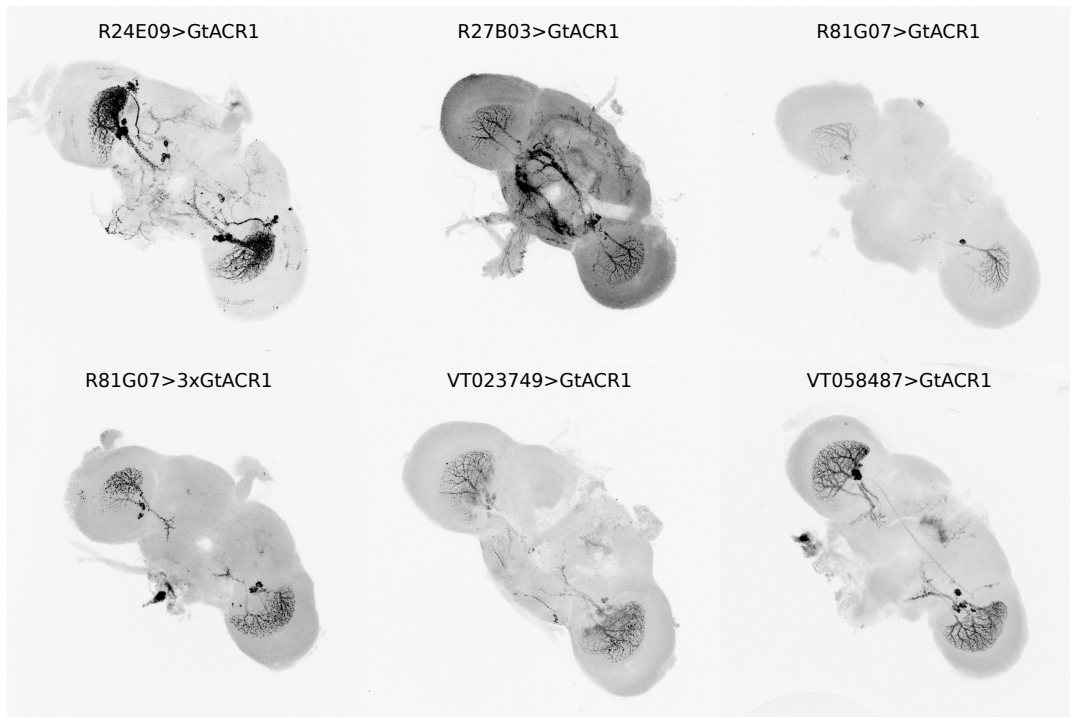


Figure S2. Expression pattern in the brain for different HS driver lines. Related to Figure 3D.

Comparison of the expression between driver lines by fluorescence imaging of EYFP-tagged GtACR1, using identical microscopy settings without any amplification step via immunostaining.

All different driver lines show expression in HS cells and some driver lines have more or less pronounced expression in central brain areas. Since optogenetic stimulation is focused on the optic lobes of the fly, expression within the ventral nerve court is likely irrelevant. Nonetheless, depending on the intensity, monocularly delivered optogenetic illumination will lead to a broader activation area, likely reaching central brain areas and the contralateral optic lobe. This means that expression within the central complex, as can be seen e.g. in line R27B03, might lead to behavioral responses not linked to HS cells. However, the coherent behavioral response across all tested driver lines (see Figure 3D), which have expression in HS cells in common, strongly suggest that the responses are evoked by HS cells.

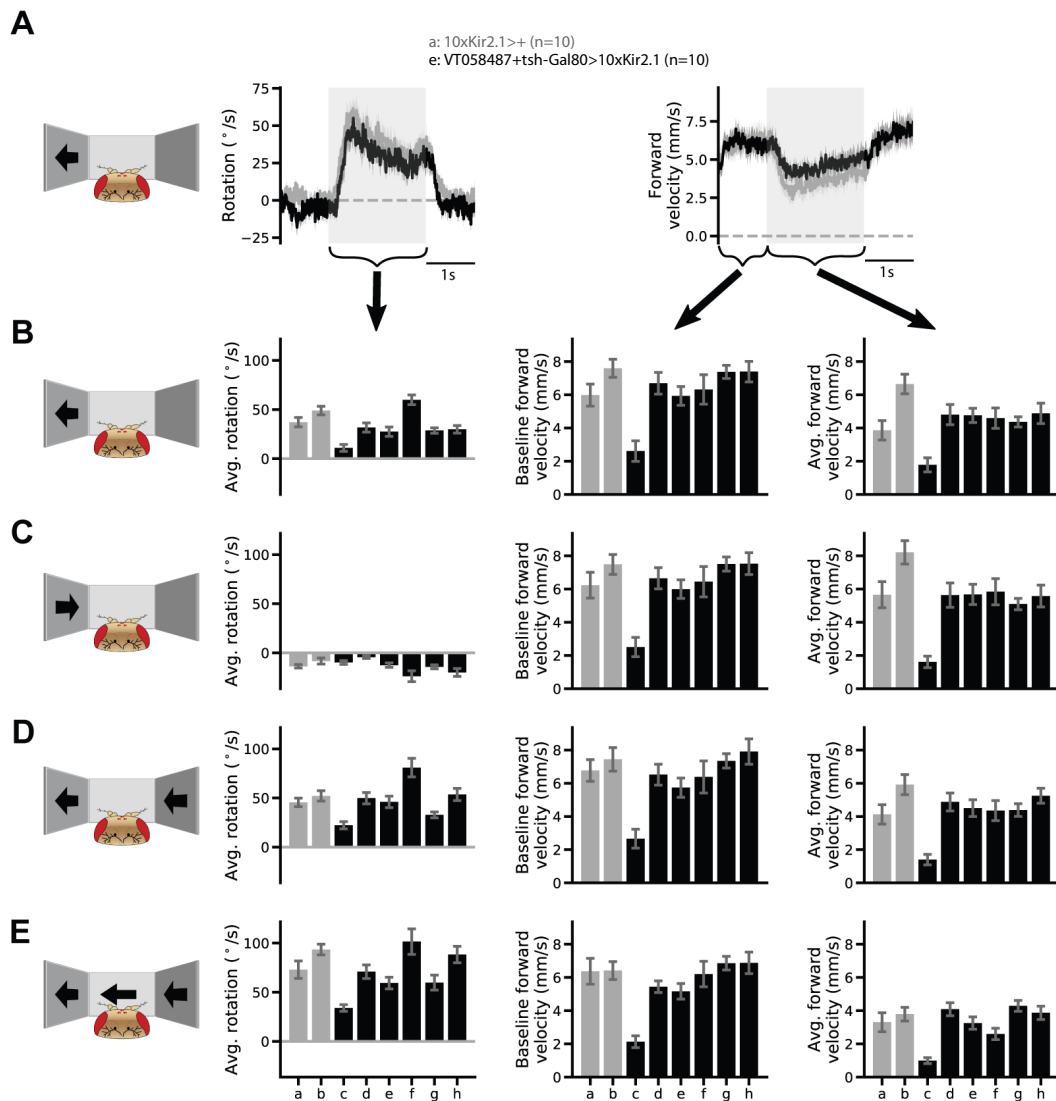


Figure S3. Silencing HS cells does not abolish optomotor turning. Related to Figure 4G.

Data is shown from HS silencing experiments using expression of non-inducible Kir2.1 with different driver lines. Therefore, the blocking effect is neither temporally nor spatially restricted during the experiments (see STAR Methods). The horizontal pattern velocity for all experiments was set to 80 $^{\circ}/s$.

(A) Exemplar averaged traces for monocular visual front-to-back stimulation for one control line (grey) as well as one HS block line (black). Both lines show similar rotational responses during pattern rotation (grey shaded area) and a reduction in forward velocity in comparison to baseline.

(B-E) Quantification of all tested genotypes for different visual stimuli, depicted in the schematics on the left.

(B) Monocular front-to-back stimulation (same experiment as shown in A).

(C) Monocular back-to-front stimulation.

(D) Binocular rotation stimulus. Flies are stimulated with visual front-to-back pattern motion on one eye (as in B), while the other eye is stimulated with back-to-front motion (as in C).

(E) Full field rotation stimulus, presenting pattern motion on two lateral screens (as in D) and an additional frontal screen.

In general, all HS block lines (c-h) show comparable responses to controls a and b, except for line c and f. The low baseline forward velocity of the driver line c (R24E09>10xKir2.1) compared to other genotypes suggests compromised motor function by unspecific effects, for instance due to off-target expression or genetic background. Thus, the reduced turning response as well as low forward velocity during stimulation only observed in this genotype is likely not due to silenced HS cells. A tendency of increased optomotor turning is observed for line f (R27B03+tubGal80ts>Kir2.1), potentially also due to (other) off-target expression. In conclusion, normal visual HS cell responses are not necessary for optomotor turning. However, a contribution of HS cell activity to optomotor turning might be masked in these experiments by a potentially saturated steering signal, conveyed by redundant neurons. Such a signal could additionally be boosted by homeostatic circuit compensation of HS cell activity loss, due to a non-inducible prolonged silencing effect of Kir2.1.

Genotypes are abbreviated as follows: a: +>10xKir2.1, b: R24E09>+, c: R24E09>10xKir2.1, d: VT058487>10xKir2.1, e: VT058487+tsh-Gal80>10xKir2.1, f: R27B03+tubGal80ts>Kir2.1, g: R81G07+tubGal80ts>Kir2.1, h: VT023749+tubGal80ts>Kir2.1. Symmetric experimental conditions are subtracted from each other for rotation and added for velocity. Data represents mean \pm standard error of the mean over flies (n=10), with 90 trials.

4 | DISCUSSION

Unravelling the neural implementation of visually guided behavior is a challenging undertaking. In order to facilitate this task, *Drosophila melanogaster*, with stereotyped visual behavior and motor reflexes, is a suitable model organism. Compared to other vertebrate model organisms, *Drosophila* has a comparatively smaller number of neurons, which reduces the overall complexity. Additionally, its neural circuits are broadly described and an important variety of genetic tools to visualize, manipulate and study them are currently available.

While the usage of optogenetic tools to test synaptic connectivity and behavioral causality has been rapidly established, there was no suitable inhibitory channel to perform acute silencing experiments within the visual system of *Drosophila*. Therefore, my colleagues and I set out to test the recently discovered anion channelrhodopsins GtACR1 and GtACR2 for their possible application in flies. We characterized their properties and performed whole-cell recordings from tangential cells expressing GtACR1. Based on our experiments, I was able to show that GtACR1 enables fast and reversible hyperpolarization of neurons within the visual circuit during tethered walking.

Next, I investigated the contribution of HS cells to walking behavior. I introduced optogenetically evoked de- and hyperpolarization in HS cells, which mimicked different types of visual motion, and thereby described two novel findings. First, HS cells transmit two visual motion directions to downstream neurons: de- and hyperpolarization evoke turning behavior into opposite directions. Second, bilateral de- and hyperpolarization of HS cells have a negative effect on walking velocity. Overall, these findings suggest that HS cells influence walking behavior bidirectionally via two decelerating pathways.

4.1 NEURAL ACTIVITY MANIPULATIONS

Silencing tools interrupt the propagation of neural signals to connect neurons and therefore are commonly used to investigate the functional requirement of individual neurons. Although hyperpolarization is often synonymously understood as silencing, this is not necessarily correct. Lobula plate tangential cells, for example, are known to respond via de- and hyperpolarization. Contrarily to silencing, induced hyperpolarization can potentially be propagated to downstream neurons and thus represent a neural output signal. Despite these differences, hyperpolarizing techniques are also very useful for investigating the functional importance of neurons.

4.1.1 Possibilities of Neural Silencing

Silencing tools use various mechanisms to block synaptic transmission at different time scales. Furthermore, as their silencing effects may or may not be controllable, individual silencing tools are generally better suited for different types of experiments.

Different Silencing Mechanisms

Signals between neurons are transmitted by chemical and electrical synapses. Chemical synapses, which can transmit more complex signals in comparison to electrical synapses, rely on neurotransmitter and neuropeptides to communicate to connected neurons. Electrical synapses, which are faster and allow bidirectional signal transmission, use intercellular channels to transmit signals. These intracellular channels, known as gap junctions, form pore structures through which small molecules and ions diffuse to the connected cell.

To completely block the transmission of neural signals, silencing tools should ideally interfere with both types of synapses. Current tools, however, usually only interfere with chemical synaptic transmissions or introduce artificial hyperpolarization. For example, *shibire*^{ts} and TNT silence transmission by chemical synapses, while Kir2.1 and GtACR1 introduce strong hyperpolarization. Thus, signal transmission over gap junctions is often left unaffected. Silencing cells that are known to have both types of synapses, such as several LPTCs, can therefore lead to only partially blocked signal transmission.

Permanent Silencing

There are different genetic tools that enable permanent silencing of neurons in *Drosophila* and are therefore useful to test the requirement of neurons for a given computation (see section 2.2.4). One of the papers presented in this thesis demonstrated that HS cells are not required for the optomotor response, as flies were still able to perform optomotor behavior despite the permanent silencing of such cells (see section 3.2).

Permanent silencing tools, however, also present challenges and disadvantages and are therefore not always well suited for certain experiments. For example, prolonged silencing can cause neural circuits to adapt to the artificial block. Signals could consequently be adjusted in amplitude, or homeostatic mechanisms counteracting the chronic inhibition might arise. Furthermore, permanent silencing can introduce developmental artifacts that alter neuronal connectivity, signal processing, or even lead to death during development. I encountered this challenge when performing experiments to permanently silence HS cells using Kir2.1, as only a few driver lines survived. I could only overcome this problem by suppressing Kir2.1 expression during development and therefore only silencing HS cells after this stage (see section 3.2).

Finally, the efficacy of synaptic silencers, such as *shibire*^{ts} and tetanus toxin light chain (TNT), may vary significantly depending on the molecular composition of the targeted cell type (Thum et al., 2006). It can therefore be

necessary to check whether the tool used sufficiently silences the cells of interest.

Short Term Silencing

Sometimes it is advantageous to silence neurons only within defined periods of time. For this purpose, it is necessary to control the silencing activity remotely. Temporal control of silencing tools is often based on temperature, whereby a threshold defines if the tool is activated or deactivated. While *shibire^{ts}* is inherently controlled by temperature, it is also possible to use the temperature-sensitive GAL4 repressor GAL80^{ts} in combination with permanent silencers. With these techniques, GAL4 is only expressed and therefore active at around 30°C.

In order to control temperature-sensitive silencing tools, it is important to be able to set a specific temperature in the experimental setup. Alternatively, it is possible to activate the silencing tool before the experiment by placing the experimental animal into a heated environment. As the silencing effect will last for certain time after neurons have been silenced, one can remove the animal from the heated environment to conduct the experiments.

As the walking behavior of flies is temperature dependent, the temperature in the tethered walking setup used during this work was precisely controlled. Consequently, temperature-sensitive silencing tools were always activated when flies were inside the setup. This greatly limited the temporal control of the silencing tools. Additionally, it is not only technically demanding to switch quickly between different temperatures, but also the silencing effect of temperature-sensitive silencers does not occur immediately. Therefore, temperature-dependent silencing tools are not well suited to introduce acute silencing, as was required for this work.

Optogenetic Silencing

Optogenetic silencers operate much faster than temperature-controlled tools and enable to reversibly de- and hyperpolarize neurons. While potent optogenetic tools to depolarize neurons were already existing, the discovery of GtACR1 enabled the introduction of strong hyperpolarizations into targeted neurons. Such strong hyperpolarizations can effectively block cells, as we described for T4/T5 cells (see section 3.1). HS cells, however, respond with de- and hyperpolarization and induced hyperpolarization can therefore act as an output signal that is transmitted to connected neurons. Furthermore, optogenetic tools are controlled by light, which further complicates the investigation of the visual system. These challenges and corresponding considerations for using optogenetics in visual circuits are discussed in the following sections.

4.1.2 Considerations for Using Optogenetic Tools

Optogenetic tools have many intrinsic parameters that need to fit the experimental needs. The successful application of optogenetics to perform cell-specific manipulations may therefore strongly depend on the selection

of the right tool. This selection, however, can be challenging because the effect of optogenetic tools varies between distinct cell types or even between different compartments within the same cell. Probably due to this or similar reasons, some silencing tools show counter-intuitive side effects, such as increased spontaneous neurotransmitter release (Mahn et al., 2016) or enhanced synaptic transmission (Mattingly et al., 2018). In addition, inconsistent effects caused by unintended changes in ion distributions have been reported (Sierra et al., 2018; Raimondo et al., 2012; Alfonsa et al., 2015; Mahn et al., 2016). Consequently, it is desirable to confirm whether the used tool shows the intended effect on targeted cells and if there are critical cell-specific artifacts.

While the properties of GtACR₁ were well suited for the experiments presented in this thesis, its overall effect depends on the chloride reversal potential of individual cells. Therefore, the use of GtACR₁ may not always result in the anticipated hyperpolarization. As shown in section 3.1, GtACR₁ effectively hyperpolarized cells and their axons in the visual system of *Drosophila*. In contrast to studies on vertebrates, no depolarization effects were observed (Wiegert and Oertner, 2016; Mahn et al., 2016; Malyshev et al., 2017). Counter-intuitive side effects described in other organisms may therefore be weaker or absent in *Drosophila*.

The second optogenetic tool used in this work was ReaChR, which has very similar spectral properties to GtACR₁. As for GtACR₁, ReaChR was proven to be well suited to manipulate cells in the visual system of *Drosophila* (see section 3.2).

Overall, both GtACR₁ and ReaChR are optogenetic tools that can be used to investigate the functional importance of neurons in visual circuits by manipulating their activity on a trial-by-trial basis, i.e. control and experimental conditions can be randomly interleaved within the same animal. This can dramatically improve the interpretation of experimental data and provide a better statistical basis for future analysis.

4.1.3 Optogenetic Manipulations in Visual Circuits

The application of optogenetics within visual circuits can be hampered by the fact that both the optogenetic tools and the endogenous photoreceptors have to be separately stimulated with light. Often there is no clear spectral separation between the optogenetic light spectrum and the endogenous photoreceptors, which can lead to significant interference with the visual system. Therefore, in order to efficiently use optogenetic within visual circuits, it is necessary to find solutions to ensure largely independent stimulation of the photoreceptors and optogenetic tools.

Spatial Separation

In principle, spatial separation could effectively solve the problem of unwanted light-induced artifacts. Under the assumption that optogenetic light can be perfectly controlled, one could ensure that it does not stimulate the photoreceptors. In this case, the wavelength of the optogenetic light would not matter. However, light is scattered upon encountering biological tissue,

which prevents optical systems from illuminating precisely defined areas within the brain (Vellekoop and Aegerter, 2010). Since primary visual circuits are usually very close to the photoreceptors, it can be very difficult to achieve spatial separation.

Light scattering could be observed in the tethered walking experiments presented in section 3.2. Depending on its intensity, optogenetic light focused on one optic lobe was even able to trigger optogenetic tools expressed in cells on the contralateral side. This example illustrates that it is not always possible to rely entirely on spatial separation to prevent optogenetic light induced artifacts.

Spectral Separation

Visual artifacts caused by optogenetic stimulation can also be avoided by using optogenetic tools with distinct activation spectra in comparison to the endogenous rhodopsins. Yet when following a spectral separation approach, it is often not possible to achieve perfect separation of both spectra. Even if the remaining overlap may seem minimal, it can still cause interference. This requires the user to pay close attention to other properties of the chosen optogenetic tools, such as sensitivity and conductance, as these properties can additionally constrain the experiment. Halorhodopsin can be seen as an example of this complication (Gradinaru et al., 2008). Although the activation spectrum extends past the visual spectrum of *Drosophila*, halorhodopsin lacks the necessary sensitivity. Consequently, the required high intensity light is still sufficient to interfere with the photoreceptors. When comparing the activation spectrum of GtACR1 with that of halorhodopsin, it can be seen that GtACR1 has a greater overlap with *Drosophila*'s rhodopsin 1. Nevertheless, since GtACR1 is very sensitive, it can be used without causing a strong interference with the photoreceptors.

Overall, a spectral separation approach to gain independent control over optogenetic tools and the visual system should be considered as a multivariate optimization problem where several properties have to be accounted for (see figure 14).

Temporal Separation

Independent stimulation of both the visual system and optogenetic tools can also be achieved by temporal separation. For this purpose, optogenetic tools based on step-function or bi-stable opsins (SFOs) can be used (see section 2.3.6). These tools can be switched on or off by short light pulses, but their effect is maintained over longer periods of time. Artifacts caused by optogenetic light decrease shortly after the stimulation has stopped. Subsequently, experimental measurements with altered neural activity and without artifacts can be performed.

Tools based on SFOs seem to be well suited for behavioral experiments. They can be activated within a short period of time during which the animal may even be spatially restricted. After activation, there is no need for further interference. However, the high light sensitivity of SFOs makes their usage challenging. Switchable tools can easily be accidentally triggered or reset

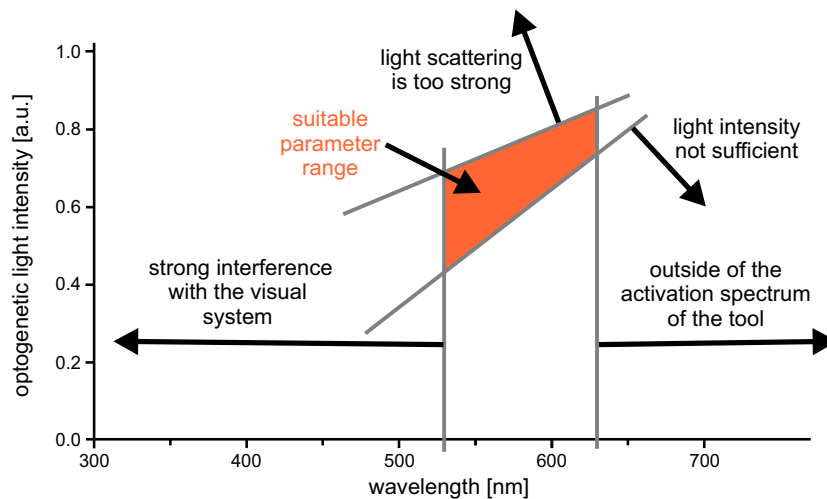


Figure 14: Exemplary illustration of the suitable parameter range (orange area) of an optogenetic tool. Several different parameters and properties restrict the range of suitable optogenetic stimulation light. For example, the wavelength of the optogenetic light is limited by the activation spectrum of the optogenetic tool and the visual range of *Drosophila*. Moreover, the light intensity must overcome a certain value to activate the tool sufficiently, but it must also not scatter into brain areas where it causes unintended manipulations.

even in low light conditions. It is therefore tricky to use these type of tools during visual tasks or light depending behaviors (Tye and Deisseroth, 2012).

Interference Caused by Visual Stimulation

Besides the interference of optogenetic light with the visual system, it is also possible that other light sources unintentionally trigger optogenetic tools. This problem becomes particularly apparent when investigating the visual system, which often requires the presentation of visual stimuli. Light sources that typically cause this type of unintentional activation include visual screens and projectors, light needed for the tracking of the animal, or laser light required to record the neural activity.

While unintended optogenetic activation can cause a constant minimal effect, it is important to detect it in order to ensure correct the interpretation of experimental results (see section 3.1). Thus, when using optogenetics, it is necessary to pay additional attention to wavelength and intensity of all nearby light sources.

Further Challenges

The expression strength of genetic tools is likely to vary between driver lines. Therefore, it is not always possible to use the same optogenetic light stimulation parameters or even the same optogenetic tool for different driver lines. For example, a stronger expression of the tool requires a lower optogenetic light intensity to achieve the same effect than tools weakly expressed. This can be problematic in cases where very specific driver lines are used. As these lines express only in a few neurons, they tend to have rather weak

expression. Thus, high light intensities are required, which can cause visual artifacts or even local changes in temperature of the brain tissue due to the absorption of light. Interestingly, recent studies have raised concerns about the side effects of optogenetically induced temperature changes during optogenetic stimulation (Vogt, 2018, 2019).

4.1.4 Optimizing GtACR1

Despite the successful application of GtACR1 in the visual system of *Drosophila*, further optimization of GtACR1 can be achieved. For this purpose, it is possible to use molecular engineering, which enables to create variants with improved properties. Since similar optimizations have already been performed for optogenetic excitatory tools, it might be possible to transfer the used approaches to optogenetic silencers. In fact, next generation of optogenetic silencers are currently being developed (Govorunova et al., 2017; Wietek et al., 2017).

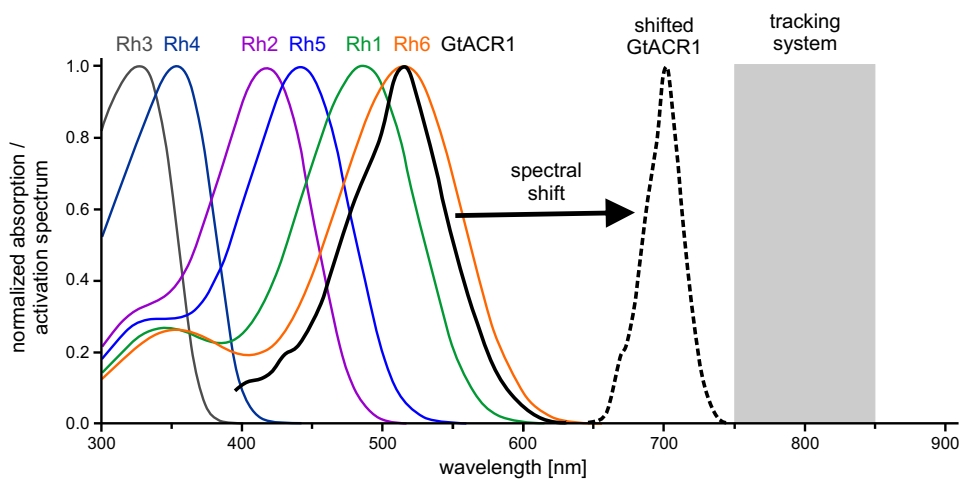


Figure 15: Proposed optimization of GtACR1 by spectral shift. Illustration of the absorption spectra of the six rhodopsins (Rh1-Rh6) expressed by *Drosophila* as well as the activation spectrum of GtACR1. The gray area indicates the wavelengths that are commonly used to track flies with infrared cameras. Figure adapted from Stavenga and Arikawa, 2008.

In order to improve GtACR1 for a lower influence onto the visual system of *Drosophila*, it could first be attempted to shift the activation spectrum into a more suitable range. As introduced in section 1.3.2, *Drosophila* has several photoreceptor types and subtypes containing different rhodopsins. These are used for various functional purposes, such as motion or color vision. Interference with any of these photoreceptors should be avoided, since it could trigger different types of artifacts.

When considering the spectral properties of all rhodopsins, it can be seen that they cover wavelengths from around 300nm up to 600nm (see figure 15). Accordingly, it would be possible to shift the activation spectrum of GtACR1 towards lower or higher wavelengths. Importantly, as the penetration of biological tissue is poorer for light of lower wavelengths than for light with

higher wavelengths, it is generally preferred to shift tools towards higher wavelengths as it facilitates stimulation of deeper lying neurons. Moreover, in order to combine the shifted optogenetic tool with tracking of flies, which is typically achieved by infrared cameras, wavelengths around 750 – 850nm must also be avoided. Taken together, GtACR₁ could be further optimized by generating red-shifted GtACR₁ with rather narrow activation spectrum that peaks around 700nm.

Alternatively, it is possible to generate switchable GtACR₁ variants by introducing slow channel kinetics. While improved spectral properties would also be desirable in that case, the possible interference with photoreceptors is limited to short periods of time and could therefore be acceptable. However, it would certainly be necessary to adjust the sensitivity of these tools so that they are not affected by visual stimuli.

4.2 THE ROLE OF HS CELLS FOR BEHAVIOR

The visual response properties of HS cells are well characterized in various fly species. From these properties and additional evidence, it is generally assumed that HS cells contribute to the control of self-motion. Past studies have therefore manipulated HS cell signals at various degrees of specificity and found behavioral phenotypes in agreement with the HS cells' role in yaw course stabilization. These studies, however, concentrated on the effect of depolarization on steering behavior and neglected hyperpolarization signals (Fujiwara et al., 2016; Haikala et al., 2013). In this thesis, further evidence is added by showing that HS cells function as bi-directional flow sensors to control turning in tethered walking *Drosophila*.

4.2.1 Response Properties Supporting Role in Course Control

HS cells are motion sensitive and directionally selective. They respond with depolarization to global horizontal motion in their preferred-direction (front-to-back) and with hyperpolarization to global horizontal motion in their null-direction (back-to-front) (Schnell et al., 2010). This response to very specific optic flow patterns is well suited to provide feedback on self-motion (Krapp et al., 1998). However, the response of individual HS cells is ambiguous. Only by considering the signals from both hemispheres is it possible to differentiate between yaw rotations and translations. For example, self-evoked yaw rotations depolarize HS cells on one hemisphere, while cells on the other side hyperpolarize. However, de- or hyperpolarization on one hemisphere can also be evoked by unilateral front-to-back stimulation, as experienced during forward motion or when passing nearby objects. Therefore, joined responses of all HS cells and additional functional logic are required to reliably use HS signals for course control. Alternatively, signals from other LPTCs can potentially be used to resolve the ambiguity of HS cell signals.

4.2.2 The Effect of Acute Manipulations on Tethered Walking

As has been shown in section 3.2, acute optogenetic unilateral de- and hyperpolarization in HS cells evokes turning responses to opposite directions. Induced depolarization evoked ipsilateral turning and hyperpolarization evoked contralateral turning. These results are consistent with the generally accepted role of HS cells for yaw stabilization. As is known from its optomotor response, *Drosophila* compensates external full field rotation by turning in the same direction. Hereby, the fly perceives front-to-back motion on one eye and back-to-front motion on the other. These visual inputs correspond to depolarization and hyperpolarization of HS cells, respectively. As I have shown in my optogenetic experiments, both de- and hyperpolarization evoke turning syndirectional with the mimicked horizontal optic flow.

Furthermore, bilateral optogenetic de- or hyperpolarization did not evoke turning responses but had a clear effect on walking velocity. Visual patterns that would evoke similar responses in HS cells are equivalent to visual feedback perceived during forward and backward translation. The observed lack of turning behavior is therefore in agreement with a yaw stabilization mechanism that appears to incorporate preferred- as well as null-direction inputs from HS cells of both optic lobes.

Overall, wide-field motion sensitive neurons in various species do not only respond with depolarization to preferred-direction, but also hyperpolarize to null-direction (Wylie et al., 1998; Duffy and Wurtz, 1991; Ibbotson, 1991). While it has already been shown that an important function of motion opponency in these kind of neurons is the improvement of flow field selectivity (Mauss et al., 2015), the findings presented in this thesis indicate that null-direction inputs further give rise to null-direction hyperpolarization, which is used as a steering signal. The hyperpolarization of HS cells is likely to be evoked by LPi neurons, as for VS cells. Thus, signals from LPi neurons are not only important for flow field selectivity, but also influence steering behavior.

4.2.3 Redundancy in the Lobula Plate Network

While it has been suggested that the primary function of HS and VS is to control head movements and therefore support gaze stability (Kim et al., 2017), there is clear evidence that HS cells also influence steering behavior during walking and flight (Haikala et al., 2013; Fujiwara et al., 2016, see section 3.2). However, silencing HS cells has only a minor effect on the optomotor behavior of *Drosophila*. Silencing experiments with Kir2.1 during tethered flight resulted in slightly slower wing response accelerations for visual patterns at high velocities, while the amplitude of wing responses was unaltered (Kim et al., 2017). In similar silencing experiments with Kir2.1 during tethered walking, I could also not observe any consistent effect regarding the optomotor response (see section 3.2). Thus, the contribution of HS cells to steering behavior appears to be part of a redundant circuit architecture. As redundant systems provide increased reliability and safety, they may be important for course control. Wrong steering signals could further destabilize moving animals and therefore lead to collisions with objects in the environment.

It is currently not known which cells in addition to the HS cells could be part of the proposed redundant system. One possibility is the existence of yet unidentified LPTCs in layer 1, alongside HS cells. It is also tempting to speculate about the contribution of LPTCs in layer 2, which show mirror-symmetrical direction selectivity. As shown in section 3.2, HS cells affect turning bi-directionally, which may well also apply to layer 2 cells. Thus, layer 1 and 2 cells may contribute to turning in a fully redundant way. One example for a layer 2 cell is H2. Unlike HS cells, H2 cells project to the contralateral hemisphere near to the axon terminals of HS cells of the other side (Cruz et al., 2019). Furthermore, H2 cells are most likely connected to descending neurons and may further provide signals onto HS cell terminals (Hausen, 1984; Haag and Borst, 2001). Because of the mirror-symmetric response profile in combination with the contralateral projection, H2 cells could potentially be connected to the same descending pathways as HS cells. Silencing HS cells would therefore not influence signals transmitted from H2 cells towards downstream areas. Additional candidate cells that could be part of the redundant system are Hx cells, which however are barely described in *Drosophila* (Wasserman et al., 2015).

Finally, tangential cells do not only provide information for downstream circuits, but further share information among each other via gap junctions and chemical synapses. Thus, LPTCs build up a tangential cell network in which signals can be transmitted to the ipsilateral as well as to the contralateral hemisphere (Borst and Weber, 2011; Haag and Borst, 2001). This connectivity among LPTCs influences the transmission of single tangential cell responses. Signals of individual tangential cell can spread through the network and thus affect connected cells. This also applies to optogenetic manipulations, which are likely to spread partially over the network. Therefore, the exact structure and connectivity of the tangential cell network may be important to gain further insights into the function of individual LPTCs.

4.2.4 Downstream Pathways

LPTCs are known to project into the posterior slope of the central brain (Strausfeld and Bassemir, 1985; Suver et al., 2016), which in turn is connected to the ventral nerve cord (VNC). The VNC is part of the central nervous system and contains motor areas that control most types of locomotor behavior. The so-called descending neurons form the link through which neural circuits within the brain communicate with the VNC. Overall, *Drosophila* has around 1100 descending neurons, from which only a small fraction is expected to transmit signals from LPTCs (Hsu and Bhandawat, 2016). While initial studies have started to systematically characterize descending neurons in *Drosophila*, additional information on connectivity and function is further required (Namiki et al., 2018). Most of the current knowledge is based on studies on larger flies and assumed to be conserved in *Drosophila* (Strausfeld and Bassemir, 1985; Strausfeld and Gronenberg, 1990; Suver et al., 2016).

Due to anatomical connectivity, it is likely that signals from tangential cells reach motor areas that control locomotion. The findings presented in this thesis further suggest that de- and hyperpolarizing signals from HS

cells are contributing to at least two separate downstream pathways. The split may occur at the level of descending neurons downstream of HS cells. It might be implemented similar to the split of photoreceptor signals into an ON and an OFF pathway, in which single photoreceptors impinge on two types of lamina cells: L1 and L2 (see section 1.3.3). Depolarization of L2 activates specific downstream neurons via excitatory cholinergic synapses, while hyperpolarization of L1 activates other downstream neurons via inhibitory sign-inverting glutamatergic synapses. Similarly, HS cell signals may be conveyed in a graded fashion to excitatory and inhibitory descending neurons with different postsynaptic targets, potentially on different sides of the body.

4.2.5 Visual Control of Walking Velocity

As presented in section 3.2, both bilateral de- and hyperpolarization as well as rotational stimuli led to a reduction in walking speed. These findings are in line with experiments performed by Creamer et al., 2018. Supporting my findings, the authors observed that back-to-front translational stimuli cause stronger slowing responses in comparison to front-to-back. In addition, they showed that the slowing response is tuned with respect to the speed of the visual stimuli and not to its temporal frequency. This finding stands in contrast with the turning responses, which are tuned to the temporal frequency. Furthermore, the authors conclude that orientation and walking speed are stabilized by algorithms that have distinct tuning but employ overlapping circuitry. They further speculate that the speed modulation of these circuits is based on T4/T5 neurons (Creamer et al., 2018), which are known inputs to HS cells. Moreover, previous studies have shown that HS cells encode translational information, suggesting that HS cells contribute to velocity control (Kern et al., 2005; Karmeier et al., 2006). Taken together, the results of Creamer et al., 2018 and the findings presented in section 3.2 indicate that HS cells are part of the proposed overlapping circuitry.

Finally, closed-loop experiments with changed visual feedback gains showed de- and accelerations in walking speed, which I did not observe in my open-loop experiments (Creamer et al., 2018). This underlines the importance of accurate visual feedback signals for velocity control. Experiments aimed at investigating velocity control may therefore need to be carried out in closed-loop configurations that better reassemble naturalistic feedback.

4.2.6 Behavioral Importance of HS Cell Signals

Although it is evident that HS cells and most probably other LPTCs influence the steering behavior of *Drosophila*, their contribution to course control and stabilization in natural behavior is not fully understood. It is often assumed that HS cells provide some kind of error signal, which captures unintended self-motion. While this idea is generally compatible with the findings presented in this thesis, it is difficult to extrapolate results from tethered walking experiments to natural behavior.

Tethered experiments suffer from altered feedback signals and artificial visual stimuli that only partially reflect natural conditions. However, studies investigating naturally occurring HS cell activity are challenging, since it is not yet possible to record from HS cells during unrestrained behavior. Currently, HS cell signals during natural behavior can only be estimated. Working with *Calliphora*, [Karmeier et al., 2006](#) reconstructed retinal input signals experienced by flies during unrestrained flight and replayed these as visual stimuli (further see [Kern et al., 2005](#)). The authors found that HS cells are substantially modulated by translational motion. While this suggests that HS cells may further be incorporated in signaling forward and sideward translations, it also shows the potential importance of the environmental structure.

Taken together, it is challenging to fully understand the contribution of HS cells for behavior. HS cells are part of a complex network with different types of modulations, redundancy, feedback, and additional input signals. Overall, HS cells are likely to contribute to yaw stabilization, velocity control, and spatial vision. They are expected not to be mutually exclusive for one task, but to be involved in many.

4.3 FUTURE DIRECTIONS

Many experiments aimed at understanding the neural basis of natural behavior are performed in highly restricted laboratory settings. This can be due to many reasons, such as the need to precisely control visual stimuli or to measure neural activity via patch clamp recordings. Insights gained from these experiments, however, cannot always be transferred to natural conditions. Therefore, restrained behavioral experiments sometimes have to be complemented with more naturalistic experiments on unrestrained animals, though at the expense of experimental control.

4.3.1 Unrestrained Behavioral Experiments

The tracking of freely moving flies is essential to understand their behavior. In addition, it is often required to interfere with the visual stimulus when investigating the visual system of *Drosophila*. While this interference can be as simple as changing the overall light conditions by switching on/off LEDs, more sophisticated setups can be advantageous, such as virtual reality setups that allow to show arbitrary visual patterns and motions.

Tracking

Tracking freely walking or flying flies within simple environments, such as empty walking arenas ([Simon and Dickinson, 2010](#)), is well established ([Götz and Wenking, 1973](#); [Straw et al., 2011](#); [Robie et al., 2017](#)). While free-flight setups require synchronized cameras as well as advanced calibration and analysis algorithms ([Li et al., 2013](#)), a single camera can often be sufficient to track freely walking flies. Additional complexity for walking setups only

arises if further requirements should be met, e.g. when high-resolution data is required or when several flies are to be tracked simultaneously.

Visual Stimulation

In contrast to tethered preparations in which the position between visual stimulus and experimental flies is fixed, freely moving flies will constantly change their pose with respect to the stimulus. Thus, visualized objects can change significantly in size and perspective. When displaying visual stimuli, it is therefore necessary to consider the current point of view of the fly to ensure a realistic visualization of the stimulus (Schuster et al., 2002). For this reason, the experimental hardware may need to be designed to perform real-time tracking and online generation of visual stimuli.

When combining visual stimulation and tracking, it is important to avoid the interference of both systems. In addition, the tracking system must not interfere with the visual system *Drosophila*, which can be achieved by spatial separation. The tracking of behavior can be performed with near-IR cameras, while visual stimuli are presented in the blue to green range.

4.3.2 Unilateral Optogenetic Manipulations during Unrestrained Behavior

While tracking freely moving flies with simultaneous visual stimulation allows the study of visually guided behavior, additional neural manipulations are often necessary to obtain a detailed understanding of neural circuits. This can be achieved by genetic tools that introduce permanent manipulations. As my colleagues and I have shown, however, acute optogenetic manipulations can be important to understand neural circuits. Therefore, it is desirable to use optogenetics in unrestrained experimental setups.

The integration of optogenetic stimulation within free walking or flying setups poses additional difficulties besides separating optogenetic light from the visual system of *Drosophila* (see section 4.1.3). It is further necessary to avoid the interference between the tracking system, the visual stimulation, and the optogenetic light. Moreover, unrestrained flies will constantly change their body and head pose with respect to the optogenetic light source, which makes precise and well calibrated stimulation of targeted neurons challenging.

Optogenetic Stimulation of a Moving Target

There are two main approaches to direct optogenetic stimulation light on a moving target. First, it is possible to focus a light point precisely on the area of interest. To this end, it would be necessary to track *Drosophila* in real-time and adjust the light source accordingly, which this is extremely complicated during walking behavior and especially during flight. The lower limit of tracking latency is currently around 30ms, i.e. walking or flying *Drosophila* will have advanced significantly when the positional signal becomes available to direct a light spot. Targeting the head, or even one side of the head, would simply be a matter of luck.

Second, it is possible to follow a global illumination approach, where large volumes are illuminated around the target. To this end, it is important to have a controllable homogeneous light source with a specific wavelength, which is usually custom made. The design of such a light source is challenging, as it requires a homogeneous illuminated area with high light density. Furthermore, global illumination will most probably induce light evoked behavioral artifacts and does not allow unilateral optical manipulation per se.

Neuron Specific Unilateral Expression Pattern

Currently, global optogenetic stimulation is the only feasible approach to use optogenetics in unrestrained behavioral experiments for *Drosophila*. However, this type of stimulation does not target specific cells within the expression pattern of a driver line. Thus, it can be necessary to ensure that there is no off-target expression. For HS cells, for instance, a line without any off-target expression does not currently exist. Therefore, I set out to screen for split-GAL4 line combinations that could potentially lead to specific HS cell expression patterns and I found combinations with highly specific expression in HS cells (see figure 16). Potential off-target expression in the ventral nerve cord can be suppressed with the so-called *T-shirt-GAL80* line, which represses GAL4 expression in the thoracic and abdominal part of the central nervous system of *Drosophila* (Clyne and Miesenböck, 2008).

Most driver lines, however, have symmetric expression patterns that impede the performance of unilateral manipulation experiments using global illumination. This can be tackled with additional genetic techniques, such as heat-shock approaches or stochastic expression methods that restrict the expression to one side. Accordingly, unilateral optogenetic stimulation in HS cells during unrestrained behavior is currently possible.

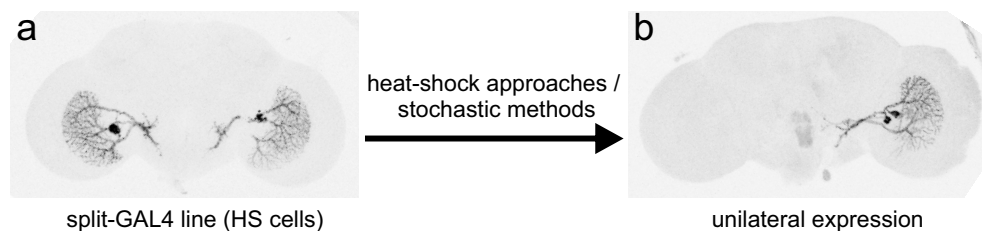


Figure 16: Symmetric and unilateral expression patterns of HS cell specific driver lines. **a** Expression pattern of a novel split-GAL4 line with HS cell specific symmetric expression (line: R27B03.AD, VT058488.DBD). **b** Selected expression pattern of a split-GAL4 line with stochastic expression mainly in HS cell (line: R39E01.AD, R81G07.DBD). Even though the random expression may be unilateral in all three HS cells, reliable unilateral expression would require heat-shock approaches or stochastic expression methods that limit expression to one side.

4.3.3 Recording Neural Activity with Bioluminescence Indicators

Simultaneous recordings of neural activity during unrestrained behavior are essential to understand neural circuits. For large animals, such as mice and birds, unrestrained recording techniques are available. Head mounted miniature fluorescence imaging microscopes, for example, enable calcium imaging while animals are moving. Originally, these devices were connected to a recording system via wires and optical fibers (Ghosh et al., 2011). Recently, however, wireless versions ideal for unrestrained behavior have been introduced (Liberti et al., 2017; Barbera et al., 2019). Unfortunately, such methods do not work for *Drosophila*.

Bioluminescence indicators are the most promising approach to enable neural recordings during free walking experiments in small animals. Recent work has successfully demonstrated that it is possible to use bioluminescence indicators to record neural activity in adult and larvae *Drosophila* (Mercier et al., 2018; Marescotti et al., 2018). However, in order to detect the emitted signals, experiments with adult flies were performed in small chambers within complete darkness. It is therefore questionable whether bioluminescence indicators can be combined with visual stimulation.

Bioluminescence represents the ability of a living organism to emit light. Genetic engineering has made it possible to develop bioluminescence indicators that emit light based on calcium concentration (for more information see Mercier et al., 2018). In contrast to calcium indicators, however, bioluminescence indicators do not need an external excitation light source in order to work. It is therefore only required to collect all emitted photons in order to measure neural activity, but emitted signals from current bioluminescence indicators are very weak. In addition, bioluminescence indicators do not capture spatial information and therefore do not allow to resolve signals from individual neurons. Recorded signals represent the overall neural activity of all neurons in which the sensor is expressed. Thus, highly specific driver lines are required in order to relate neural signals to specific neurons or neural populations.

Even though bioluminescence indicators are promising tools, they are still at an early stage of development. Improvements are required in order to combine bioluminescence recordings with visual stimulation or optogenetics.

4.4 CONCLUSION

In the course of this work, I investigated the application of GtACR1, a novel optogenetic tool, within the visual system of *Drosophila melanogaster*. Together with my colleagues, I demonstrated that GtACR1 is well suited to introduce strong hyperpolarization within the visual system of *Drosophila* without causing major visual artifacts. Subsequently, I studied the contribution of HS cell signals to walking behavior. I could induce rotational responses by introducing unilateral artificial de- or hyperpolarization in HS cells and thus show their effects on steering behavior. Furthermore, I showed that both signals negatively influence walking speed. However, silencing HS

cells did not abolish the optomotor response, which suggests the existence of a redundant system. LPTCs in layer 2, which show mirror-symmetrical direction selectivity, might participate in the suggested redundant system by also affecting turning bi-directionally. A circuit architecture that combines HS and layer 2 cell signals could potentially create the proposed redundant system. Therefore, future work will focus on the investigation of LPTCs in layer 2 and their behavioral role for *Drosophila melanogaster*.

BIBLIOGRAPHY

Adelson, E. H. and J. R. Bergen

1985. Spatiotemporal energy models for the perception of motion. *Journal of the Optical Society of America. A, Optics and Image Science*, 2 2:284–99.

Alberio, L., A. Locarno, A. Saponaro, E. Romano, V. Bercier, S. Albadri, F. Simeoni, S. Moleri, S. Pelucchi, A. Porro, E. Marcello, N. Barsotti, K. Kukovetz, A. J. Boender, A. Contestabile, S. Luo, A. Moutal, Y. Ji, G. Romani, M. Beltrame, F. Del Bene, M. Di Luca, R. Khanna, H. M. Colecraft, M. Pasqualetti, G. Thiel, R. Tonini, and A. Moroni

2018. A light-gated potassium channel for sustained neuronal inhibition. *Nature Methods*, 15(11):969–976.

Albright, T. D.

1984. Direction and orientation selectivity of neurons in visual area MT of the macaque. *Journal of Neurophysiology*, 52(6):1106–1130.

Alfonsa, H., E. M. Merricks, N. K. Codadu, M. O. Cunningham, K. Deisseroth, C. Racca, and A. J. Trevelyan

2015. The contribution of raised intraneuronal chloride to epileptic network activity. *The Journal of Neuroscience : the Official Journal of the Society for Neuroscience*, 35(25995461):7715–7726.

Arenz, A., M. S. Drews, F. G. Richter, G. Ammer, and A. Borst

2017. The temporal tuning of the *Drosophila* motion detectors is determined by the dynamics of their input elements. *Current Biology*, 27(7):929–944.

AzimiHashemi, N., K. Erbguth, A. Vogt, T. Riemensperger, E. Rauch, D. Woodmansee, J. Nagpal, M. Brauner, M. Sheves, A. Fiala, L. Kattner, D. Trauner, P. Hegemann, A. Gottschalk, and J. F. Liewald

2014. Synthetic retinal analogues modify the spectral and kinetic characteristics of microbial rhodopsin optogenetic tools. *Nature Communications*, 5:5810.

Bahl, A., G. Ammer, T. Schilling, and A. Borst

2013. Object tracking in motion-blind flies. *Nature Neuroscience*, 16:730.

Baines, R. A., J. P. Uhler, A. Thompson, S. T. Sweeney, and M. Bate

2001. Altered electrical properties in *Drosophila* neurons developing without synaptic transmission. *Journal of Neuroscience*, 21(5):1523.

Barbera, G., B. Liang, L. Zhang, Y. Li, and D.-T. Lin

2019. A wireless miniscope for deep brain imaging in freely moving mice. *Journal of Neuroscience Methods*, 323:56–60.

Barlow, H. B. and R. M. Hill

1963. Selective sensitivity to direction of movement in ganglion cells of the rabbit retina. *Science*, 139(3553):412.

- Barlow, H. B. and W. R. Levick
1965. The mechanism of directionally selective units in rabbit's retina. *The Journal of Physiology*, 178(3):477–504.
- Bartussek, J. and F.-O. Lehmann
2016. Proprioceptive feedback determines visuomotor gain in *Drosophila*. *Royal Society Open Science*, 3(1):150562.
- Bausenwein, B., A. P. M. Dittrich, and K. F. Fischbach
1992. The optic lobe of *Drosophila melanogaster*. *Cell and Tissue Research*, 267(1):17–28.
- Beck, S., J. Yu-Strzelczyk, D. Pauls, O. M. Constantin, C. E. Gee, N. Ehmann, R. J. Kittel, G. Nagel, and S. Gao
2018. Synthetic light-activated ion channels for optogenetic activation and inhibition. *Frontiers in Neuroscience*, 12:643.
- Behnia, R., D. A. Clark, A. G. Carter, T. R. Clandinin, and C. Desplan
2014. Processing properties of on and off pathways for *Drosophila* motion detection. *Nature*, 512:427.
- Behnia, R. and C. Desplan
2015. Visual circuits in flies: beginning to see the whole picture. *Current Opinion in Neurobiology*, 34:125–132.
- Bello, B., D. Resendez-Perez, and W. J. Gehring
1998. Spatial and temporal targeting of gene expression in *Drosophila* by means of a tetracycline-dependent transactivator system. *Development*, 125(12):2193.
- Bender, J. A. and M. H. Dickinson
2006. A comparison of visual and haltere-mediated feedback in the control of body saccades in *Drosophila melanogaster*. *J. Exp. Biol.*, 209(23):4597.
- Berndt, A., S. Y. Lee, J. Wietek, C. Ramakrishnan, E. E. Steinberg, A. J. Rashid, H. Kim, S. Park, A. Santoro, P. W. Frankland, S. M. Iyer, S. Pak, S. Ährlund Richter, S. L. Delp, R. C. Malenka, S. A. Josselyn, M. Carlén, P. Hegemann, and K. Deisseroth
2016. Structural foundations of optogenetics: Determinants of channel-rhodopsin ion selectivity. *Proceedings of the National Academy of Sciences of the United States of America*, 113(4):822.
- Berndt, A., P. Schoenenberger, J. Mattis, K. M. Tye, K. Deisseroth, P. Hegemann, and T. G. Oertner
2011. High-efficiency channelrhodopsins for fast neuronal stimulation at low light levels. *Proceedings of the National Academy of Sciences of the United States of America*, 108(21504945):7595–7600.
- Berndt, A., O. Yizhar, L. A. Gunaydin, P. Hegemann, and K. Deisseroth
2008. Bi-stable neural state switches. *Nature Neuroscience*, 12:229.
- Bieschke, E. T., J. C. Wheeler, and J. Tower
1998. Doxycycline-induced transgene expression during *Drosophila* development and aging. *Molecular and General Genetics MGG*, 258(6):571–579.

- Bischof, J., R. K. Maeda, M. Hediger, F. Karch, and K. Basler
2007. An optimized transgenesis system for *Drosophila* using germ-line-specific phiC31 integrases. *Proceedings of the National Academy of Sciences of the United States of America*, 104(9):3312.
- Bishop, L. G. and D. G. Keehn
1967. Neural correlates of the optomotor response in the fly. *Kybernetik*, 3(6):288–295.
- Blondeau, J.
1981. Electrically evoked course control in the fly *Calliphora erythrocephala*. *Journal of Experimental Biology*, 92(1):143.
- Blondeau, J. and M. Heisenberg
1982. The three-dimensional optomotor torque system of *Drosophila melanogaster*. *Journal of Comparative Physiology*, 145(3):321–329.
- Boergens, K. M., C. Kapfer, M. Helmstaedter, W. Denk, and A. Borst
2018. Full reconstruction of large lobula plate tangential cells in *Drosophila* from a 3D EM dataset. *PLOS ONE*, 13(11):e0207828.
- Bohm, R. A., W. P. Welch, L. K. Goodnight, L. W. Cox, L. G. Henry, T. C. Gunter, H. Bao, and B. Zhang
2010. A genetic mosaic approach for neural circuit mapping in *Drosophila*. *Proceedings of the National Academy of Sciences of the United States of America*, 107(37):16378.
- Borst, A.
2007. Correlation versus gradient type motion detectors: the pros and cons. *Philosophical Transactions of the Royal Society B: Biological Sciences*, 362(1479):369–374.
- Borst, A.
2014. Neural circuits for motion vision in the fly. *Cold Spring Harbor Symposia on Quantitative Biology*, 79:131–139.
- Borst, A. and H. D. I. Abarbanel
2007. Relating a calcium indicator signal to the unperturbed calcium concentration time-course. *Theoretical Biology and Medical Modelling*, 4(1):7.
- Borst, A. and M. Egelhaaf
1989. Principles of visual motion detection. *Trends in Neurosciences*, 12(8):297–306.
- Borst, A. and J. Haag
2002. Neural networks in the cockpit of the fly. *Journal of Comparative Physiology A*, 188(6):419–437.
- Borst, A., J. Haag, and D. F. Reiff
2010. Fly motion vision. *Annual Review of Neuroscience*, 33(1):49–70.
- Borst, A. and F. Weber
2011. Neural action fields for optic flow based navigation: A simulation study of the fly lobula plate network. *PLOS ONE*, 6(1):e16303.

- Brand, A. H. and N. Perrimon
1993. Targeted gene expression as a means of altering cell fates and generating dominant phenotypes. *Development*, 118(2):401.
- Briggman, K. L., M. Helmstaedter, and W. Denk
2011. Wiring specificity in the direction-selectivity circuit of the retina. *Nature*, 471:183.
- Buchner, E.
1971. *Dunkelanregung des stationären Flugs der Fruchtfliege Drosophila*. PhD thesis, Universität Tübingen.
- Buchner, E.
1976. Elementary movement detectors in an insect visual system. *Biological Cybernetics*, 24(2):85–101.
- Busch, C., A. Borst, and A. S. Mauss
2018. Bi-directional control of walking behavior by horizontal optic flow sensors. *Current Biology*, 28(24):4037–4045.e5.
- Cao, G., J. Platasa, V. Pieribone, D. Raccuglia, M. Kunst, and M. Nitabach
2013. Genetically targeted optical electrophysiology in intact neural circuits. *Cell*, 154(4):904–913.
- Chalfie, M., Y. Tu, G. Euskirchen, W. W. Ward, and D. C. Prasher
1994. Green fluorescent protein as a marker for gene expression. *Science*, 263(5148):802.
- Chamberland, S., H. H. Yang, M. M. Pan, S. W. Evans, S. Guan, M. Chavarha, Y. Yang, C. Salesse, H. Wu, J. C. Wu, T. R. Clandinin, K. Toth, M. Z. Lin, F. St-Pierre, and K. Scott
2017. Fast two-photon imaging of subcellular voltage dynamics in neuronal tissue with genetically encoded indicators. *eLife*, 6:e25690.
- Chen, T.-W., T. J. Wardill, Y. Sun, S. R. Pulver, S. L. Renninger, A. Baohan, E. R. Schreiter, R. A. Kerr, M. B. Orger, V. Jayaraman, L. L. Looger, K. Svoboda, and D. S. Kim
2013. Ultrasensitive fluorescent proteins for imaging neuronal activity. *Nature*, 499:295.
- Chiang, A.-S., C.-Y. Lin, C.-C. Chuang, H.-M. Chang, C.-H. Hsieh, C.-W. Yeh, C.-T. Shih, J.-J. Wu, G.-T. Wang, Y.-C. Chen, C.-C. Wu, G.-Y. Chen, Y.-T. Ching, P.-C. Lee, C.-Y. Lin, H.-H. Lin, C.-C. Wu, H.-W. Hsu, Y.-A. Huang, J.-Y. Chen, H.-J. Chiang, C.-F. Lu, R.-F. Ni, C.-Y. Yeh, and J.-K. Hwang
2011. Three-dimensional reconstruction of brain-wide wiring networks in *Drosophila* at single-cell resolution. *Current Biology*, 21(1):1–11.
- Chiappe, M. E., J. D. Seelig, M. B. Reiser, and V. Jayaraman
2010. Walking modulates speed sensitivity in *Drosophila* motion vision. *Current Biology*, 20(16):1470–1475.

- Chou, W.-H., K. J. Hall, D. B. Wilson, C. L. Wideman, S. M. Townson, L. V. Chadwell, and S. G. Britt
1996. Identification of a novel *Drosophila* opsin reveals specific patterning of the R7 and R8 photoreceptor cells. *Neuron*, 17(6):1101–1115.
- Chow, B. Y., X. Han, A. S. Dobry, X. Qian, A. S. Chuong, M. Li, M. A. Henninger, G. M. Belfort, Y. Lin, P. E. Monahan, and E. S. Boyden
2010. High-performance genetically targetable optical neural silencing by light-driven proton pumps. *Nature*, 463:98.
- Clyne, J. D. and G. Miesenböck
2008. Sex-specific control and tuning of the pattern generator for courtship song in *Drosophila*. *Cell*, 133(2):354–363.
- Collett, T. S.
1980. Some operating rules for the optomotor system of a hoverfly during voluntary flight. *Journal of Comparative Physiology*, 138(3):271–282.
- Collett, T. S. and M. F. Land
1975. Visual control of flight behaviour in the hoverfly *Syrirta pipiens* l. *Journal of Comparative Physiology*, 99(1):1–66.
- Cosens, D. and N. LeBlanc
1980. Frequency dependent flicker response enhancement in the lamina ganglionaris of *Drosophila*. *Journal of Comparative Physiology*, 137(4):341–351.
- Cosentino, C., L. Alberio, S. Gazzarrini, M. Aquila, E. Romano, S. Cerneni, P. Zuccolini, J. Petersen, M. Beltrame, J. L. Van Etten, J. M. Christie, G. Thiel, and A. Moroni
2015. Engineering of a light-gated potassium channel. *Science*, 348(6235):707.
- Creamer, M. S., O. Mano, and D. A. Clark
2018. Visual control of walking speed in *Drosophila*. *Neuron*.
- Cruz, T., T. Fujiwara, N. Varela, F. Mohammad, A. Claridge-Chang, and M. E. Chiappe
2019. Motor context coordinates visually guided walking in *Drosophila*. *bioRxiv*, P. 572792.
- Dana, H., Y. Sun, B. Mohar, B. Hulse, J. P. Hasseman, G. Tsegaye, A. Tsang, A. Wong, R. Patel, J. J. Macklin, Y. Chen, A. Konnerth, V. Jayaraman, L. L. Looger, E. R. Schreier, K. Svoboda, and D. S. Kim
2018. High-performance GFP-based calcium indicators for imaging activity in neuronal populations and microcompartments. *bioRxiv*, P. 434589.
- Dawydow, A., R. Gueta, D. Ljaschenko, S. Ullrich, M. Hermann, N. Ehmman, S. Gao, A. Fiala, T. Langenhan, G. Nagel, and R. J. Kittel
2014. Channelrhodopsin-2-XXL, a powerful optogenetic tool for low-light applications. *Proceedings of the National Academy of Sciences of the United States of America*, 111(38):13972–13977.

- Denk, W., J. H. Strickler, and W. W. Webb
1990. Two-photon laser scanning fluorescence microscopy. *Science*, 248(4951):73.
- Dickinson, M. H.
1999. Haltere-mediated equilibrium reflexes of the fruit fly, *Drosophila melanogaster*. *Philosophical transactions of the Royal Society of London. Series B, Biological Sciences*, 354(10382224):903–916.
- Dionne, H., K. L. Hibbard, A. Cavallaro, J.-C. Kao, and G. M. Rubin
2018. Genetic reagents for making split-GAL4 lines in *Drosophila*. *Genetics*, 209(29535151):31–35.
- Duffy, C. J. and R. H. Wurtz
1991. Sensitivity of MST neurons to optic flow stimuli. I. A continuum of response selectivity to large-field stimuli. *Journal of Neurophysiology*, 65(6):1329–1345.
- Duffy, J. B.
2002. GAL4 system in *Drosophila*: A fly geneticist's swiss army knife. *Genesis*, 34(1-2):1–15.
- Duistermars, B. J., D. M. Chow, M. Condro, and M. A. Frye
2007. The spatial, temporal and contrast properties of expansion and rotation flight optomotor responses in *Drosophila*. *Journal of Experimental Biology*, 210(18):3218.
- Eckert, H. and D. R. Dvorak
1983. The centrifugal horizontal cells in the lobula plate of the blowfly, *Phaenicia sericata*. *Journal of Insect Physiology*, 29(7):547–560.
- Egelhaaf, M.
1985. On the neuronal basis of figure-ground discrimination by relative motion in the visual system of the fly. *Biological Cybernetics*, 52(3):195–209.
- Egelhaaf, M., N. Böldcker, R. Kern, R. Kurtz, and J. Lindemann
2012. Spatial vision in insects is facilitated by shaping the dynamics of visual input through behavioral action. *Frontiers in Neural Circuits*, 6:108.
- Feiler, R., R. Bjornson, K. Kirschfeld, D. Mismar, G. M. Rubin, D. P. Smith, M. Socolich, and C. S. Zuker
1992. Ectopic expression of ultraviolet-rhodopsins in the blue photoreceptor cells of *Drosophila*: visual physiology and photochemistry of transgenic animals. *Journal of Neuroscience*, 12(10):3862.
- Feinberg, E. H., M. K. VanHoven, A. Bendesky, G. Wang, R. D. Fetter, K. Shen, and C. I. Bargmann
2008. GFP reconstitution across synaptic partners (GRASP) defines cell contacts and synapses in living nervous systems. *Neuron*, 57(3):353–363.
- Fennema, C. L. and W. B. Thompson
1979. Velocity determination in scenes containing several moving objects. *Computer Graphics and Image Processing*, 9(4):301–315.

- Fenko, L., O. Yizhar, and K. Deisseroth
2011. The development and application of optogenetics. *Annual Review of Neuroscience*, 34(1):389–412.
- Fiala, A., A. Suska, and O. M. Schlüter
2010. Optogenetic approaches in neuroscience. *Current Biology*, 20(20):R897–R903.
- Fischbach, K. F. and A. P. M. Dittrich
1989. The optic lobe of *Drosophila melanogaster*. I. A golgi analysis of wild-type structure. *Cell and Tissue Research*, 258(3):441–475.
- Fortini, M. E. and G. M. Rubin
1990. Analysis of *cis*-acting requirements of the Rh3 and Rh4 genes reveals a bipartite organization to rhodopsin promoters in *Drosophila melanogaster*. *Genes & Development*, 4(3):444–463.
- Freyberg, Z., M. S. Sonders, J. I. Aguilar, T. Hiranita, C. S. Karam, J. Flores, A. B. Pizzo, Y. Zhang, Z. J. Farino, A. Chen, C. A. Martin, T. A. Kopajtich, H. Fei, G. Hu, Y.-Y. Lin, E. V. Mosharov, B. D. McCabe, R. Freyberg, K. Wimalasena, L.-W. Hsin, D. Sames, D. E. Krantz, J. L. Katz, D. Sulzer, and J. A. Javitch
2016. Mechanisms of amphetamine action illuminated through optical monitoring of dopamine synaptic vesicles in *Drosophila* brain. *Nature Communications*, 7:10652.
- Fujiwara, T. and E. Chiappe
2017. Motor-driven modulation in visual neural circuits. In *Decoding Neural Circuit Structure and Function: Cellular Dissection Using Genetic Model Organisms*, A. Çelik and M. F. Wernet, eds., Pp. 261–281. Cham: Springer International Publishing.
- Fujiwara, T., T. L. Cruz, J. P. Bohnslav, and M. E. Chiappe
2016. A faithful internal representation of walking movements in the *Drosophila* visual system. *Nature Neuroscience*, 20(1):72–81.
- Ganapathy, S., O. Bécheau, H. Venselaar, S. Frölich, J. van der Steen, Q. Chen, S. Radwan, J. Lugtenburg, K. Hellingwerf, H. M. de Groot, and W. de Grip
2015. Modulation of spectral properties and pump activity of proteorhodopsins by retinal analogues. *Biochemical Journal*, 467(2):333.
- Gao, S., S.-y. Takemura, C.-Y. Ting, S. Huang, Z. Lu, H. Luan, J. Rister, A. S. Thum, M. Yang, S.-T. Hong, J. W. Wang, W. F. Odenwald, B. H. White, I. A. Meinertzhagen, and C.-H. Lee
2008. The neural substrate of spectral preference in *Drosophila*. *Neuron*, 60(2):328–342.
- Gauck, V. and A. Borst
1999. Spatial response properties of contralateral inhibited lobula plate tangential cells in the fly visual system. *Journal of Comparative Neurology*, 406(1):51–71.

- Geiger, G. and D. R. Nässel
1981. Visual orientation behaviour of flies after selective laser beam ablation of interneurons. *Nature*, 293(5831):398–399.
- Ghosh, K. K., L. D. Burns, E. D. Cocker, A. Nimmerjahn, Y. Ziv, A. E. Gamal, and M. J. Schnitzer
2011. Miniaturized integration of a fluorescence microscope. *Nature Methods*, 8:871.
- Gibson, J. J.
1950. *The perception of the visual world*. Houghton Mifflin.
- Golic, K. G. and S. Lindquist
1989. The FLP recombinase of yeast catalyzes site-specific recombination in the *Drosophila* genome. *Cell*, 59(3):499–509.
- Govorunova, E. G., O. A. Sineshchekov, R. Janz, X. Liu, and J. L. Spudich
2015. Natural light-gated anion channels: A family of microbial rhodopsins for advanced optogenetics. *Science*, 349(6248):647–650.
- Govorunova, E. G., O. A. Sineshchekov, E. M. Rodarte, R. Janz, O. Morelle, M. Melkonian, G. K.-S. Wong, and J. L. Spudich
2017. The expanding family of natural anion channelrhodopsins reveals large variations in kinetics, conductance, and spectral sensitivity. *Scientific Reports*, 7:43358.
- Gradinaru, V., K. R. Thompson, and K. Deisseroth
2008. eNpHR: a natronomonas halorhodopsin enhanced for optogenetic applications. *Brain Cell Biology*, 36(1):129–139.
- Gradinaru, V., F. Zhang, C. Ramakrishnan, J. Mattis, R. Prakash, I. Diester, I. Goshen, K. R. Thompson, and K. Deisseroth
2010. Molecular and cellular approaches for diversifying and extending optogenetics. *Cell*, 141(20303157):154–165.
- Grether, M. E., J. M. Abrams, J. Agapite, K. White, and H. Steller
1995. The head involution defective gene of *Drosophila melanogaster* functions in programmed cell death. *Genes & Development*, 9(14):1694–1708.
- Gronenberg, W., J. J. Milde, and N. J. Strausfeld
1995. Oculomotor control in calliphorid flies: Organization of descending neurons to neck motor neurons responding to visual stimuli. *Journal of Comparative Neurology*, 361(2):267–284.
- Gronenberg, W. and N. J. Strausfeld
1990. Descending neurons supplying the neck and flight motor of diptera: Physiological and anatomical characteristics. *Journal of Comparative Neurology*, 302(4):973–991.
- Groth, A. C., M. Fish, R. Nusse, and M. P. Calos
2004. Construction of transgenic *Drosophila* by using the site-specific integrase from phage phiC31. *Genetics*, 166(15126397):1775–1782.

- Gruntman, E., S. Romani, and M. B. Reiser
2018. Simple integration of fast excitation and offset, delayed inhibition computes directional selectivity in *Drosophila*. *Nature Neuroscience*, 21(2):250–257.
- Götz, K. G.
1964. Optomotorische Untersuchung des visuellen systems einiger Augenmutanten der Fruchtfliege *Drosophila*. *Kybernetik*, 2(2):77–92.
- Götz, K. G.
1965. Die optischen Übertragungseigenschaften der Komplexaugen von *Drosophila*. *Kybernetik*, 2(5):215–221.
- Götz, K. G. and H. Wenking
1973. Visual control of locomotion in the walking fruitfly *Drosophila*. *Journal of Comparative Physiology*, 85(3):235–266.
- Gunaydin, L. A., O. Yizhar, A. Berndt, V. S. Sohal, K. Deisseroth, and P. Hegemann
2010. Ultrafast optogenetic control. *Nature Neuroscience*, 13:387.
- Guru, A., R. J. Post, Y.-Y. Ho, and M. R. Warden
2015. Making sense of optogenetics. *The International Journal of Neuropsychopharmacology*, 18(26209858):pyv079.
- Haag, J., A. Arenz, E. Serbe, F. Gabbiani, A. Borst, and F. Rieke
2016. Complementary mechanisms create direction selectivity in the fly. *eLife*, 5:e17421.
- Haag, J. and A. Borst
2001. Recurrent network interactions underlying flow-field selectivity of visual interneurons. *Journal of Neuroscience*, 21(15):5685.
- Haag, J., A. Mishra, A. Borst, and F. Rieke
2017. A common directional tuning mechanism of *Drosophila* motion-sensing neurons in the ON and in the OFF pathway. *eLife*, 6:e29044.
- Hadjieconomou, D., S. Rotkopf, C. Alexandre, D. M. Bell, B. J. Dickson, and I. Salecker
2011. Flybow: Genetic multicolor cell labeling for neural circuit analysis in *Drosophila melanogaster*. *Nature Methods*, 8:260.
- Haikala, V., M. Joesch, A. Borst, and A. S. Mauss
2013. Optogenetic control of fly optomotor responses. *Journal of Neuroscience*, 33(34):13927.
- Hall, J. M., D. P. McLoughlin, N. D. Kathman, A. M. Yarger, S. Mureli, and J. L. Fox
2015. Kinematic diversity suggests expanded roles for fly halteres. *Biology Letters*, 11(11):20150845.
- Hamada, F. N., M. Rosenzweig, K. Kang, S. R. Pulver, A. Ghezzi, T. J. Jegla, and P. A. Garrity
2008. An internal thermal sensor controlling temperature preference in *Drosophila*. *Nature*, 454:217.

- Hampel, S., P. Chung, C. E. McKellar, D. Hall, L. L. Looger, and J. H. Simpson
2011. *Drosophila* Brainbow: A recombinase-based fluorescence labeling technique to subdivide neural expression patterns. *Nature Methods*, 8:253.
- Han, D. D., D. Stein, and L. M. Stevens
2000. Investigating the function of follicular subpopulations during *Drosophila* oogenesis through hormone-dependent enhancer-targeted cell ablation. *Development*, 127(3):573.
- Han, X., B. Chow, H. Zhou, N. Klapoetke, A. Chuong, R. Rajimehr, A. Yang, M. Baratta, J. Winkle, R. Desimone, and E. Boyden
2011. A high-light sensitivity optical neural silencer: Development and application to optogenetic control of non-human primate cortex. *Frontiers in Systems Neuroscience*, 5:18.
- Hardie, R. C.
1985. Functional organization of the fly retina. In *Progress in Sensory Physiology*, H. Autrum, D. Ottoson, E. R. Perl, R. F. Schmidt, H. Shimazu, and W. D. Willis, eds., Pp. 1–79. Berlin, Heidelberg: Springer Berlin Heidelberg.
- Hardie, R. C.
2001. Phototransduction in *Drosophila melanogaster*. *Journal of Experimental Biology*, 204(20):3403.
- Hardie, R. C.
2011. Phototransduction mechanisms in *Drosophila* microvillar photoreceptors. *WIREs Membrane Transport and Signaling*, 1(2):162–187.
- Hardie, R. C. and M. Juusola
2015. Phototransduction in *Drosophila*. *Current Opinion in Neurobiology*, 34:37–45.
- Hardie, R. C. and P. Raghu
2001. Visual transduction in *Drosophila*. *Nature*, 413:186.
- Hassenstein, B.
1951. Ommatidienraster und afferente Bewegungsintegration. *Zeitschrift für Vergleichende Physiologie*, 33(4):301–326.
- Hassenstein, B. and W. Reichardt
1956. Systemtheoretische Analyse der Zeit-, Reihenfolgen- und Vorzeichenbewertung bei der Bewegungsperzeption des Rüsselkäfers *Chlorophanus*. *Zeitschrift für Naturforschung B*, 11(9-10):513.
- Hausen, K.
1984. The lobula-complex of the fly: Structure, function and significance in visual behaviour. In *Photoreception and Vision in Invertebrates*, M. A. Ali, ed., Pp. 523–559. Boston, MA: Springer US.
- Hausen, K. and C. Wehrhahn
1983. Microsurgical lesion of horizontal cells changes optomotor yaw responses in the blowfly *Calliphora erythrocephala*. *Proceedings of the Royal Society of London B: Biological Sciences*, 219(1215):211–216.

- Hausen, K. and C. Wehrhahn
1990. Neural circuits mediating visual flight control in flies. II. Separation of two control systems by microsurgical brain lesions. *Journal of Neuroscience*, 10(1):351.
- Heisenberg, M. and E. Buchner
1977. The rôle of retinula cell types in visual behavior of *Drosophila melanogaster*. *Journal of Comparative Physiology*, 117(2):127–162.
- Heisenberg, M. and R. Wolf
1984. *Vision in Drosophila: Genetics of Microbehavior*, Experimental Brain Research Supplementum. Springer-Verlag.
- Heisenberg, M., R. Wonneberger, and R. Wolf
1978. Optomotor-blind^{H31} - a *Drosophila* mutant of the lobula plate giant neurons. *Journal of Comparative Physiology*, 124(4):287–296.
- Hengstenberg, R.
1988. Mechanosensory control of compensatory head roll during flight in the blowfly *Calliphora erythrocephala* meig. *Journal of Comparative Physiology A*, 163(2):151–165.
- Herwig, L., A. J. Rice, C. N. Bedbrook, R. K. Zhang, A. Lignell, J. K. B. Cahn, H. Renata, S. C. Dodani, I. Cho, L. Cai, V. Gradinaru, and F. H. Arnold
2017. Directed evolution of a bright near-infrared fluorescent rhodopsin using a synthetic chromophore. *Cell Chemical Biology*, 24(3):415–425.
- Hidalgo, A., J. Urban, and A. H. Brand
1995. Targeted ablation of glia disrupts axon tract formation in the *Drosophila* CNS. *Development*, 121(11):3703.
- Hildreth, E. C. and C. Koch
1987. The analysis of visual motion: From computational theory to neuronal mechanisms. *Annual Review of Neuroscience*, 10(1):477–533.
- Honjo, K., R. Y. Hwang, and J. Tracey, William Daniel
2012. Optogenetic manipulation of neural circuits and behavior in *Drosophila* larvae. *Nature protocols*, 7(22790083):1470–1478.
- Hopp, E., A. Borst, and J. Haag
2014. Subcellular mapping of dendritic activity in optic flow processing neurons. *Journal of Comparative Physiology A*, 200(5):359–370.
- Hsu, C. T. and V. Bhandawat
2016. Organization of descending neurons in *Drosophila melanogaster*. *Scientific Reports*, 6:20259.
- Huang, T.-h., P. Niesman, D. Arasu, D. Lee, A. L. De La Cruz, A. Callejas, E. J. Hong, C. Lois, and M. Ramaswami
2017. Tracing neuronal circuits in transgenic animals by transneuronal control of transcription (TRACT). *eLife*, 6:e32027.

- Ibbotson, M. R.
1991. Wide-field motion-sensitive neurons tuned to horizontal movement in the honeybee, *Apis mellifera*. *Journal of Comparative Physiology A*, 168(1):91–102.
- Inada, K., H. Kohsaka, E. Takasu, T. Matsunaga, and A. Nose
2011. Optical dissection of neural circuits responsible for *Drosophila* larval locomotion with halorhodopsin. *PLOS ONE*, 6(12):e29019.
- Inagaki, H. K., Y. Jung, E. D. Hoopfer, A. M. Wong, N. Mishra, J. Y. Lin, R. Y. Tsien, and D. J. Anderson
2014. Optogenetic control of *Drosophila* using a red-shifted channel-rhodopsin reveals experience-dependent influences on courtship. *Nature Methods*, 11(24363022):325–332.
- Jenett, A., G. Rubin, T.-T. B. Ngo, D. Shepherd, C. Murphy, H. Dionne, B. Pfeiffer, A. Cavallaro, D. Hall, J. Jeter, N. Iyer, D. Fetter, J. Hausenfluck, H. Peng, E. Trautman, R. Svirskas, E. Myers, Z. Iwinski, Y. Aso, G. DePasquale, A. Enos, P. Hulamm, S. Lam, H.-H. Li, T. Laverty, F. Long, L. Qu, S. Murphy, K. Rokicki, T. Safford, K. Shaw, J. Simpson, A. Sowell, S. Tae, Y. Yu, and C. Zugates
2012. A GAL4-driver line resource for *Drosophila* neurobiology. *Cell Reports*, 2(4):991–1001.
- Joesch, M., J. Plett, A. Borst, and D. F. Reiff
2008. Response properties of motion-sensitive visual interneurons in the lobula plate of *Drosophila melanogaster*. *Current Biology*, 18(5):368–374.
- Joesch, M., B. Schnell, S. V. Raghu, D. F. Reiff, and A. Borst
2010. On and off pathways in *Drosophila* motion vision. *Nature*, 468:300.
- Johns, D. C., R. Marx, R. E. Mains, B. O'Rourke, and E. Marbán
1999. Inducible genetic suppression of neuronal excitability. *Journal of Neuroscience*, 19(5):1691.
- Karmeier, K., J. Van Hateren, R. Kern, and M. Egelhaaf
2006. Encoding of naturalistic optic flow by a population of blowfly motion-sensitive neurons. *Journal of Neurophysiology*, 96(3):1602–1614.
- Karuppururai, T., T.-Y. Lin, C.-Y. Ting, R. Pursley, K. Melnattur, F. Diao, B. White, L. Macpherson, M. Gallio, T. Pohida, and C.-H. Lee
2014. A hard-wired glutamatergic circuit pools and relays UV signals to mediate spectral preference in *Drosophila*. *Neuron*, 81(3):603–615.
- Kern, R., J. H. van Hateren, C. Michaelis, J. P. Lindemann, and M. Egelhaaf
2005. Function of a fly motion-sensitive neuron matches eye movements during free flight. *PLOS Biology*, 3(6):e171.
- Kim, A. J., L. M. Fenk, C. Lyu, and G. Maimon
2017. Quantitative predictions orchestrate visual signaling in *Drosophila*. *Cell*, 168(1-2):280–294.e12.

- Kim, A. J., J. K. Fitzgerald, and G. Maimon
2015. Cellular evidence for efference copy in *Drosophila* visuomotor processing. *Nature Neuroscience*, 18(9):1247–1255.
- Kirschfeld, K.
1967. Die Projektion der optischen Umwelt auf das Raster der Rhabdomere im Komplexauge von *Musca*. *Experimental Brain Research*, 3(3):248–270.
- Kitamoto, T.
2000. Conditional modification of behavior in *Drosophila* by targeted expression of a temperature-sensitive shibire allele in defined neurons. *Journal of Neurobiology*, 47(2):81–92.
- Klapoetke, N. C., Y. Murata, S. S. Kim, S. R. Pulver, A. Birdsey-Benson, Y. K. Cho, T. K. Morimoto, A. S. Chuong, E. J. Carpenter, Z. Tian, J. Wang, Y. Xie, Z. Yan, Y. Zhang, B. Y. Chow, B. Surek, M. Melkonian, V. Jayaraman, M. Constantine-Paton, G. K.-S. Wong, and E. S. Boyden
2014. Independent optical excitation of distinct neural populations. *Nature Methods*, 11(3):338–346.
- Kleinlogel, S., K. Feldbauer, R. E. Dempski, H. Fotis, P. G. Wood, C. Bamann, and E. Bamberg
2011. Ultra light-sensitive and fast neuronal activation with the Ca²⁺-permeable channelrhodopsin CatCh. *Nature Neuroscience*, 14:513.
- Knoll, M. and E. Ruska
1932. Das Elektronenmikroskop. *Zeitschrift für Physik*, 78(5):318–339.
- Koenderink, J. J. and A. J. van Doorn
1987. Facts on optic flow. *Biological Cybernetics*, 56(4):247–254.
- Krapp, H. G., B. Hengstenberg, and R. Hengstenberg
1998. Dendritic structure and receptive-field organization of optic flow processing interneurons in the fly. *Journal of Neurophysiology*, 79:1902–1917.
- Krapp, H. G. and R. Hengstenberg
1996. Estimation of self-motion by optic flow processing in single visual interneurons. *Nature*, 384(6608):463–466.
- Kremers, G.-J., S. G. Gilbert, P. J. Cranfill, M. W. Davidson, and D. W. Piston
2011. Fluorescent proteins at a glance. *Journal of Cell Science*, 124(2):157.
- Lai, S.-L. and T. Lee
2006. Genetic mosaic with dual binary transcriptional systems in *Drosophila*. *Nature Neuroscience*, 9:703.
- Land, M. F.
1997. Visual acuity in insects. *Annual Review of Entomology*, 42(1):147–177.
- Lappe, M., F. Bremmer, and A. V. van den Berg
1999. Perception of self-motion from visual flow. *Trends in Cognitive Sciences*, 3(9):329–336.

- Laughlin, S. B. and D. Osorio
1989. Mechanisms for neural signal enhancement in the blowfly compound eye. *Journal of Experimental Biology*, 144(1):113.
- Levy, P. and C. Larsen
2013. Odd-skipped labels a group of distinct neurons associated with the mushroom body and optic lobe in the adult *Drosophila* brain. *The Journal of Comparative Neurology*, 521(23749685):3716–3740.
- Li, B., L. Heng, K. Koser, and M. Pollefeys
2013. A multiple-camera system calibration toolbox using a feature descriptor-based calibration pattern. In *2013 IEEE/RSJ International Conference on Intelligent Robots and Systems*, Pp. 1301–1307.
- Liberti, W. A., L. N. Perkins, D. P. Leman, and T. J. Gardner
2017. An open source, wireless capable miniature microscope system. *Journal of Neural Engineering*, 14(4):045001.
- Lima, S. Q. and G. Miesenböck
2005. Remote control of behavior through genetically targeted photostimulation of neurons. *Cell*, 121(1):141–152.
- Limb, J. O. and J. A. Murphy
1975. Estimating the velocity of moving images in television signals. *Computer Graphics and Image Processing*, 4(4):311–327.
- Lin, J. Y., P. M. Knutsen, A. Muller, D. Kleinfeld, and R. Y. Tsien
2013. ReaChR: A red-shifted variant of channelrhodopsin enables deep transcranial optogenetic excitation. *Nature Neuroscience*, 16(10):1499–1508.
- Lin, J. Y., M. Z. Lin, P. Steinbach, and R. Y. Tsien
2009. Characterization of engineered channelrhodopsin variants with improved properties and kinetics. *Biophysical Journal*, 96(5):1803–1814.
- Lin, M. Z. and M. J. Schnitzer
2016. Genetically encoded indicators of neuronal activity. *Nature Neuroscience*, 19(9):1142–1153.
- Longden, K. D. and H. G. Krapp
2009. State-dependent performance of optic-flow processing interneurons. *Journal of Neurophysiology*, 102(6):3606–3618.
- Lott, G. K., M. J. Rosen, and R. R. Hoy
2007. An inexpensive sub-millisecond system for walking measurements of small animals based on optical computer mouse technology. *Journal of Neuroscience Methods*, 161(1):55–61.
- Luan, H., N. C. Peabody, C. Vinson, and B. H. White
2006. Refined spatial manipulation of neuronal function by combinatorial restriction of transgene expression. *Neuron*, 52(3):425–436.
- Ma, J. and M. Ptashne
1987. The carboxy-terminal 30 amino acids of GAL4 are recognized by GAL80. *Cell*, 50(1):137–142.

- Mahn, M., M. Prigge, S. Ron, R. Levy, and O. Yizhar
2016. Biophysical constraints of optogenetic inhibition at presynaptic terminals. *Nature Neuroscience*, 19:554.
- Maimon, G., A. D. Straw, and M. H. Dickinson
2010. Active flight increases the gain of visual motion processing in *Drosophila*. *Nature Neuroscience*, 13:393.
- Maisak, M. S., J. Haag, G. Ammer, E. Serbe, M. Meier, A. Leonhardt, T. Schilling, A. Bahl, G. M. Rubin, A. Nern, B. J. Dickson, D. F. Reiff, E. Hopp, and A. Borst
2013. A directional tuning map of *Drosophila* elementary motion detectors. *Nature*, 500:212.
- Malyshev, A. Y., M. V. Roshchin, G. R. Smirnova, D. A. Dolgikh, P. M. Balaban, and M. A. Ostrovsky
2017. Chloride conducting light activated channel GtACR2 can produce both cessation of firing and generation of action potentials in cortical neurons in response to light. *Neuroscience Letters*, 640:76–80.
- Mamiya, A., P. Gurung, and J. C. Tuthill
2018. Neural coding of leg proprioception in *Drosophila*. *Neuron*, 100(3):636–650.e6.
- Marescotti, M., K. Lagogiannis, B. Webb, R. W. Davies, and J. D. Armstrong
2018. Monitoring brain activity and behaviour in freely moving *Drosophila* larvae using bioluminescence. *Scientific Reports*, 8(1):9246.
- Marvin, J. S., B. G. Borghuis, L. Tian, J. Cichon, M. T. Harnett, J. Akerboom, A. Gordus, S. L. Renninger, T.-W. Chen, C. I. Bargmann, M. B. Orger, E. R. Schreiter, J. B. Demb, W.-B. Gan, S. A. Hires, and L. L. Looger
2013. An optimized fluorescent probe for visualizing glutamate neurotransmission. *Nature Methods*, 10:162.
- Mattingly, M., K. Weineck, J. Costa, and R. L. Cooper
2018. Hyperpolarization by activation of halorhodopsin results in enhanced synaptic transmission: Neuromuscular junction and CNS circuit. *PLOS ONE*, 13(7):e0200107.
- Mauss, A. S. and A. Borst
2016. Electrophysiological recordings from lobula plate tangential cells in *Drosophila*. In *Drosophila: Methods and Protocols*, C. Dahmann, ed., Pp. 321–332. New York, NY: Springer New York.
- Mauss, A. S., M. Meier, E. Serbe, and A. Borst
2014. Optogenetic and pharmacologic dissection of feedforward inhibition in *Drosophila* motion vision. *Journal of Neuroscience*, 34(6):2254.
- Mauss, A. S., K. Pankova, A. Arenz, A. Nern, G. M. Rubin, and A. Borst
2015. Neural circuit to integrate opposing motions in the visual field. *Cell*, 162(2):351–362.

- Mauss, A. S., A. Vlasits, A. Borst, and M. Feller
2017. Visual circuits for direction selectivity. *Annual Review of Neuroscience*, 40(1):211–230.
- McGuire, S. E., P. T. Le, A. J. Osborn, K. Matsumoto, and R. L. Davis
2003. Spatiotemporal rescue of memory dysfunction in *Drosophila*. *Science*, 302(5651):1765.
- Meier, M., E. Serbe, M. Maisak, J. Haag, B. Dickson, and A. Borst
2014. Neural circuit components of the *Drosophila* OFF motion vision pathway. *Current Biology*, 24(4):385–392.
- Meinertzhagen, I. A. and S. D. O’Neil
1991. Synaptic organization of columnar elements in the lamina of the wild type in *Drosophila melanogaster*. *Journal of Comparative Neurology*, 305(2):232–263.
- Melnattur, K. V., R. Pursley, T.-Y. Lin, C.-Y. Ting, P. D. Smith, T. Pohida, and C.-H. Lee
2014. Multiple redundant medulla projection neurons mediate color vision in *Drosophila*. *Journal of Neurogenetics*, 28(3-4):374–388.
- Mercier, D., Y. Tsuchimoto, K. Ohta, and H. Kazama
2018. Olfactory landmark-based communication in interacting *Drosophila*. *Current Biology*.
- Miesenböck, G., D. A. De Angelis, and J. E. Rothman
1998. Visualizing secretion and synaptic transmission with pH-sensitive green fluorescent proteins. *Nature*, 394:192.
- Mondal, K., A. G. Dastidar, G. Singh, S. Madhusudhanan, S. L. Gande, K. VijayRaghavan, and R. Varadarajan
2007. Design and isolation of temperature-sensitive mutants of GAL4 in yeast and *Drosophila*. *Journal of Molecular Biology*, 370(5):939–950.
- Morante, J. and C. Desplan
2004. Building a projection map for photoreceptor neurons in the *Drosophila* optic lobes. *Seminars in Cell & Developmental Biology*, 15(1):137–143.
- Mronz, M. and F.-O. Lehmann
2008. The free-flight response of *Drosophila* to motion of the visual environment. *Journal of Experimental Biology*, 211(13):2026.
- Murthy, M., I. Fiete, and G. Laurent
2008. Testing odor response stereotypy in the *Drosophila* mushroom body. *Neuron*, 59(6):1009–1023.
- Nagel, G., T. Szellas, W. Huhn, S. Kateriya, N. Adeishvili, P. Berthold, D. Ollig, P. Hegemann, and E. Bamberg
2003. Channelrhodopsin-2, a directly light-gated cation-selective membrane channel. *Proceedings of the National Academy of Sciences of the United States of America*, 100(24):13940.

- Nakai, J., M. Ohkura, and K. Imoto
2001. A high signal-to-noise Ca²⁺ probe composed of a single green fluorescent protein. *Nature Biotechnology*, 19:137.
- Namiki, S., M. H. Dickinson, A. M. Wong, W. Korff, G. M. Card, and K. Scott
2018. The functional organization of descending sensory-motor pathways in *Drosophila*. *eLife*, 7:e34272.
- Nern, A., B. D. Pfeiffer, and G. M. Rubin
2015. Optimized tools for multicolor stochastic labeling reveal diverse stereotyped cell arrangements in the fly visual system. *Proceedings of the National Academy of Sciences*, 112(22):E2967–E2976.
- Niell, C. M. and M. P. Stryker
2010. Modulation of visual responses by behavioral state in mouse visual cortex. *Neuron*, 65(20188652):472–479.
- Nitabach, M. N., Y. Wu, V. Sheeba, W. C. Lemon, J. Strumbos, P. K. Zelensky, B. H. White, and T. C. Holmes
2006. Electrical hyperexcitation of lateral ventral pacemaker neurons desynchronizes downstream circadian oscillators in the fly circadian circuit and induces multiple behavioral periods. *Journal of Neuroscience*, 26(2):479.
- Néric, N. and C. Desplan
2016. From the eye to the brain: Development of the *Drosophila* visual system. *Current Topics in Developmental Biology*, 116(26970623):247–271.
- Osterwalder, T., K. S. Yoon, B. H. White, and H. Keshishian
2001. A conditional tissue-specific transgene expression system using inducible GAL4. *Proceedings of the National Academy of Sciences of the United States of America*, 98(22):12596.
- Otsuna, H. and K. Ito
2006. Systematic analysis of the visual projection neurons of *Drosophila melanogaster*. I. Lobula-specific pathways. *The Journal of Comparative Neurology*, 497(6):928–958.
- Pfeiffer, B. D., T.-T. B. Ngo, K. L. Hibbard, C. Murphy, A. Jenett, J. W. Truman, and G. M. Rubin
2010. Refinement of tools for targeted gene expression in *Drosophila*. *Genetics*, 186(2):735.
- Pfeiffer, B. D., J. W. Truman, and G. M. Rubin
2012. Using translational enhancers to increase transgene expression in *Drosophila*. *Proceedings of the National Academy of Sciences of the United States of America*, 109(17):6626.
- Platasa, J. and V. A. Pieribone
2018. Genetically encoded fluorescent voltage indicators: Are we there yet? *Current Opinion in Neurobiology*, 50:146–153.

- Potter, C. J., B. Tasic, E. V. Russler, L. Liang, and L. Luo
2010. The Q system: A repressible binary system for transgene expression, lineage tracing, and mosaic analysis. *Cell*, 141(3):536–548.
- Potters, M. and W. Bialek
1994. Statistical mechanics and visual signal processing. *Journal de Physique I*, 4(11):1755–1775.
- Pringle, J. W. S. and J. Gray
1948. The gyroscopic mechanism of the halteres of *Diptera*. *Philosophical Transactions of the Royal Society of London. Series B, Biological Sciences*, 233(602):347–384.
- Raimondo, J. V., L. Kay, T. J. Ellender, and C. J. Akerman
2012. Optogenetic silencing strategies differ in their effects on inhibitory synaptic transmission. *Nature Neuroscience*, 15:1102.
- Ramón y Cajal, S., D. Sánchez, and U. C. de Madrid. Laboratorio de Investigaciones Biológicas
1915. *Contribución al conocimiento de los centros nerviosos de los insectos*. Madrid: Imprenta de Hijos de Nicolás Moya,.
- Ready, D. F., T. E. Hanson, and S. Benzer
1976. Development of the *Drosophila* retina, a neurocrystalline lattice. *Developmental Biology*, 53(2):217–240.
- Reiff, D. F., J. Plett, M. Mank, O. Griesbeck, and A. Borst
2010. Visualizing retinotopic half-wave rectified input to the motion detection circuitry of *Drosophila*. *Nature Neuroscience*, 13(8):973–978.
- Rein, M. L. and J. M. Deussing
2012. The optogenetic (r)evolution. *Molecular Genetics and Genomics*, 287(2):95–109.
- Riabinina, O., D. Luginbuhl, E. Marr, S. Liu, M. N. Wu, L. Luo, and C. J. Potter
2015. Improved and expanded Q-system reagents for genetic manipulations. *Nature Methods*, 12:219.
- Riemensperger, T., R. J. Kittel, and A. Fiala
2016. Optogenetics in *Drosophila* neuroscience. In *Optogenetics: Methods and Protocols*, A. Kianianmomeni, ed., Pp. 167–175. New York, NY: Springer New York.
- Rister, J., D. Pauls, B. Schnell, C.-Y. Ting, C.-H. Lee, I. Sinakevitch, J. Morante, N. J. Strausfeld, K. Ito, and M. Heisenberg
2007. Dissection of the peripheral motion channel in the visual system of *Drosophila melanogaster*. *Neuron*, 56(1):155–170.
- Rivera-Alba, M., S. Vitaladevuni, Y. Mishchenko, Z. Lu, S.-y. Takemura, L. Scheffer, I. Meinertzhagen, D. Chklovskii, and G. de Polavieja
2011. Wiring economy and volume exclusion determine neuronal placement in the *Drosophila* brain. *Current Biology*, 21(23):2000–2005.

- Robie, A. A., J. Hirokawa, A. W. Edwards, L. A. Umayam, A. Lee, M. L. Phillips, G. M. Card, W. Korff, G. M. Rubin, J. H. Simpson, M. B. Reiser, and K. Branson
2017. Mapping the neural substrates of behavior. *Cell*, 170(2):393–406.e28.
- Robie, A. A., A. D. Straw, and M. H. Dickinson
2010. Object preference by walking fruit flies, *Drosophila melanogaster*, is mediated by vision and graviperception. *The Journal of Experimental Biology*, 213(20581279):2494–2506.
- Rodriguez, E. A., R. E. Campbell, J. Y. Lin, M. Z. Lin, A. Miyawaki, A. E. Palmer, X. Shu, J. Zhang, and R. Y. Tsien
2017. The growing and glowing toolbox of fluorescent and photoactive proteins. *Trends in Biochemical Sciences*, 42(2):111–129.
- Roman, G., K. Endo, L. Zong, and R. L. Davis
2001. P{Switch}, a system for spatial and temporal control of gene expression in *Drosophila*. *Proceedings of the National Academy of Sciences of the United States of America*, 98(22):12602.
- Rosenzweig, M., K. M. Brennan, T. D. Tayler, P. O. Phelps, A. Patapoutian, and P. A. Garrity
2005. The *Drosophila* ortholog of vertebrate TRPA1 regulates thermotaxis. *Genes & Development*, 19(15681611):419–424.
- Rubin, G. M. and A. C. Spradling
1982. Genetic transformation of *Drosophila* with transposable element vectors. *Science*, 218(4570):348.
- Sakmann, B. and E. Neher
1984. Patch clamp techniques for studying ionic channels in excitable membranes. *Annual Review of Physiology*, 46(1):455–472.
- Schnaitmann, C., C. Garbers, T. Wachtler, and H. Tanimoto
2013. Color discrimination with broadband photoreceptors. *Current Biology*, 23(23):2375–2382.
- Schnell, B., M. Joesch, F. Forstner, S. V. Raghu, H. Otsuna, K. Ito, A. Borst, and D. F. Reiff
2010. Processing of horizontal optic flow in three visual interneurons of the *Drosophila* brain. *Journal of Neurophysiology*, 103(3):1646–1657.
- Schnell, B., I. G. Ros, and M. H. Dickinson
2017. A descending neuron correlated with the rapid steering maneuvers of flying *Drosophila*. *Current Biology*, 27(28392112):1200–1205.
- Schuster, S., R. Strauss, and K. G. Götz
2002. Virtual-reality techniques resolve the visual cues used by fruit flies to evaluate object distances. *Current Biology*, 12(18):1591–1594.
- Seelig, J. D., M. E. Chiappe, G. K. Lott, A. Dutta, J. E. Osborne, M. B. Reiser, and V. Jayaraman
2010. Two-photon calcium imaging from head-fixed *Drosophila* during optomotor walking behavior. *Nature Methods*, 7:535.

- Sepehri Rad, M., Y. Choi, L. B. Cohen, B. J. Baker, S. Zhong, D. A. Storage, and O. R. Braubach
2017. Voltage and calcium imaging of brain activity. *Biophysical Journal*, 113(10):2160–2167.
- Serbe, E., M. Meier, A. Leonhardt, and A. Borst
2016. Comprehensive characterization of the major presynaptic elements to the *Drosophila* off motion detector. *Neuron*, 89(4):829–841.
- Shaner, N. C., P. A. Steinbach, and R. Y. Tsien
2005. A guide to choosing fluorescent proteins. *Nature Methods*, 2:905.
- Shih, C.-T., O. Sporns, S.-L. Yuan, T.-S. Su, Y.-J. Lin, C.-C. Chuang, T.-Y. Wang, C.-C. Lo, R. J. Greenspan, and A.-S. Chiang
2015. Connectomics-based analysis of information flow in the *Drosophila* brain. *Current Biology*, 25(10):1249–1258.
- Shinomiya, K., G. Huang, Z. Lu, T. Parag, C. S. Xu, R. Aniceto, N. Ansari, N. Cheatham, S. Lauchie, E. Neace, O. Ogundeyi, C. Ordish, D. Peel, A. Shinomiya, C. Smith, S. Takemura, I. Talebi, P. K. Rivlin, A. Nern, L. K. Scheffer, S. M. Plaza, I. A. Meinertzhagen, and A. Borst
2019. Comparisons between the ON- and OFF-edge motion pathways in the *Drosophila* brain. *eLife*, 8:e40025.
- Shinomiya, K., T. Karuppudurai, T.-Y. Lin, Z. Lu, C.-H. Lee, and I. Meinertzhagen
2014. Candidate neural substrates for OFF-edge motion detection in *Drosophila*. *Current Biology*, 24(10):1062–1070.
- Sierra, Y. A. B., B. R. Rost, M. Pofahl, A. M. Fernandes, R. A. Kopton, S. Moser, D. Holtkamp, N. Masala, P. Beed, J. J. Tukker, S. Oldani, W. Bönigk, P. Kohl, H. Baier, F. Schneider-Warme, P. Hegemann, H. Beck, R. Seifert, and D. Schmitz
2018. Potassium channel-based optogenetic silencing. *Nature Communications*, 9(1):4611.
- Simon, J. C. and M. H. Dickinson
2010. A new chamber for studying the behavior of *Drosophila*. *PLOS ONE*, 5(1):e8793.
- Simpson, J. H. and L. L. Looger
2018. Functional imaging and optogenetics in *Drosophila*. *Genetics*, 208(29618589):1291–1309.
- Sineshchekov, O. A., E. G. Govorunova, J. Wang, and J. L. Spudich
2012. Enhancement of the long-wavelength sensitivity of optogenetic microbial rhodopsins by 3,4-dehydroretinal. *Biochemistry*, 51(22):4499–4506.
- Smith, D. J.
2008. Ultimate resolution in the electron microscope? *Materials Today*, 11:30–38.

- Stavenga, D. G.
1995. Insect retinal pigments: Spectral characteristics and physiological functions. *Progress in Retinal and Eye Research*, 15(1):231–259.
- Stavenga, D. G. and K. Arikawa
2008. One rhodopsin per photoreceptor: Iro-c genes break the rule. *PLOS Biology*, 6(4):e115.
- Stebbins, M. J., S. Urlinger, G. Byrne, B. Bello, W. Hillen, and J. C. Yin
2001. Tetracycline-inducible systems for *Drosophila*. *Proceedings of the National Academy of Sciences of the United States of America*, 98(11517299):10775–10780.
- Stebbins, M. J. and J. C. P. Yin
2001. Adaptable doxycycline-regulated gene expression systems for *Drosophila*. *Gene*, 270(1):103–111.
- Strausfeld, N. J.
1976. Atlas of an insect brain. In *Springer Berlin Heidelberg*.
- Strausfeld, N. J.
1989. Beneath the compound eye: Neuroanatomical analysis and physiological correlates in the study of insect vision. In *Facets of Vision*, D. G. Stavenga and R. C. Hardie, eds., Pp. 317–359, Berlin, Heidelberg. Springer Berlin Heidelberg.
- Strausfeld, N. J. and U. K. Bassemir
1985. Lobula plate and ocellar interneurons converge onto a cluster of descending neurons leading to neck and leg motor neuropil in *Calliphora erythrocephala*. *Cell and Tissue Research*, 240(3):617–640.
- Strausfeld, N. J. and W. Gronenberg
1990. Descending neurons supplying the neck and flight motor of diptera: Organization and neuroanatomical relationships with visual pathways. *Journal of Comparative Neurology*, 302(4):954–972.
- Straw, A. D., K. Branson, T. R. Neumann, and M. H. Dickinson
2011. Multi-camera real-time three-dimensional tracking of multiple flying animals. *Journal of The Royal Society Interface*, 8(56):395–409.
- Strother, J. A., S.-T. Wu, E. M. Rogers, J. L. M. Eliason, A. M. Wong, A. Nern, and M. B. Reiser
2018. Behavioral state modulates the ON visual motion pathway of *Drosophila*. *Proceedings of the National Academy of Sciences of the United States of America*, 115(1):E102.
- Struhl, G. and K. Basler
1993. Organizing activity of wingless protein in *Drosophila*. *Cell*, 72(4):527–540.
- Sunkara, A., G. C. DeAngelis, D. E. Angelaki, and R. Romo
2015. Role of visual and non-visual cues in constructing a rotation-invariant representation of heading in parietal cortex. *eLife*, 4:e04693.

- Suver, M., A. Mamiya, and M. Dickinson
2012. Octopamine neurons mediate flight-induced modulation of visual processing in *Drosophila*. *Current Biology*, 22(24):2294–2302.
- Suver, M. P., A. Huda, N. Iwasaki, S. Safarik, and M. H. Dickinson
2016. An array of descending visual interneurons encoding self-motion in *Drosophila*. *Journal of Neuroscience*, 36(46):11768.
- Sweeney, S. T., K. Broadie, J. Keane, H. Niemann, and C. J. O’Kane
1995. Targeted expression of tetanus toxin light chain in *Drosophila* specifically eliminates synaptic transmission and causes behavioral defects. *Neuron*, 14(2):341–351.
- Takemura, S., A. Bharioke, Z. Lu, A. Nern, S. Vitaladevuni, P. K. Rivlin, W. T. Katz, D. J. Olbris, S. M. Plaza, P. Winston, T. Zhao, J. A. Horne, R. D. Fetter, S. Takemura, K. Blazek, L.-A. Chang, O. Ogundeyi, M. A. Saunders, V. Shapiro, C. Sigmund, G. M. Rubin, L. K. Scheffer, I. A. Meinertzhagen, and D. B. Chklovskii
2013. A visual motion detection circuit suggested by *Drosophila* connectomics. *Nature*, 500:175.
- Takemura, S., Z. Lu, and I. A. Meinertzhagen
2008. Synaptic circuits of the *Drosophila* optic lobe: The input terminals to the medulla. *The Journal of Comparative Neurology*, 509(18537121):493–513.
- Takemura, S., A. Nern, D. B. Chklovskii, L. K. Scheffer, G. M. Rubin, and I. A. Meinertzhagen
2017. The comprehensive connectome of a neural substrate for ‘ON’ motion detection in *Drosophila*. *eLife*, 6.
- Takemura, S., C. S. Xu, Z. Lu, P. K. Rivlin, T. Parag, D. J. Olbris, S. Plaza, T. Zhao, W. T. Katz, L. Umayam, C. Weaver, H. F. Hess, J. A. Horne, J. Nunez-Iglesias, R. Aniceto, L.-A. Chang, S. Lauchie, A. Nasca, O. Ogundeyi, C. Sigmund, S. Takemura, J. Tran, C. Langille, K. L. Lacheur, S. McLin, A. Shinomiya, D. B. Chklovskii, I. A. Meinertzhagen, and L. K. Scheffer
2015. Synaptic circuits and their variations within different columns in the visual system of *Drosophila*. *Proceedings of the National Academy of Sciences*, 112(44):13711–13716.
- Talay, M., E. B. Richman, N. J. Snell, G. G. Hartmann, J. D. Fisher, A. Sorkaç, J. F. Santoyo, C. Chou-Freed, N. Nair, M. Johnson, J. R. Szymanski, and G. Barnea
2017. Transsynaptic mapping of second-order taste neurons in flies by *trans-tango*. *Neuron*, 96(4):783–795.e4.
- Thorson, J.
1966. Small-signal analysis of a visual reflex in the locust. *Kybernetik*, 3(2):53–66.

- Thum, A. S., S. Knapek, J. Rister, E. Dierichs-Schmitt, M. Heisenberg, and H. Tanimoto
2006. Differential potencies of effector genes in adult drosophila. *Journal of Comparative Neurology*, 498(2):194–203.
- Tirian, L. and B. Dickson
2017. The VT GAL4, LexA, and split-GAL4 driver line collections for targeted expression in the *Drosophila* nervous system. *bioRxiv*, P. 198648.
- Tuthill, J., A. Nern, S. Holtz, G. Rubin, and M. Reiser
2013. Contributions of the 12 neuron classes in the fly lamina to motion vision. *Neuron*, 79(1):128–140.
- Tye, K. M. and K. Deisseroth
2012. Optogenetic investigation of neural circuits underlying brain disease in animal models. *Nature Reviews Neuroscience*, 13:251.
- Vallerga, S.
1994. The phylogenetic evolution of the visual system. In *Human and Machine Vision: Analogies and Divergencies*, V. Cantoni, ed., Pp. 1–12. Boston, MA: Springer US.
- van Santen, J. G. and G. Sperling
1985. Elaborated reichardt detectors. *Journal of the Optical Society of America. A, Optics and Image Science*, 2 2:300–21.
- van Santen, J. P. H. and G. Sperling
1984. Temporal covariance model of human motion perception. *Journal of the Optical Society of America A, Optics and Image Science*, 1(5):451–473.
- Vellekoop, I. M. and C. Aegerter
2010. Focusing light through living tissue. *Proceedings of SPIE*, 7554:755430.
- Venken, K. T., J. Simpson, and H. Bellen
2011. Genetic manipulation of genes and cells in the nervous system of the fruit fly. *Neuron*, 72(2):202–230.
- Vogt, K. and K. Kirschfeld
1984. Chemical identity of the chromophores of fly visual pigment. *Naturwissenschaften*, 71(4):211–213.
- Vogt, N.
2018. Modeling temperature during optogenetic illumination. *Nature Methods*, 15(10):763–763.
- Vogt, N.
2019. Optogenetics turns up the heat. *Nature Methods*, 16(8):681–681.
- Von Helmholtz, H.
1867. *Handbuch der physiologischen Optik*, volume 9. Voss.
- von Holst, E. and H. Mittelstaedt
1950. Das Reafferenzprinzip. *Naturwissenschaften*, 37(20):464–476.

- von Philipsborn, A. C., T. Liu, J. Y. Yu, C. Masser, S. S. Bidaye, and B. J. Dickson
2011. Neuronal control of *Drosophila* courtship song. *Neuron*, 69(3):509–522.
- Wardill, T. J., O. List, X. Li, S. Dongre, M. McCulloch, C.-Y. Ting, C. J. O’Kane, S. Tang, C.-H. Lee, R. C. Hardie, and M. Juusola
2012. Multiple spectral inputs improve motion discrimination in the *Drosophila* visual system. *Science*, 336(6083):925–931.
- Waschuk, S. A., A. G. Bezerra, L. Shi, and L. S. Brown
2005. *Leptosphaeria* rhodopsin: Bacteriorhodopsin-like proton pump from a eukaryote. *Proceedings of the National academy of Sciences of the United States of America*, 102(19):6879.
- Wasserman, S. M., J. W. Aptekar, P. Lu, J. Nguyen, A. L. Wang, M. F. Keles, A. Grygoruk, D. E. Krantz, C. Larsen, and M. A. Frye
2015. Olfactory neuromodulation of motion vision circuitry in *Drosophila*. *Current Biology*, 25(25619767):467–472.
- Webster, M. A.
2015. Visual adaptation. *Annual Review of Vision Science*, 1(1):547–567.
- Wehner, R.
1987. ‘Matched filters’ – neural models of the external world. *Journal of Comparative Physiology A*, 161(4):511–531.
- Weir, P. T. and M. H. Dickinson
2012. Flying *Drosophila* orient to sky polarization. *Current Biology*, 22(1):21–27.
- Wernet, M., M. Velez, D. Clark, F. Baumann-Klausener, J. Brown, M. Klovs-tad, T. Labhart, and T. Clandinin
2012. Genetic dissection reveals two separate retinal substrates for polarization vision in *Drosophila*. *Current Biology*, 22(1):12–20.
- Wernet, M. F. and C. Desplan
2004. Building a retinal mosaic: Cell-fate decision in the fly eye. *Trends in Cell Biology*, 14(10):576–584.
- Wernet, M. F., T. Labhart, F. Baumann, E. O. Mazzoni, F. Pichaud, and C. Desplan
2003. Homothorax switches function of *Drosophila* photoreceptors from color to polarized light sensors. *Cell*, 115(3):267–279.
- White, K., M. E. Grether, J. M. Abrams, L. Young, K. Farrell, and H. Steller
1994. Genetic control of programmed cell death in *Drosophila*. *Science*, 264(5159):677.
- White, K., E. Tahaoglu, and H. Steller
1996. Cell killing by the *Drosophila* gene reaper. *Science*, 271(5250):805.

- Wiegert, J. S., M. Mahn, M. Prigge, Y. Printz, and O. Yizhar
2017. Silencing neurons: Tools, applications, and experimental constraints. *Neuron*, 95(3):504–529.
- Wiegert, J. S. and T. G. Oertner
2016. How (not) to silence long-range projections with light. *Nature Neuroscience*, 19:527.
- Wietek, J., R. Beltramo, M. Scanziani, P. Hegemann, T. G. Oertner, and J. S. Wiegert
2015. An improved chloride-conducting channelrhodopsin for light-induced inhibition of neuronal activity in vivo. *Scientific Reports*, 5:14807.
- Wietek, J., S. Rodriguez-Rozada, J. Tutas, F. Tenedini, C. Grimm, T. G. Oertner, P. Soba, P. Hegemann, and J. S. Wiegert
2017. Anion-conducting channelrhodopsins with tuned spectra and modified kinetics engineered for optogenetic manipulation of behavior. *Scientific Reports*, 7(1):14957.
- Wietek, J., J. S. Wiegert, N. Adeishvili, F. Schneider, H. Watanabe, S. P. Tsunoda, A. Vogt, M. Elstner, T. G. Oertner, and P. Hegemann
2014. Conversion of channelrhodopsin into a light-gated chloride channel. *Science*, 344(6182):409–412.
- Wilson, R. I., G. C. Turner, and G. Laurent
2004. Transformation of olfactory representations in the *Drosophila* antennal lobe. *Science*, 303(5656):366.
- Wing, J. P., L. Zhou, L. M. Schwartz, and J. R. Nambu
1998. Distinct cell killing properties of the *Drosophila* reaper, head involution defective, and grim genes. *Cell Death And Differentiation*, 5:930.
- Wu, M., A. Nern, W. R. Williamson, M. M. Morimoto, M. B. Reiser, G. M. Card, G. M. Rubin, and K. Scott
2016. Visual projection neurons in the *Drosophila* lobula link feature detection to distinct behavioral programs. *eLife*, 5:e21022.
- Wylie, D. R. W., W. F. Bischof, and B. J. Frost
1998. Common reference frame for neural coding of translational and rotational optic flow. *Nature*, 392(6673):278–282.
- Xu, Y., P. Zou, and A. E. Cohen
2017. Voltage imaging with genetically encoded indicators. *Current Opinion in Chemical Biology*, 39:1–10.
- Yamaguchi, S., R. Wolf, C. Desplan, and M. Heisenberg
2008. Motion vision is independent of color in *Drosophila*. *Proceedings of the National Academy of Sciences of the United States of America*, 105(12):4910.
- Yang, H., F. St-Pierre, X. Sun, X. Ding, M. Lin, and T. Clandinin
2016. Subcellular imaging of voltage and calcium signals reveals neural processing in vivo. *Cell*, 166(1):245–257.

- Yizhar, O., L. E. Fenno, M. Prigge, F. Schneider, T. J. Davidson, D. J. O'Shea, V. S. Sohal, I. Goshen, J. Finkelstein, J. T. Paz, K. Stehfest, R. Fudim, C. Ramakrishnan, J. R. Huguenard, P. Hegemann, and K. Deisseroth
2011. Neocortical excitation/inhibition balance in information processing and social dysfunction. *Nature*, 477(7363):171–178.
- Zheng, Z., J. S. Lauritzen, E. Perlman, C. G. Robinson, M. Nichols, D. Milkie, O. Torrens, J. Price, C. B. Fisher, N. Sharifi, S. A. Calle-Schuler, L. Kmecova, I. J. Ali, B. Karsh, E. T. Trautman, J. A. Bogovic, P. Hanslovsky, G. S. X. E. Jefferis, M. Kazhdan, K. Khairy, S. Saalfeld, R. D. Fetter, and D. D. Bock
2018. A complete electron microscopy volume of the brain of adult *Drosophila melanogaster*. *Cell*, 174(3):730–743.e22.
- Zhou, L., A. Schnitzler, J. Agapite, L. M. Schwartz, H. Steller, and J. R. Nambu
1997. Cooperative functions of the reaper and head involution defective genes in the programmed cell death of *Drosophila* central nervous system midline cells. *Proceedings of the National Academy of Sciences of the United States of America*, 94(10):5131.
- Zhu, Y.
2013. The *Drosophila* visual system: From neural circuits to behavior. *Cell Adhesion & Migration*, 7(23880926):333–344.

ACKNOWLEDGEMENTS

First and foremost, I would like to thank Axel for being a great supervisor throughout the time of my PhD. I really enjoyed the scientific and experimental freedom you gave me, which allowed me to dive into the field of neuroscience. I am grateful for your very valuable support steering my work to ensure scientific success, particularly in key moments.

Special thanks also go to Alex for his intensive support. I could always count on your help and I am thankful for your many useful advises! Thank you also for reviewing my thesis. I would also like to thank everyone who contributed in my research projects: all my colleagues and friends for supporting me throughout this time. I want to thank Aljoscha for supporting me with the behavior setup, software and analysis. I thank Inês and Sandra for helping me with any kind of genetic or biological work and questions. I also thank Nikolai for organizing many events and keeping a great social atmosphere. I am very grateful to Wolfgang, Michael, Renate, Christian, and Romina for their excellent technical assistance. Special thanks go to Stefan, who was a tremendous help with all kinds of mechanical, electrical and optical engineering challenges. I am obliged to the whole Borst department, and to all of my colleagues at the institute as well as the administrative team and members of the Graduate School for Systemic Neurosciences for sharing with me this great experience. Additionally, I want to thank Ruben Portugues and Christian Leibold for their advice as part of my thesis committee.

Finally, I would also like to thank my parents and my sister, for always being interested in my thesis and holding my back. Most importantly I want to thank Laia for making the past years so amazing and for supporting me during challenging times! Thanks for helping me improve my thesis. Y muchas gracias Laia por todo!!!